

STATISTICAL ANALYSIS OF REINFORCING STEEL PROPERTIES

A thesis presented for the degree of
Master of Engineering in Mechanical Engineering
in the University of Canterbury

by

LIM Wai Tat

University of Canterbury
Christchurch, New Zealand

June 1991

ABSTRACT

The previous Grade 275 and Grade 380 reinforcing steels have been respectively replaced by Grade 300 and Grade 430 steels confirming to the new standard NZS 3402, released in December 1989. Grade 300 is similar to, but a little stronger than, the previous Grade 275. Grade 430 has a significantly higher yield strength, lower strain hardening rate and is more ductile and readily weldable when compared to the old Grade 380.

This project was carried out to investigate the distribution of mechanical properties for NZS 3402 Grade 300, and the micro-alloyed Grade 430 reinforcing steel manufactured by Pacific Steel Ltd. The investigation was based on data supplied by Pacific Steel Ltd and on data generated from mechanical tests carried out in the Materials Laboratory of the Mechanical Engineering Department, University of Canterbury. Tensile testing was carried out on the supplied material in the as rolled (deformed reinforcing bar) condition and on standard tensile specimens machined from these bars. One machined tensile specimen was pre-strained 5% and artificially aged to determine a strain ageing index for each cast supplied.

For both grades of steel distributions of lower yield strength, tensile strength, elongation at fracture, Luder strain at the yield point, strain hardening parameters n and k , and three parameters measuring strain ageing index were determined. The characteristic yield strength, minimum and maximum yield strength ranges obtained were found to comply with the specified tensile properties in the new specification.

Multiple linear regression techniques were used to investigate relationships between the determined mechanical properties and the steels chemical composition as determined by Pacific Steel Ltd. The regression analysis yielded simple linear equations which can be used to predict the mechanical properties of bars from production variations in chemical composition.

These equations reveal that the improved properties of Grade 430 reinforcing steel is mainly attributed to the addition of 0.04% vanadium. Grade 430 steel is found to be less susceptible to strain ageing and can be used in plastic hinge zones in reinforced concrete structures.

ACKNOWLEDGEMENTS

I wish to express my gratitude to Professor L.A. Erasmus for his support and supervision of this project. His invaluable advice, encouragement and concern is deeply appreciated.

My special thanks to Pacific Steel Ltd of Auckland for the Harold A. Longden Scholarship award in 1990 and for the additional allowance provided for 1991. This financial support has been very helpful in enabling me to undertake postgraduate research. My thanks also go to its Technical Services Department, particularly the Manager, Mr N.M. Corry, for providing the experimental steels, valuable data and information, and also for enabling me to visit the Company.

The technical support and assistance from the staff of the Department of Mechanical Engineering, University of Canterbury, especially Dr J.S. Smaill, Dr J.M. Cowling, Messrs M.J. Flaws, D.K. Healy and H.A. Mobbs and the meticulous typing of Mrs J.M. Kerby are gratefully acknowledged.

Finally, I wish to express my deep gratitude and appreciation to my parents for their constant support and encouragement.

TABLE OF CONTENTS

	Page
Abstract	ii
Acknowledgements	iv
Table of Contents	v
List of Figures	vii
List of Tables	xi
Chapter One : Introduction	
1.1 General	1
1.2 Scope of Thesis	3
Chapter Two : Experimental Procedure	
2.1 Types and Sample Size of Reinforcing Steel	4
2.2 Chemical Composition of Reinforcing Steel	5
2.3 Tensile Testing	7
Chapter Three : Distribution of Reinforcing Steel Properties	
3.1 Introduction	9
3.2 Definition of Parameters	9
3.3 Distribution of Lower Yield Strength	16
3.4 Distribution of Tensile Strength	35
3.5 Distribution of Elongation at Fracture	44
3.6 Distribution of Luder Strain	48
3.7 Distribution of Strain Hardening Exponent and Coefficient	53
3.8 Distribution of Strain Ageing Index	57
3.9 Special "Low Carbon Trial Heats"	63
3.10 Summary	63
Chapter Four : Multiple Linear Regression	66
Chapter Five : Multiple Linear Regression of Reinforcing Steel Properties	
5.1 Introduction	73
5.2 The Regression of Lower Yield Strength	78
5.3 The Regression of Tensile Strength	86
5.4 The Regression of Elongation at Fracture	91
5.5 The Regression of Luder Strain	96
5.6 The Regression of Strain Hardening Exponent and Coefficient	99
5.7 The Regression of Strain Ageing Index	103
5.8 Summary	107

	Page
Chapter Six : Conclusions	112
References	114
Appendix A : Chemical Composition of Reinforcing Steel	120
Appendix B : Detailed Dimension of the Machined Specimen	128
Appendix C : Tensile Results of Reinforcing Steel	131

LIST OF FIGURES

Figure	Page
3.1: The idealized steel stress-strain curve	10
3.2: Schematic tensile load/elongation curve for a structural grade steel	10
3.3: Mander's stress-strain model	12
3.4: Effect of strain ageing on the load-elongation curve for low carbon steel	15
3.5: Distribution of lower yield strength of Grade 300 machined specimen data	17
3.6: Distribution of lower yield strength of Grade 300 lab deformed data	17
3.7: Distribution of lower yield strength of Grade 300 P.S. deformed data	18
3.8: Distribution of lower yield strength of Grade 430 machined specimen data	19
3.9: Distribution of lower yield strength of Grade 430 lab deformed data	19
3.10: Distribution of lower yield strength of Grade 430 P.S. deformed data	20
3.11: Graph of lower yield strength of machined specimen vs lab deformed (Grade 300)	21
3.12: Graph of lower yield strength of machined specimen vs lab deformed (Grade 430)	22
3.13: Graph of lower yield strength of machined specimen vs lab deformed	23
3.14: Graph of lower yield strength of machined specimen vs P.S. deformed	25
3.15: Graph of lower yield strength of lab deformed vs P.S. deformed	26
3.16: Variation of cross section areas of 10 mm and 12 mm lab deformed bars	30

Figure	Page
3.17: Variation of cross section areas of 20 mm and 24 mm lab deformed bars	31
3.18: Variation of cross section areas of 28 mm and 32 mm lab deformed bars	32
3.19: Distribution of tensile strength of Grade 300 machined specimen data	36
3.20: Distribution of tensile strength of Grade 300 lab deformed data	36
3.21: Distribution of tensile strength of Grade 300 P.S. deformed data	37
3.22: Distribution of tensile strength of Grade 430 machined specimen data	38
3.23: Distribution of tensile strength of Grade 430 lab deformed data	38
3.24: Distribution of tensile strength of Grade 430 P.S. deformed data	39
3.25: Graph of tensile strength of machined specimen vs P.S. deformed	41
3.26: Graph of tensile strength of lab deformed vs P.S. deformed	42
3.27: Distribution of % elongation at fracture of Grade 300 machined specimen data	45
3.28: Distribution of % elongation at fracture of Grade 300 P.S. deformed data	45
3.29: Distribution of % elongation at fracture of Grade 430 machined specimen data	46
3.30: Distribution of % elongation at fracture of Grade 430 P.S. deformed data	46
3.31: Graph of % elongation at fracture of machined specimen vs P.S. deformed	47
3.32: Distribution of % Luder strain of Grade 300 machined specimen data	49
3.33: Distribution of % Luder strain of Grade 300 lab deformed data	49
3.34: Distribution of % Luder strain of Grade 430 machined specimen data	50

Figure	Page
3.35: Distribution of % Luder strain of Grade 430 lab deformed data	50
3.36: Graph of % Luder strain of machined specimen vs lab deformed	51
3.37: Distribution of strain hardening exponent of Grade 300 machined specimen data	54
3.38: Distribution of strain hardening exponent of Grade 430 machined specimen data	54
3.39: Distribution of strain hardening coefficient of Grade 300 machined specimen data	55
3.40: Distribution of strain hardening coefficient of Grade 430 machined specimen data	55
3.41: Mean strain hardening rate for Grade 300 and Grade 430 reinforcing steels	58
3.42: Distribution of strain ageing index ΔY of Grade 300 machined specimen data	59
3.43: Distribution of strain ageing index ΔY of Grade 430 machined specimen data	59
3.44: Distribution of strain ageing index ΔU of Grade 300 machined specimen data	60
3.45: Distribution of strain ageing index ΔU of Grade 430 machined specimen data	60
3.46: Distribution of strain ageing index ΔEl of Grade 300 machined specimen data	61
3.47: Distribution of strain ageing index ΔEl of Grade 430 machined specimen data	61
5.1: Calculated and observed lower yield strength for Grade 300 and Grade 430 reinforcing steels using Equation 5.4	81
5.2: Calculated and observed lower yield strength for Grade 300 and Grade 430 reinforcing steels using Equation 5.5	82
5.3: Calculated and observed lower yield strength for "low carbon trial heats" using Equation 5.2	87

Figure	Page
5.4: Calculated and observed tensile strength for Grade 300 and Grade 430 reinforcing steels using Equation 5.8	89
5.5: Calculated and observed tensile strength for "low carbon trial heats" using Equation 5.7	92
5.6: Calculated and observed % elongation at fracture for Grade 300 and Grade 430 reinforcing steels using Equation 5.11	94
5.7: Calculated and observed % Luder strain for Grade 300 and Grade 430 reinforcing steels using Equation 5.14	97
5.8: Calculated and observed strain hardening exponent n for Grade 300 and Grade 430 reinforcing steels using Equation 5.18	100
5.9: Calculated and observed strain hardening coefficient k for Grade 300 and Grade 430 reinforcing steels using Equation 5.21	102
5.10: Calculated and observed strain ageing index ΔY for Grade 430 reinforcing steel using Equation 5.22	105

LIST OF TABLES

Table	Page
2.1: Sample size of deformed reinforcing bars used in the analysis	4
2.2: Statistical means and ranges of the chemical composition for Grade 300 and Grade 430 samples	6
3.1: Comparison of linear regression equations of lower yield strength for machined specimens	24
3.2: Statistical means and ranges of lower yield strength for Grade 300 reinforcing steel	28
3.3: Statistical means and ranges of lower yield strength for Grade 430 reinforcing steel	28
3.4: Nominal and effective cross section area of lab deformed bars	29
3.5: Comparison of mean lower yield strength of lab deformed bars which fractured inside/outside the gauge length	33
3.6: Comparison of mean tensile strength of lab deformed bars which fractured inside/outside the gauge length	43
3.7: Statistical means and ranges of tensile strength for Grade 300 and Grade 430 reinforcing steels	43
3.8: Statistical means and ranges of % elongation at fracture for Grade 300 and Grade 430 reinforcing steels	48
3.9: Statistical means and ranges of % Luder strain for Grade 300 and Grade 430 reinforcing steels	52
3.10: Statistical means and ranges of strain hardening exponent and coefficient for Grade 300 and Grade 430 reinforcing steels	53
3.11: Comparison of strain hardening rates between current and previous grades of reinforcing steel	56
3.12: Statistical means and ranges of ΔY , ΔU and ΔEI for Grade 300 and Grade 430 reinforcing steels	62
3.13: Statistical means and ranges for parameters of Grade 300 reinforcing steel	64
3.14: Statistical means and ranges for parameters of Grade 430 reinforcing steel	65

Table	Page
4.1: Multiple linear regression printout 1	70
4.2: Multiple linear regression printout 2	71
4.3 t values extracted from t-test tables	72
5.1 Statistical means and ranges for variables of Grade 300 reinforcing steel examined by multiple linear regression	75
5.2 Statistical means and ranges for variables of Grade 430 reinforcing steel examined by multiple linear regression	76
5.3: Statistical means and ranges for variables of combined grades examined by multiple linear regression	77
5.4: Summary of significant equations from multiple linear regression analysis	109

CHAPTER 1

INTRODUCTION

1.1 GENERAL

Concrete is strong in compression but weak in tension. In reinforced concrete structure, steel which is equally strong in compression and tension, is used to combine with concrete to improve the resistance of concrete to tensile force¹. The steel used to provide reinforcement in concrete structures is termed reinforcing steel.

In earthquake resistance reinforced concrete structures, reinforcing steel plays an extremely important role which is significantly more demanding than its basic function. This is due to the philosophy of capacity design of reinforced concrete structures to utilise both strength and energy dissipation characteristics of the system². The energy dissipation characteristics are utilised to absorb and dissipate the dynamic seismic loads to avoid brittle failures. This energy dissipation mechanism relies on the ductility of the structure in the post-elastic range. In the strong column-weak beam design concept, the ductility of the structure is ensured by the development of plastic hinges in beams adjacent to column-beam joints in preference to hinges forming in the columns^{2,3}.

The absorption and dissipation of energy by post-elastic deformation in plastic hinges depends almost entirely on the ductility of the reinforcing steel². Steels used for reinforcement in this structure should be capable of accommodating significant amounts of plastic strain without failure. Therefore, the ductility of reinforcing steel becomes an important requirement in the design of earthquake resistant reinforced concrete.

The plastic hinge behaviour of reinforced concrete members is also very dependent on the stress-strain characteristic of the reinforcing steel³. During a severe earthquake, strains in the steel of plastic hinge regions may increase beyond the

Luder strain, consequently strain-hardening occurs. This strain increase may lead to large strength increases, particularly if the strain hardening rate of the steel is high and if the steel has a short Luder strain which results in strain hardening occurring soon after yielding. Ideally, the Luder strain should be as large as possible so that the plastic strain is accommodated with a minimum of strain hardening.

As a result of this flexural overstrength, during subsequent earthquakes, plastic hinges may be formed in regions which have not been designed as such. Thus, relocation of the plastic hinge within the structure could give rise to an undesirable failure mode. In the design of seismic resisting concrete structures, an overstrength factor which is greater than unity is included in the calculation of the steel stress at the beam plastic hinges to take into account the possibly large increase in flexural strength.

Strain ageing of reinforcing steel also has a significant effect on the properties of seismic reinforced concrete structures². Strain ageing of the longitudinal reinforcing steel at plastic hinges subsequent to the first formidable seismic loading can increase the flexural strength at the plastic hinges as a result of the increase in yield strength of the steel during the ageing process. The flexural overstrength brings the same effect as when strain hardening of steel occurs, i.e. causing the plastic hinges to form at alternative and undesirable regions in the structure during subsequent earthquakes.

Cold bent reinforcing bars in the form of standard bends, returns or hooks contained in most regions in reinforced concrete structure will strain age during service at ambient temperature⁴. As a result of strain age embrittlement, these strain aged regions will be susceptible to brittle failure, which may cause catastrophic fracture of the structure. It is therefore, very important to understand the effect of strain ageing on the mechanical properties of reinforcing steel used in earthquake resistant reinforced concrete structures. Unfortunately, information regarding strain hardening and strain ageing of reinforcing steels are not specified in appropriate standards, nor is the data on Luder strain.

1.2 SCOPE OF THESIS

In view of the importance and demanding roles of reinforcing steels in earthquake resistant reinforced concrete structures, accurate information on tensile properties and quantitative data on strain hardening and strain ageing of the steels should be available, so that this information can be used at the design stage. This project was therefore carried out to investigate the distribution of mechanical properties, strain hardening rate and strain ageing index for NZS 3402 Grade 300 and the micro-alloyed Grade 430 reinforcing steels manufactured by Pacific Steel Ltd. The data obtained in the study can be used to determine the flexural over-strength factors of both grades of steel for use in the capacity design of reinforced concrete structures.

In the steelmaking process, production variations in chemical composition is unavoidable. Included in this variation is the residual element content of steels produced from scrap (as at Pacific Steel Ltd). The second aim of the project is to investigate any relationship between determined mechanical properties and the material chemical composition of Grade 300 and Grade 430 reinforcing steels by the use of Multiple Linear Regression technique. It was hoped that the effect of chemical composition variation on bar properties could be represented by simple linear equations. This data will be of value to Pacific Steel Ltd in predicting the mechanical properties of bars from production variations on chemical composition.

CHAPTER 2

EXPERIMENTAL PROCEDURE

2.1 TYPES AND SAMPLE SIZE OF REINFORCING STEEL

There are basically two grades of reinforcing steel being tested in this project, namely Grade 300 and the micro-alloyed Grade 430. Both grades of steel are manufactured by Pacific Steel Ltd based on the new standard of NZS 3402:1989⁵. In addition to this, there are 12 samples classified as "low carbon trial heats" included in the analysis.

The sample size of each grade of reinforcing steel and the "low carbon trial heats" steel are listed in Table 2.1.

Table 2.1: Sample size (number of heats) of deformed reinforcing bars used in the analysis

Grade	Diameter of bar (mm)						Total of samples
	10	12	20	24	28	32	
300	-	-	15	14	17	9	55
430	6	11	1	23	34	38	113
"low carbon trial heats"	-	-	3	3	3	3	12

The "low carbon trial heats" are micro-alloyed with vanadium and were produced to investigate the effect of carbon content and bar size on the mechanical properties. Data generated from these trial heats was grouped in Grade 430 data in the analysis since these steels are micro-alloyed. The overall data range provided by combining these two sets of data will be wider and this may improve the regression results.

2.2 CHEMICAL COMPOSITION OF REINFORCING STEEL

Grade 300 is similar to the Grade 275 steel. The carbon contents of these two grades are identical. Generally, Grade 430 reinforcing steel has higher carbon, manganese and silicon contents than Grade 300 and is micro-alloyed with 0.04% vanadium. Chemical analysis of Grade 300 samples shows a mean vanadium content of 0.0027%. As vanadium is not deliberately added in Grade 300 steel, it is a residual element. The chemical composition of the "low carbon trial heats" is generally similar to Grade 430. The only significant differences are a lower carbon content and slightly lower vanadium content in these trial heats.

The chemical composition of each bar (given in Appendix A) was determined by Pacific Steel Ltd who also supplied the individual cast analysis. Chemical composition determined from bars analysis was used in the regression analysis. Additional chemical analysis was carried out on all the 180 bars tested in the Materials Laboratory to ensure that the supplied chemical composition was being assigned correctly to the bars. A summary of the means and statistical ranges of the chemical composition for Grade 300 and Grade 430 sample investigated in this project is shown in Table 2.2.

Table 2.2: Statistical means and ranges of the chemical composition for Grade 300 and Grade 430 samples

Chemical Analysis	Grade 300 (Data Sets 55)				Grade 430 (Data Sets 113)			
	Mean	Standard Deviation	Maximum	Minimum	Mean	Standard Deviation	Maximum	Minimum
C	0.1858	0.0193	0.24	0.15	0.2000	0.0282	0.25	0.11
Mn	0.5651	0.0526	0.82	0.49	1.2542	0.0747	1.50	1.12
Si	0.1564	0.0325	0.33	0.11	0.3265	0.0354	0.44	0.23
S	0.0328	0.0075	0.044	0.019	0.0324	0.0065	0.047	0.011
P	0.0230	0.0089	0.05	0.009	0.0254	0.0078	0.049	0.011
Ni	0.1053	0.0136	0.16	0.090	0.1038	0.0150	0.16	0.08
Cr	0.0938	0.0227	0.15	0.05	0.0983	0.0195	0.15	0.05
Mo	0.0166	0.0026	0.023	0.011	0.0171	0.0035	0.027	0.011
Cu	0.3853	0.0629	0.56	0.24	0.3861	0.0772	0.75	0.24
Sn	0.0358	0.0055	0.056	0.02	0.0346	0.0045	0.049	0.026
V	0.0027	0.0009	0.007	0.001	0.0403	0.0038	0.056	0.033

2.3 TENSILE TESTING

For each of the supplied bars, data on lower yield strength, tensile strength and % elongation at fracture were supplied by Pacific Steel Ltd. These production test results were obtained from bars tested in the as rolled condition. These test results from Pacific Steel Ltd were duplicated, but since the individual results did not differ by much, they were represented by a single average value in the analysis.

Mechanical tests carried out in the Materials Laboratory of the Department involved tensile testing of the supplied material in the as rolled (deformed) condition and on standard tensile specimens machined from these bars. The dimensions of the standard tensile specimens are given in Appendix B.

The as rolled deformed bars were tested using the Baldwin universal testing machine. However, both ends of the deformed bar were machined to provide smooth gripping surfaces to avoid damage to the machine grips. Using a 75 mm gauge length extensometer attached to the bar gauge length, a load vs elongation curve was obtained. This data incorporated lower yield strength, Luder strain, tensile strength and % elongation at fracture. However, out of 180 deformed bars tested, 57 bars fractured outside the specimen gauge length. The locations of these fractures were observed to be at the upper machined end of the bars. As a result, there was no complete set of data on % elongation at fracture. It was therefore decided to exclude the remaining data in the analysis. Calculations of lower yield strength and tensile strength were based on the effective cross section areas of the deformed bars. Pacific Steel Ltd uses nominal areas for the determination of stress in their test specimens.

Standard tensile specimens were tested using the Satec testing machine. However, tensile specimens machined from deformed bars of diameter 10 mm and 12 mm were tested using the Instron testing machine. This enables a 25 mm gauge length extensometer to be used on these smaller tensile specimens which would not have been possible on the Satec testing machine.

In addition to recording the lower yield strength, tensile strength, % elongation at fracture and Luder strain, the strain hardening characteristics over the initial 8% plastic strain were determined from the stress vs strain graphs for the machined specimens. Determination of strain hardening exponent n and strain hardening coefficient k is described in Chapter 3.

To study the strain ageing characteristics of Grade 300 and Grade 430 reinforcing steel, one machined tensile specimen was pre-strained 5% and artificially aged at 100°C for three hours to determine the strain ageing index for each cast supplied. According to Hundy's equation⁶, this ageing is equivalent to natural ageing at 15°C at one year. Pre-straining of tensile specimens and the final testing of the artificially aged specimens were carried out on the Satec and Instron testing machines. From the continuous record of stress vs strain during the initial 5% prestrained of the specimen, a further set of data incorporating lower yield strength and Luder strain was obtained. Average values of lower yield strength and Luder strain from two tensile specimens was therefore used in the analysis.

Change in yield stress ΔY due to 5% strain ageing was determined from the recorded stress-strain curve based on the same specimen. However, changes in tensile strength ΔU and elongation ΔEl were determined by comparison with the initial tensile test result.

The tensile results produced from different types of specimen of all the supplied bars are given in Appendix C.

CHAPTER 3

DISTRIBUTION OF REINFORCING STEEL PROPERTIES

3.1 INTRODUCTION

Reinforcing steel conforming to the new standard NZS 3402:1989 has been commercially available and widely used over the past year. Grade 300 is similar to, but a slightly improved form of the previous Grade 275. However, Grade 430 is a completely new steel, micro-alloyed with vanadium and designed to provide a high yield strength range, high ductility and low strain age hardening⁵. In order to evaluate the mechanical properties of this steel, statistical studies were carried out based on extensive measured data.

For the two grades of reinforcing steel, the distribution of lower yield strength, tensile strength, % elongation at fracture, Luder strain at the yield point, strain hardening parameters and three parameters measuring the strain ageing index were determined based on data generated from tensile tests on machined specimens. The distribution of lower yield strength, tensile strength and % elongation at fracture were also determined from data supplied by Pacific Steel Ltd, for comparison with a similar set of data from deformed reinforcing bar tested in the Materials Laboratory at the University of Canterbury.

Linear regression analyses were carried out on different sets of data to investigate the correlation between the properties.

3.2 DEFINITION OF PARAMETERS

NZS 3101:1982⁸ assumes an elastic perfectly plastic stress-strain relationship for reinforcing steel which ignores the strength increase due to strain hardening. The idealised steel stress-strain curve is shown in Figure 3.1. This model is inappropriate

for capacity design consideration since the strength at the plastic hinge regions can be increased significantly by strain hardening at strains beyond the yield point.

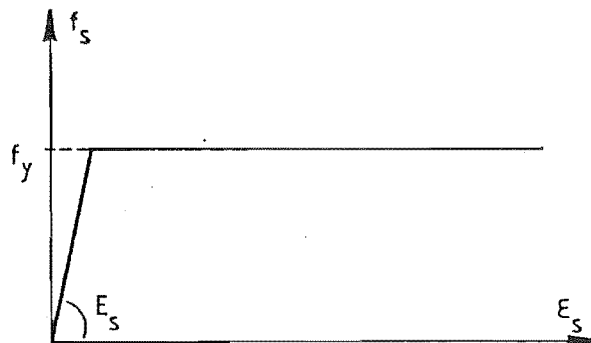


Figure 3.1: The idealized steel stress-strain curve

A typical stress-strain relationship for reinforcing steel used in reinforced concrete structures is shown in Figure 3.2. The corresponding properties investigated in this project are summarised below:-

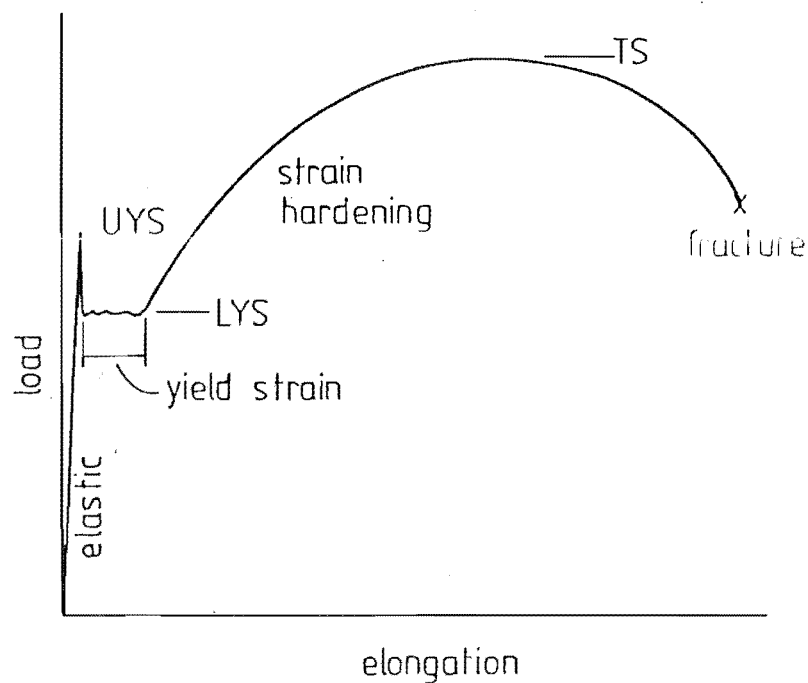


Figure 3.2: Schematic tensile load/elongation curve for a structural grade steel

3.2.1 Lower Yield Strength

As shown in Figure 3.2, the curve indicates an initial linear elastic portion up to a point. When this point is reached, a sudden drop of load occurs. This point is called the upper yield point and corresponds to the stress where plastic deformation is initiated. Following this drop the load fluctuates about an approximately constant value inhabiting Luder bands form and spread along the specimen gauge length. The lowest value measured is called the lower yield point. The stress at the lower yield point is referred to as the lower yield strength.

3.2.2 Luder Strain

Luder strain or yield point elongation refers to the elongation which occurs at the lower yield stress. This is the region of the stress-strain curve where the strain is approximately independent of stress. The extent of the Luder strain is generally a function of the strength of the steel. High-strength high-carbon steels usually have a much shorter Luder strain than lower-strength low-carbon steels. When the concrete structure is subjected to seismic loadings, Luder strain of the reinforcing steel will accommodate the post-elastic deformation which occurs at plastic hinges. The larger the Luder strain, the more plastic strain can be accommodated with a minimum of strain hardening.

3.2.3 Strain Hardening

The strain hardening region of a typical stress-strain curve of reinforcing steel commences when the stress increases at the end of the Luder strain extension. When steel strain hardens, increasing force must be applied in order that deformation may continue. The rate of stress increase over the uniform strain hardening region is governed by strain hardening rate which is a property of the material. With increasing strain, the rate of strain hardening diminishes due to the dynamic recovery processes within the metal.

In the design of seismic resisting reinforced concrete structures, a flexural over-strength factor is used in the calculation of stress at plastic hinges in order to account for any increase in strength due to the strain hardening of the reinforcing steel. The commencement of strain hardening is determined by the extent of the Luder strain. Hence, a large Luder strain will minimise the influence of strain hardening. Luder

strain and strain hardening rate are very important properties of reinforcing steel. However, this data is normally not specified in the relevant standards.

In the stress-strain model proposed by Mander et al⁹, a strain hardening modulus was used to define the strain hardening curve. The strain hardening modulus (E_{sh}) is the tangent to the strain-hardening curve at its starting point, as shown in Figure 3.3.

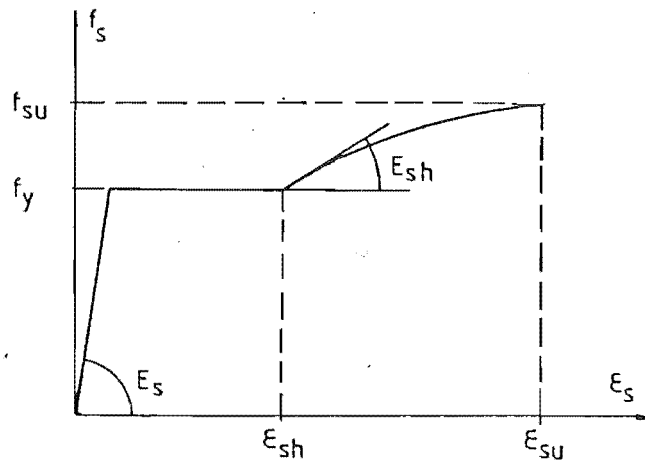


Figure 3.3: Mander's stress-strain model

The strain hardening modulus is equivalent to the strain hardening rate at the commencement of uniform strain hardening. However, this model does not consider the variation of strain hardening rates beyond the starting point of the strain hardening curve. This model also has a limitation in that the accuracy of the strain hardening modulus depends entirely on the accuracy in defining the starting point of the strain hardening curve and on the accuracy of drawing the tangent line through this point.

In this study, a different approach is employed to determine the strain hardening rate. In analysing the strain hardening characteristics, the tensile curve for the initial 8% strain was assumed to obey an exponential relationship of the form

$$\sigma = k\epsilon^n \quad \text{- Eqn. 3.1}$$

where,

σ = true stress

ϵ = true strain

k = strain hardening coefficient

n = strain hardening exponent.

Stresses at intervals of 1% strain for the initial 8% of strain were obtained from the stress-strain curve produced on the Satec testing machine. The corresponding true stress and true strain were calculated using Equations 3.2 and 3.3.

$$\sigma = f(1 + \lambda) \quad \text{- Eqn. 3.2}$$

$$\epsilon = \ln(1 + \lambda) \quad \text{- Eqn. 3.3}$$

where,

f = engineering stress

λ = engineering strain.

Equation 3.1 can be rewritten as

$$\ln \sigma = n \ln \epsilon + \ln k \quad \text{- Eqn. 3.4}$$

By plotting a graph of $\ln \sigma$ versus $\ln \epsilon$ and using the linear regression technique to obtain the best fit line, n and k are easily determined.

The strain hardening rate during plastic deformation is then given by

$$\frac{d\sigma}{d\epsilon} = nk(\epsilon)^{n-1} \quad \text{- Eqn. 3.5}$$

and can be determined if n and k are known. This method of determining the strain hardening rate is based on a large portion of the strain hardening curve to obtain the mean values of n and k . Therefore, the strain hardening rate determined in this way more accurately represents the true behaviour of the steel during plastic deformation.

3.2.4 Tensile Strength

When stressed to beyond the elastic limit ductile metals usually flow plastically, and because the metal strain hardens, increasing force must be applied in order that deformation may continue. Consequently, a maximum force is recorded at the point of plastic instability. Further increasing the strain beyond the point will cause a reduction in force or load. Eventually a point is reached in the tensile test where fracture occurs. The tensile strength is defined as the maximum recorded force divided by the tensile specimen's original cross-sectional area. The tensile strength is one of the reinforcing steel properties used to determine the flexural overstrength factor in the theoretical moment-curvature analysis³.

3.2.5 Elongation at Fracture

The elongation measured over the gauge length at fracture as a percentage of the original gauge length is used to represent the ductility of the steel. Ductility is also a function of the strength of steels in a similar way to Luder strain. In general, higher-strength high-carbon steels are less ductile than lower-strength low-carbon steels. In the design of reinforced concrete structures, it is essential for the safety of the structure that the reinforcing steel should be sufficiently ductile to undergo large plastic strains. The necessary elongation at fracture of steels is specified in the relevant standards.

3.2.6 Strain Ageing in Reinforcing Steel

When a specimen of low-carbon steel is strained to beyond the yield point elongation (Luder strain) and then unloaded followed by ageing at ambient (natural ageing) or elevated temperature (artificial ageing), the yield point re-emerges at a higher stress. This return of the yield point is referred to as strain ageing and is accompanied by an increase in tensile strength and a reduction in ductility. The new lower yield point is higher than the flow stress at the end of prestraining. Strain ageing is measured by values of ΔY , ΔU and ΔEI as shown in Figure 3.4. In addition to the changes in tensile properties, strain ageing also causes an increase in the fracture mode transition temperature which is referred to as strain age embrittlement.

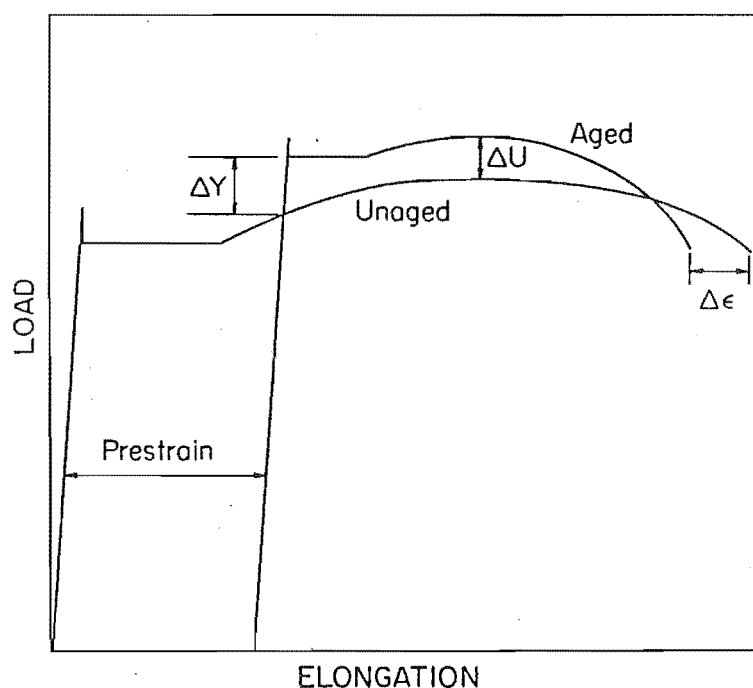


Figure 3.4: Effect of strain ageing on the load-elongation curve for low carbon steel.

Strain ageing is caused by the 'locking' of newly formed dislocations resulting from plastic straining. This 'locking' occurs by the segregation of interstitial atoms to these dislocation sites, and hence results in the re-emergence of the discontinuous yield point. It has been shown¹⁰ that "active" nitrogen (nitrogen not combined with elements which form stable nitrides) results in strain ageing at ambient and elevated temperatures, whereas carbon only contributes to strain ageing at elevated temperature.

An increase in the yield strength of the steel during the strain ageing process will increase the flexural strength at plastic hinges of the reinforced concrete structures. As a result, the energy absorbing deformation will occur at an alternative location within the structure. Strain age embrittlement associated with the strain aged region in concrete structures could also result in cleavage fracture of reinforcing bar causing catastrophic failure of the structure during a seismic event. It is, therefore, essential to make a quantitative assessment of the effect of strain ageing in reinforcing steel by means of measuring the strain ageing parameters. This was carried out in this

investigation. However, the change in fracture transition temperature was not determined, but this has been reported elsewhere¹¹.

3.3 DISTRIBUTION OF LOWER YIELD STRENGTH

Distributions of lower yield strength of Grade 300 reinforcing steel for different sets of data are shown in Figures 3.5, 3.6 and 3.7. As can be seen from the figures, the mean lower yield strength for machined specimen tested at the University of Canterbury (machined specimen), deformed bar tested at the University of Canterbury (lab deformed), and deformed bar tested by Pacific Steel (P.S. deformed) are 339.8 MPa, 310.4 MPa and 329 MPa respectively. Figures 3.8, 3.9 and 3.10 show the distributions of lower yield strength of Grade 430 reinforcing steel produced from the different sets of data, with the respective means of 466.7 MPa, 438.3 MPa and 467.5 MPa. The small cluster of data observed at the lower 'tail' of the distributions results from 12 samples of special low carbon heats produced for trial purposes. These samples are of lower carbon content than the normal Grade 430 steel and the lower yield strengths fall in the range between 370 MPa and 430 MPa.

Simple linear regression was used to investigate the variation of lower yield strength between different sets of data. The regression analysis carried out based on Grade 300 data is of low significance level and can be misleading. This is because of the small number of data sets (55) spreading over a relatively small range of values, as shown in Figure 3.11. The regression line obtained from the analysis of Grade 430 data does not compare well with the expected correlation as shown in Figure 3.12. When the data from Grade 300 bars is combined with that for the Grade 430 bars, the combined data set is larger and the range of values is wider. Consequently, the accuracy of the regression analysis is substantially improved as shown in Table 3.1 and Figure 3.13. It is justifiable to use the combined data because the regression analysis was carried out mainly to investigate the correlation between different test specimen geometry and not between grades.

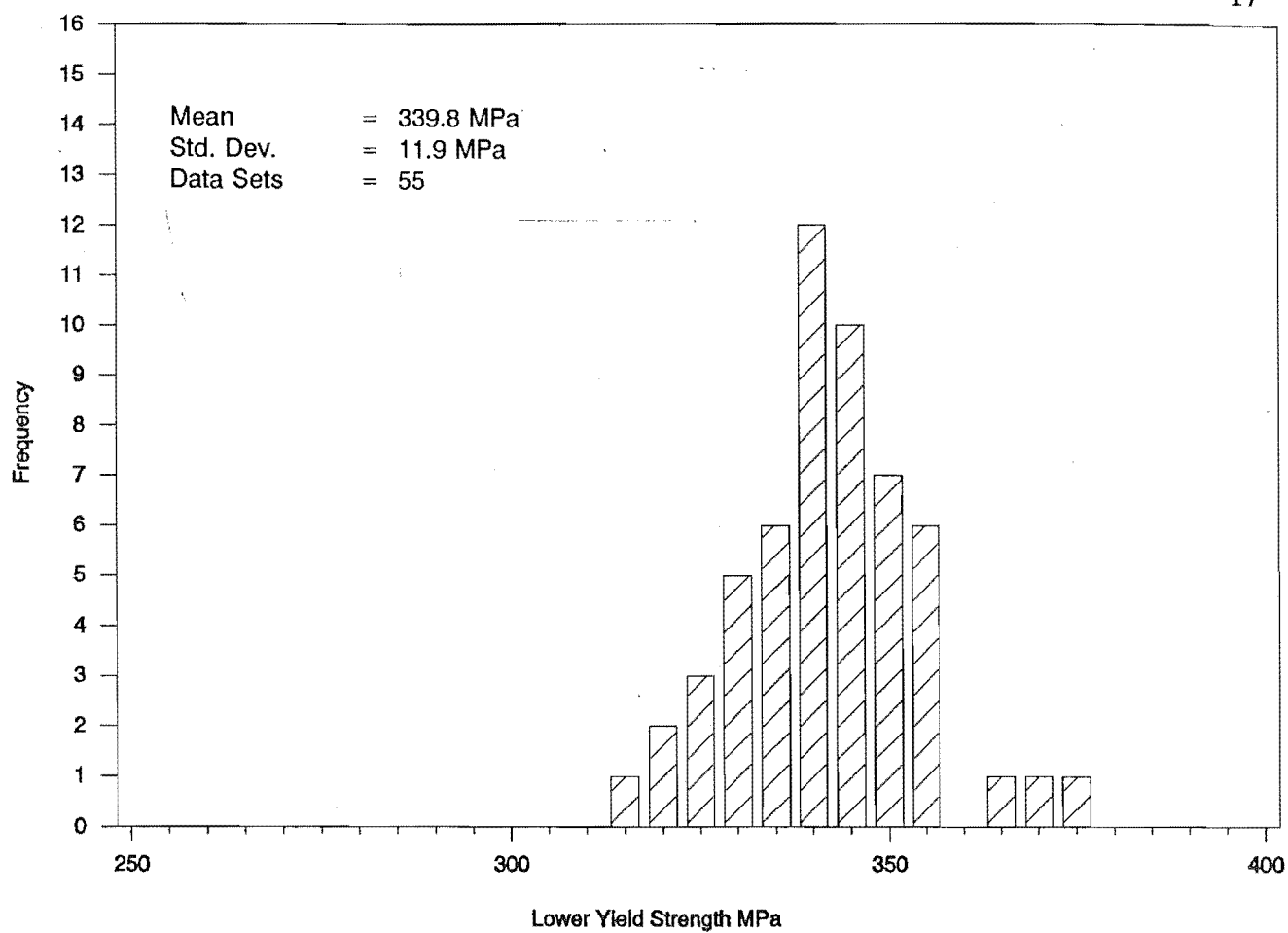


Figure 3.5: Distribution of lower yield strength of Grade 300 machined specimen data

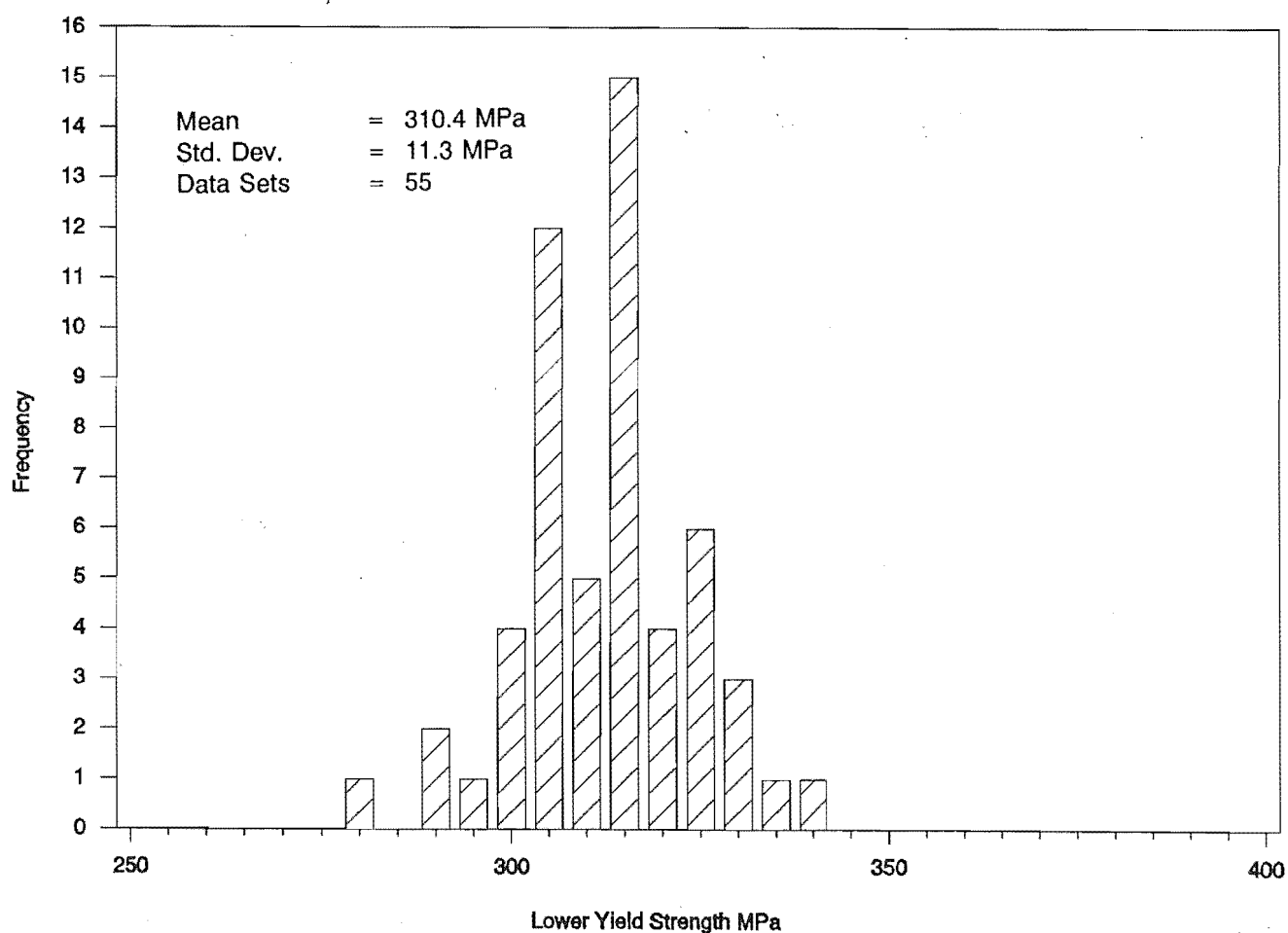


Figure 3.6: Distribution of lower yield strength of Grade 300 lab deformed data

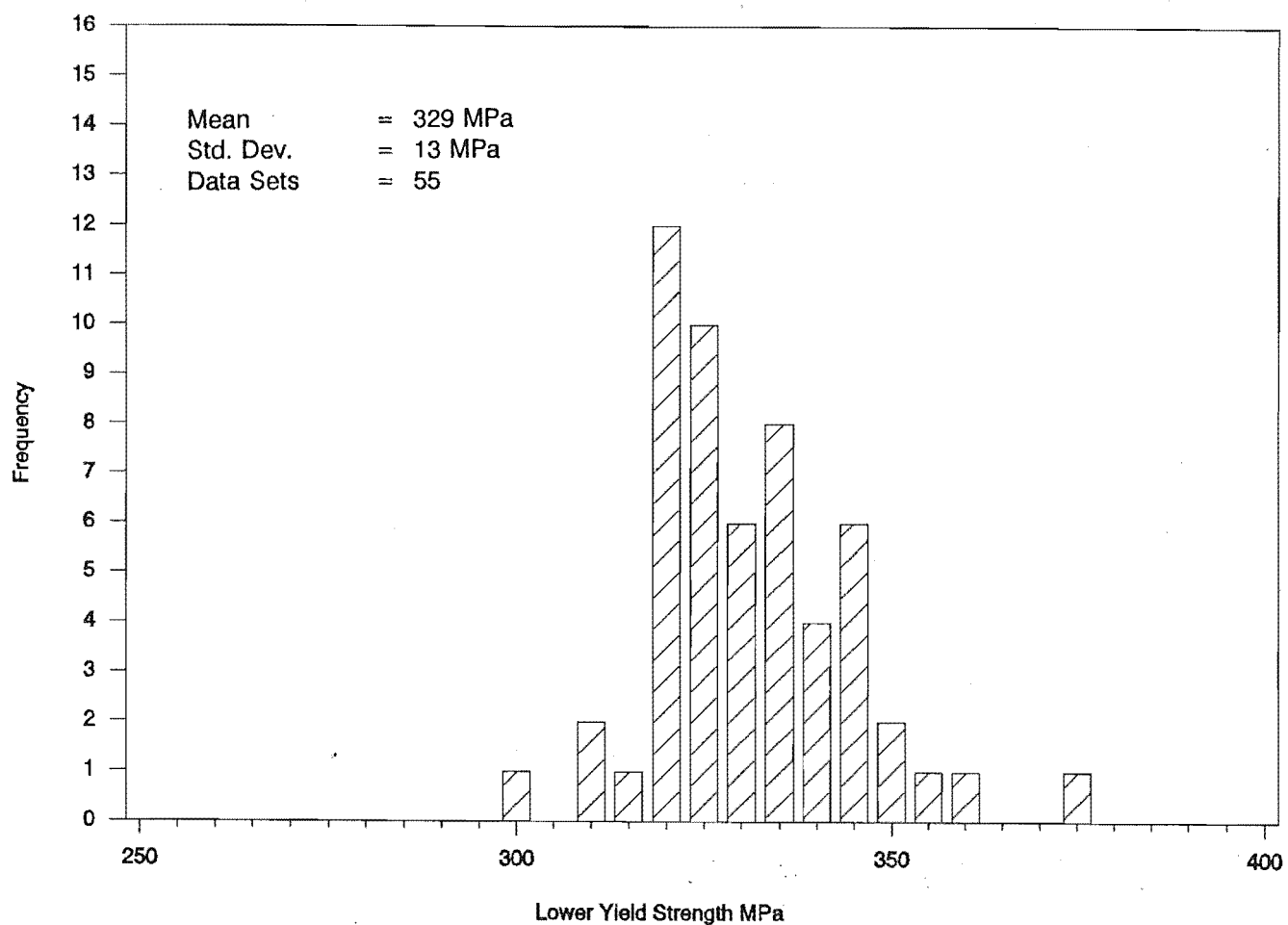


Figure 3.7: Distribution of lower yield strength of Grade 300 P.S. deformed data

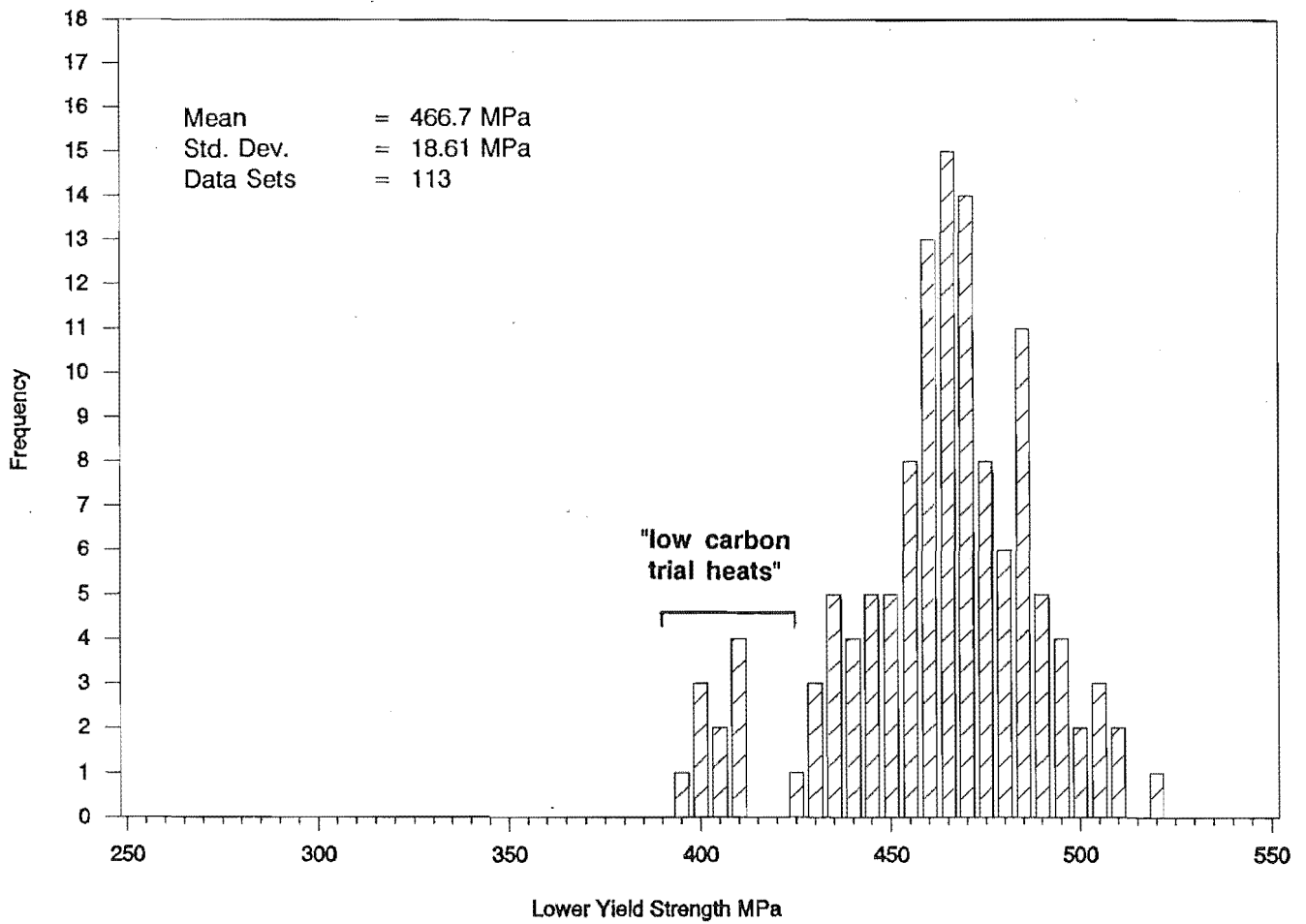


Figure 3.8: Distribution of lower yield strength of Grade 430 machined specimen data

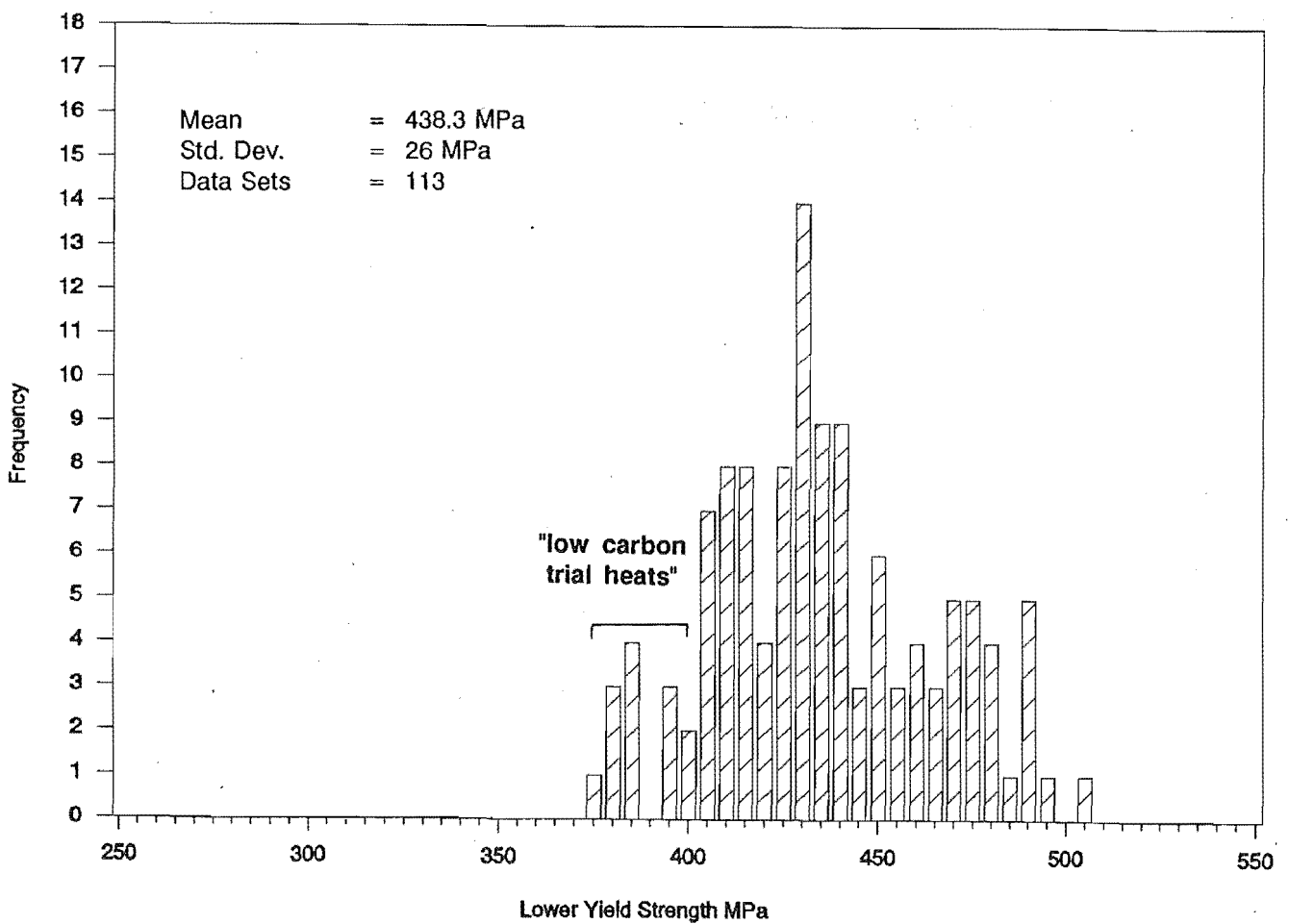


Figure 3.9: Distribution of lower yield strength of Grade 430 lab deformed data

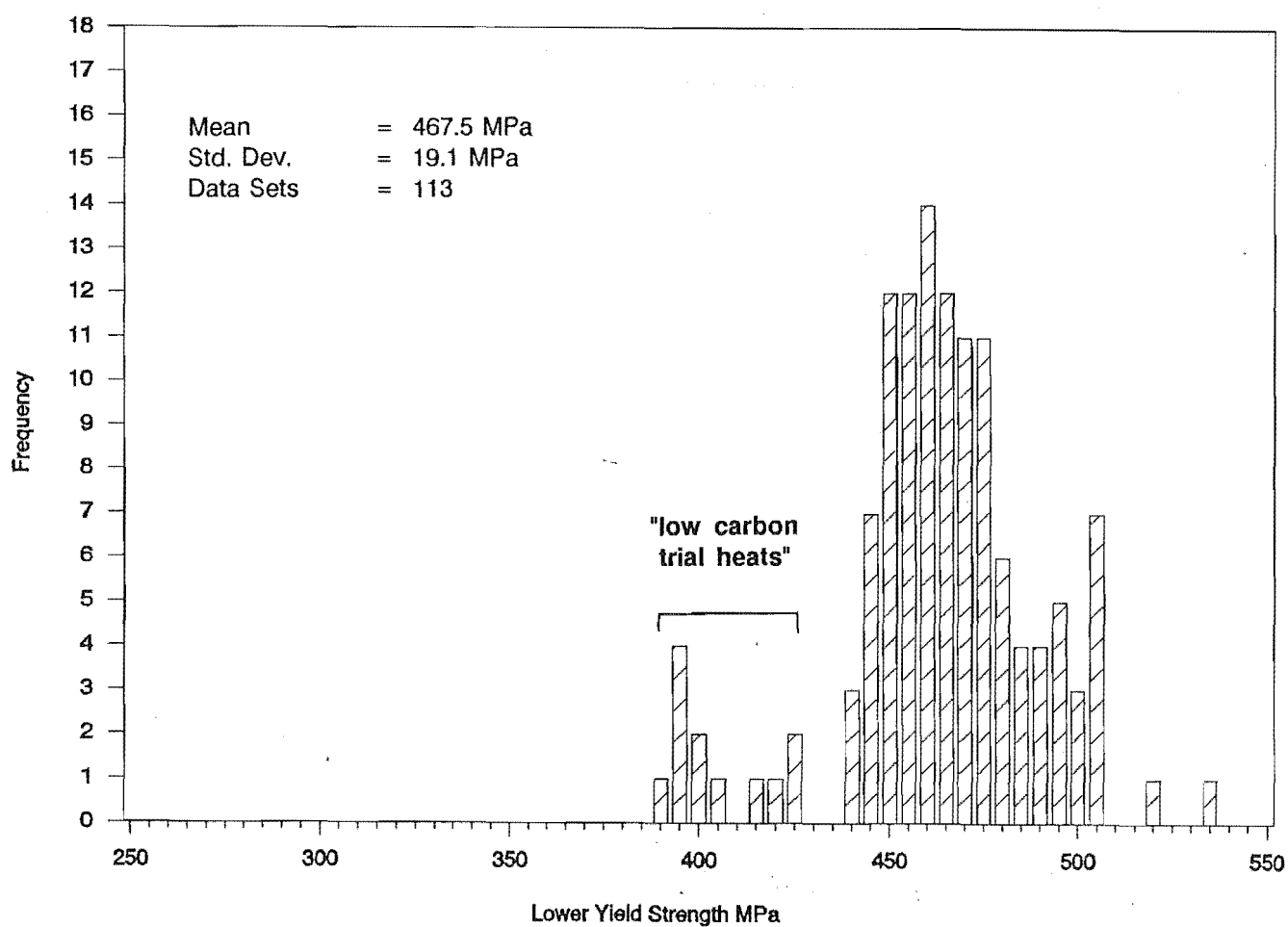


Figure 3.10: Distribution of lower yield strength of Grade 430 P.S. deformed data

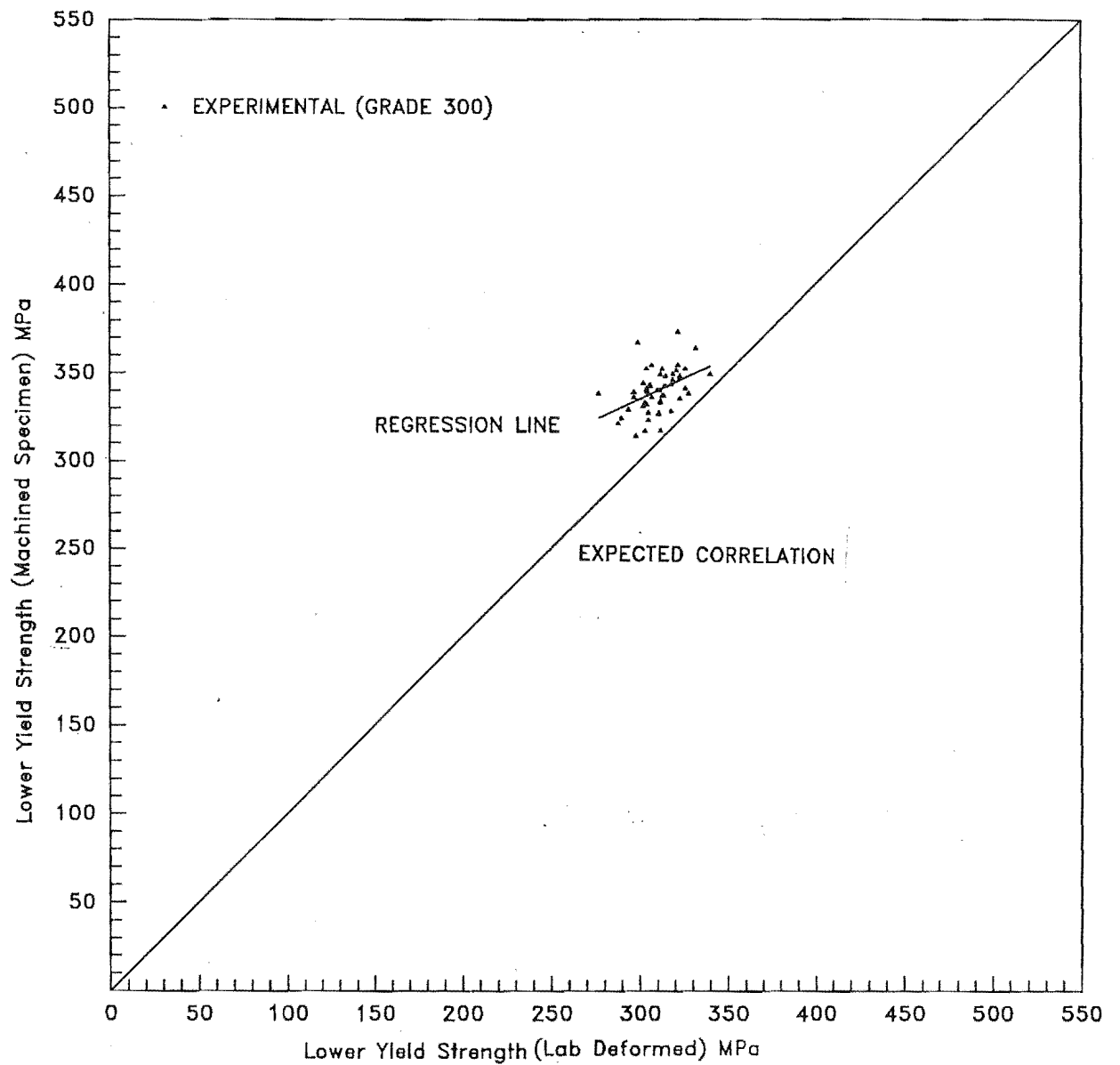


Figure 3.11: Graph of lower yield strength of machined specimen vs lab deformed (Grade 300)

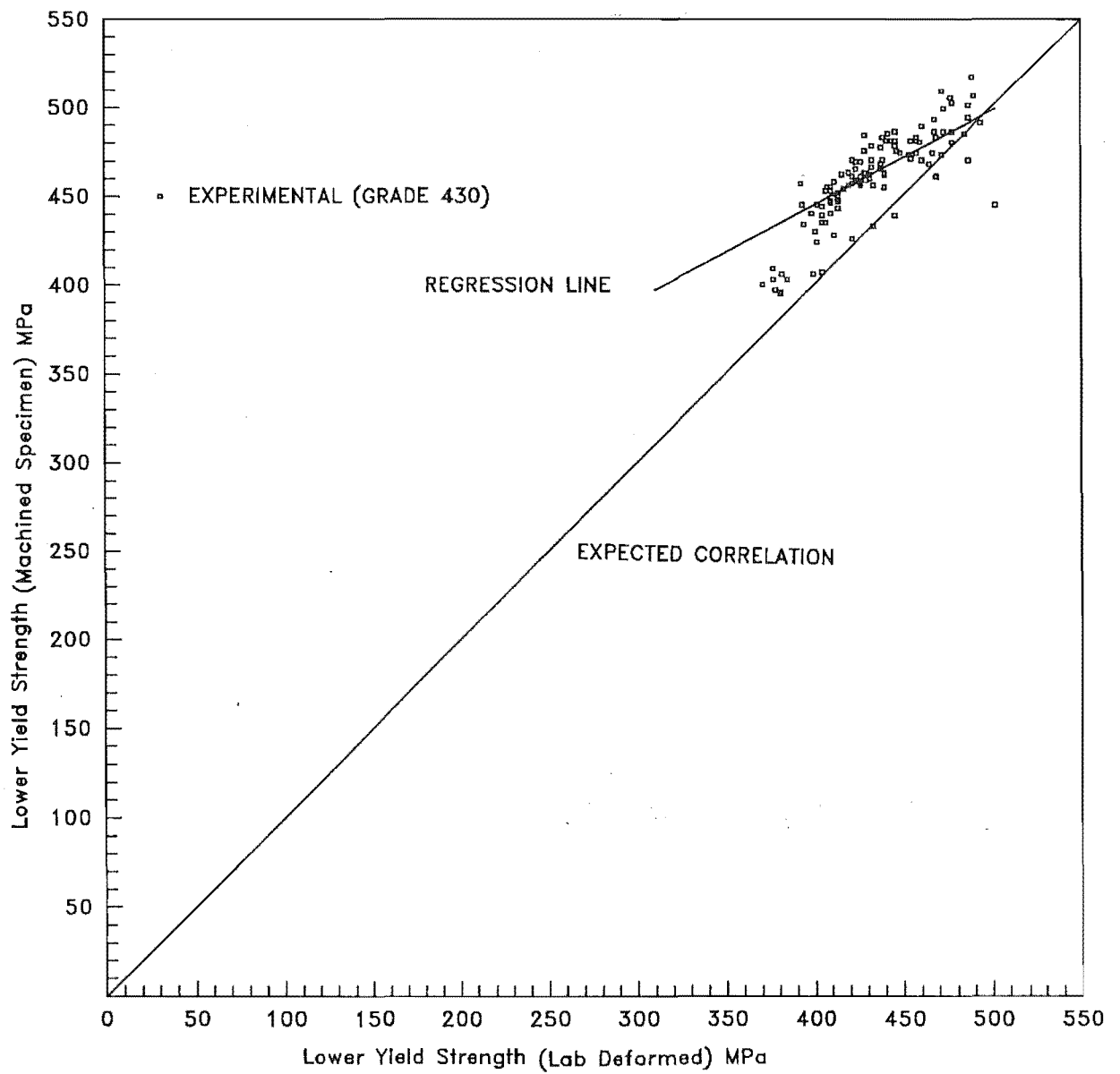


Figure 3.12: Graph of lower yield strength of machined specimen vs lab deformed (Grade 430)

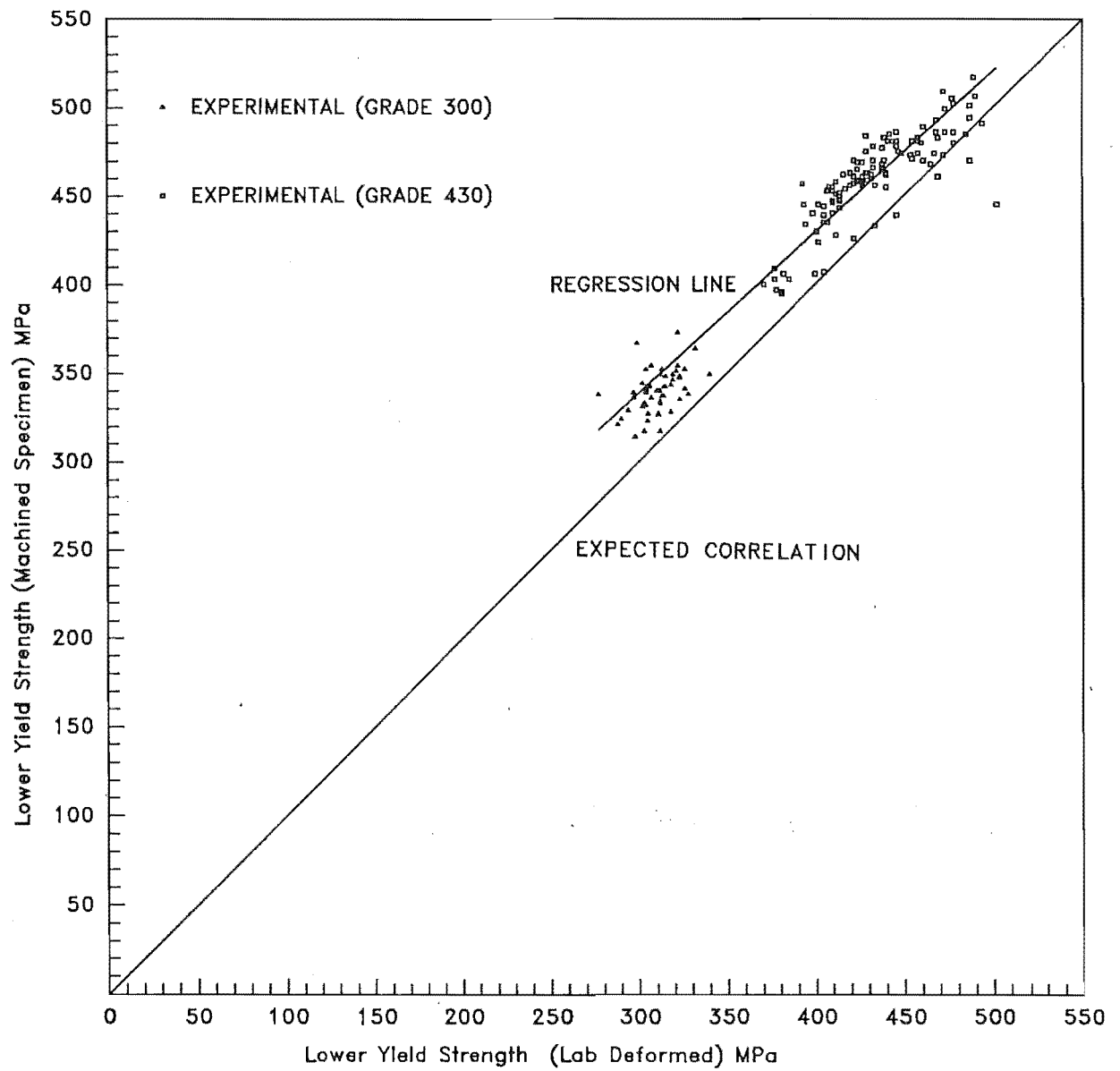


Figure 3.13: Graph of lower yield strength of machined specimen vs lab deformed

Table 3.1: Comparison of linear regression equation of lower yield strength of machined specimens

Grade	Data Sets	Linear Regression Equations	Eqn. t Value	Eqn. Significance Level
300	55	$LYS_{mach} = 0.466 LYS_{def} + 195$	3.61	0.1%
430	125	$LYS_{mach} = 0.525 LYS_{def} + 235$	10.8	>> 0.00002%
Combined	180	$LYS_{mach} = 0.908 LYS_{def} + 66$	37.11	>> 0.00002%

Note: LYS_{mach} = lower yield strength of machined specimen

LYS_{def} = lower yield strength of lab deformed bar

Figure 3.13 reveals that lower yield strength for machined specimens are greater than those of the lab deformed bars. Whereas, regression of lower yield strength based on machined specimen data and P.S. deformed data yielded a regression line that agrees very well with the expected correlation as shown in Figure 3.14. The regression line is represented by Equation 3.6.

$$LYS_{mach} = 0.892 LYS_{PS} + 48 \quad - \text{Eqn. 3.6}$$

where,

LYS_{PS} = lower yield strength of Pacific Steel deformed bar.

Regression analysis carried out on the two sets of data from deformed bars reveals that lower yield strengths recorded by Pacific Steel Ltd are generally greater than those for similar bars tested in the Materials Laboratory, see Figure 3.15. Assuming the parts of the regression line associated with Grade 300 and Grade 430 data are respectively parallel to the expected correlation, differences of 20 MPa and 30 MPa can be estimated.

For Grade 300 steel, the distribution produced from lab deformed data (Figure 3.6) has the lowest mean value of 310.4 MPa. The differences in mean values between Figure 3.6 and data produced from machined specimens (Figure 3.5) and data produced by Pacific Steel (Figure 3.7) are 29.4 MPa and 18.6 MPa respectively. The

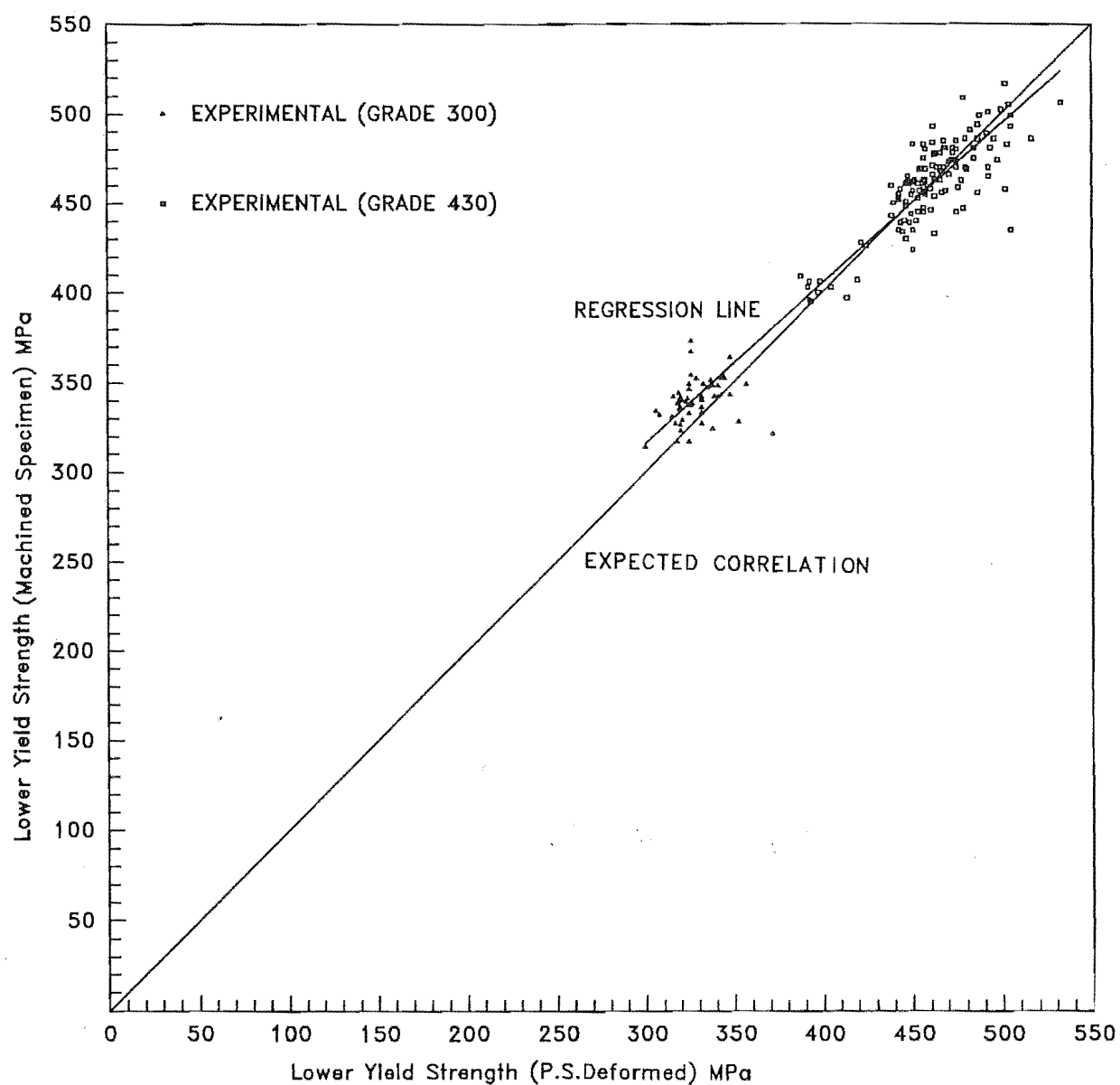


Figure 3.14: Graph of lower yield strength of machined specimen vs P.S. deformed

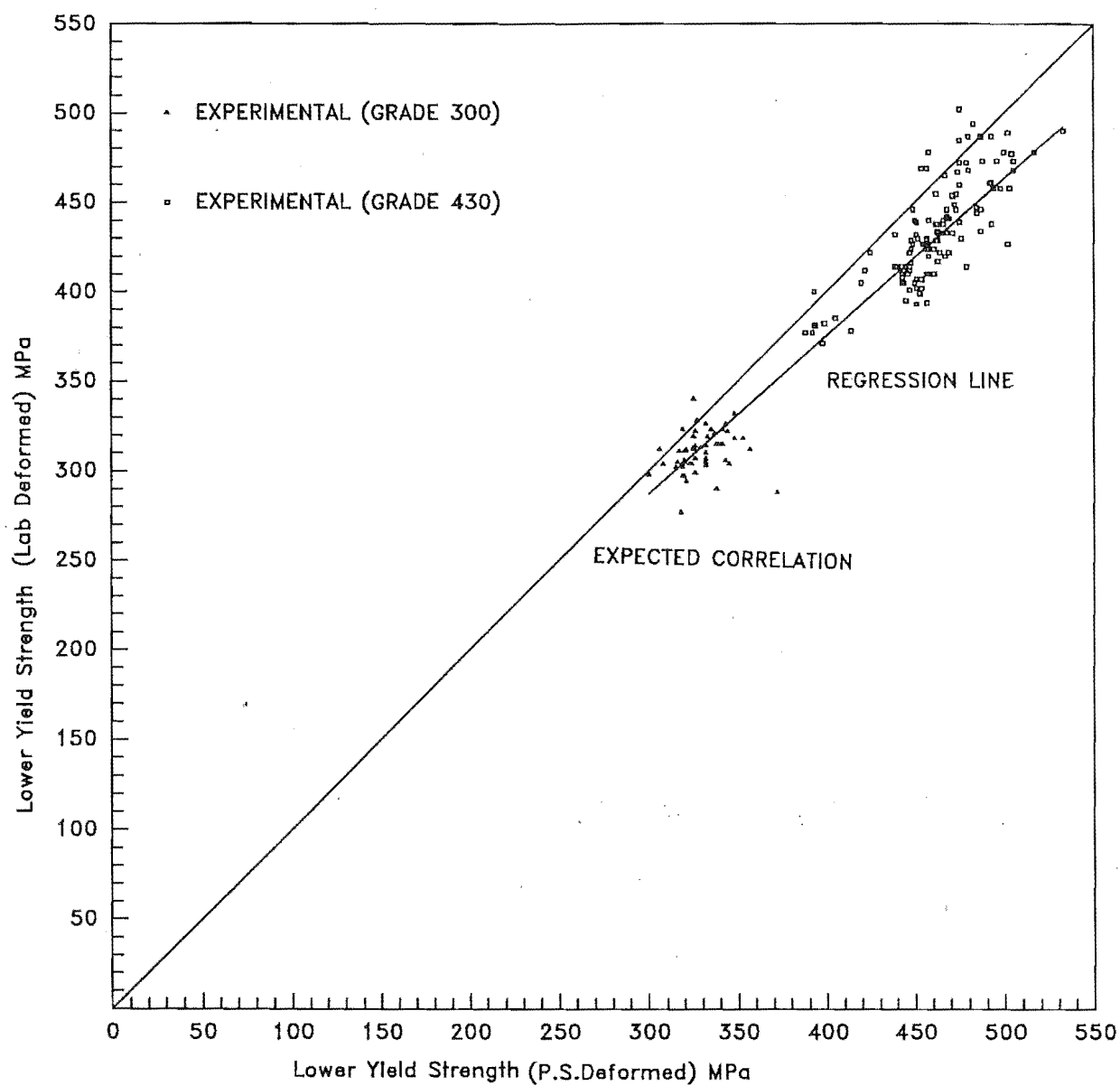


Figure 3.15: Graph of lower yield strength of lab deformed vs P.S. deformed

latter figure is consistent with the difference of 20 MPa estimated from Figure 3.15. The difference in mean values between Figures 3.5 and 3.7 is 10.8 MPa. Generally, these distributions do not appear to be normal, probably because of the small number of data sets examined.

Comparison of Figures 3.8 and 3.10 for Grade 430 steel shows that the distributions for these data sets are closely comparable. The difference in mean is less than 1.0 MPa. However, distribution produced from lab deformed data shows a mean 28.4 MPa less than that shown in Figure 3.8. When comparing Figures 3.9 and 3.10, P.S. deformed data is found to have a mean 29.2 MPa higher than the lab deformed data. This figure agrees well with the 30 MPa difference estimated from Figure 3.15.

Tables 3.2 and 3.3 show the comparison of the statistical means and the ranges of lower yield strengths with the properties specified in NZS 3402:1989. It should be noted that the statistical data of all parameters in the study for Grade 430 steel were determined based on data from the 113 samples only. This is because the mean values of the parameters, particularly lower yield strength and tensile strength, were found to be affected substantially if data from the "low carbon trial heats" were included in the analysis.

Table 3.2 shows that all the lower yield strength data for Grade 300 steel supplied by Pacific Steel Ltd and generated in the Materials Laboratory were found to lie within the specified range for yield strength. When considering the characteristic strength, the lower characteristic strength determined from lab deformed data is less than the specified value and the upper characteristic strength of machined specimen data is 4.4 MPa higher than the specified value. For Grade 430 steel, lab deformed data does not fulfil the specified minimum yield strength and the lower characteristic strength. The differences are 17 MPa and 34.5 MPa respectively. However, machined specimen data and P.S. deformed data generally agree with the specified values.

Table 3.2: Statistical means and ranges of lower yield strength for Grade 300 reinforcing steel (Data Sets 55)

Source	Mean MPa	Standard Deviation MPa	Yield Strength		Characteristic Strength	
			Minimum MPa	Maximum MPa	Lower MPa	Upper MPa
Specified Properties (NZS 3402:1989)			275	380	300.0	355.0
Machined Specimen	339.8	11.90	314	373	320.2	359.4
Lab Deformed	310.4	11.33	277	340	291.8	329.0
P.S. Deformed	329.0	13.00	300	372	307.5	350.5

Table 3.3: Statistical means and ranges of lower yield strength for Grade 430 reinforcing steel (Data Sets 113)

Source	Mean MPa	Standard Deviation MPa	Yield Strength		Characteristic Strength	
			Minimum MPa	Maximum MPa	Lower MPa	Upper MPa
Specified Properties (NZS 3402:1989)			410	520	430	500
Machined Specimen	466.7	18.61	424	517	436	497.3
Lab Deformed	438.3	26.00	393	502	395.5	481.1
P.S. Deformed	467.5	19.1	439	533	436.1	498.9

Note: The Lower and Upper characteristic strength values are respectively the expected 5 and 95 percentiles for the distribution of tested yield strength.

In both grades of steel, statistical data of machined specimens is in good agreement with P.S. deformed data, but data of lab deformed bars is lower than the other two sets. The differences may have resulted from the following factors.

(1) Variation in the area of cross section of the bar

As mentioned earlier in Chapter Two, Pacific Steel Ltd calculated the stress based on the nominal areas of the deformed bars. Tensile test results obtained in the Materials Laboratory are based on the effective (actual) cross-sectional areas (ECSA) of the deformed bars, calculated from individual bar weights using Equation 3.7.

$$\text{ECSA (mm}^2\text{)} = \frac{\text{weight of bar (kg)}}{\text{length of bar (mm)}} \times 127388.54 \quad - \text{Eqn. 3.7}$$

Previous investigations¹² have shown that the measured cross-sectional areas of reinforcing bars deviate from the nominal areas. Figures 3.16, 3.17 and 3.18 show variations of effective cross section areas of all the reinforcing bars tested in the laboratory. Table 3.4 shows the comparison between the nominal and the mean effective cross section area and the associated reduction. It should be noted that only six 10 mm bars were tested and the mean calculated could easily be affected by an extreme value.

Table 3.4: Nominal and effective cross section area of lab deformed bars

Bar Diameter <i>mm</i>	No. of Bar <i>Tested</i>	Cross Section Area <i>mm</i> ²		% Reduction
		Nominal	Effective	
10	6	78.54	79.30	- 0.9
12	11	113.10	111.43	1.5
20	19	314.16	311.64	0.8
24	40	452.40	449.74	0.6
28	54	615.75	612.45	0.6
32	50	804.25	795.24	1.1

Figures 3.16, 3.17 and 3.18 show that the effective cross-sectional areas of different sizes of reinforcing bar are generally smaller than the nominal cross-

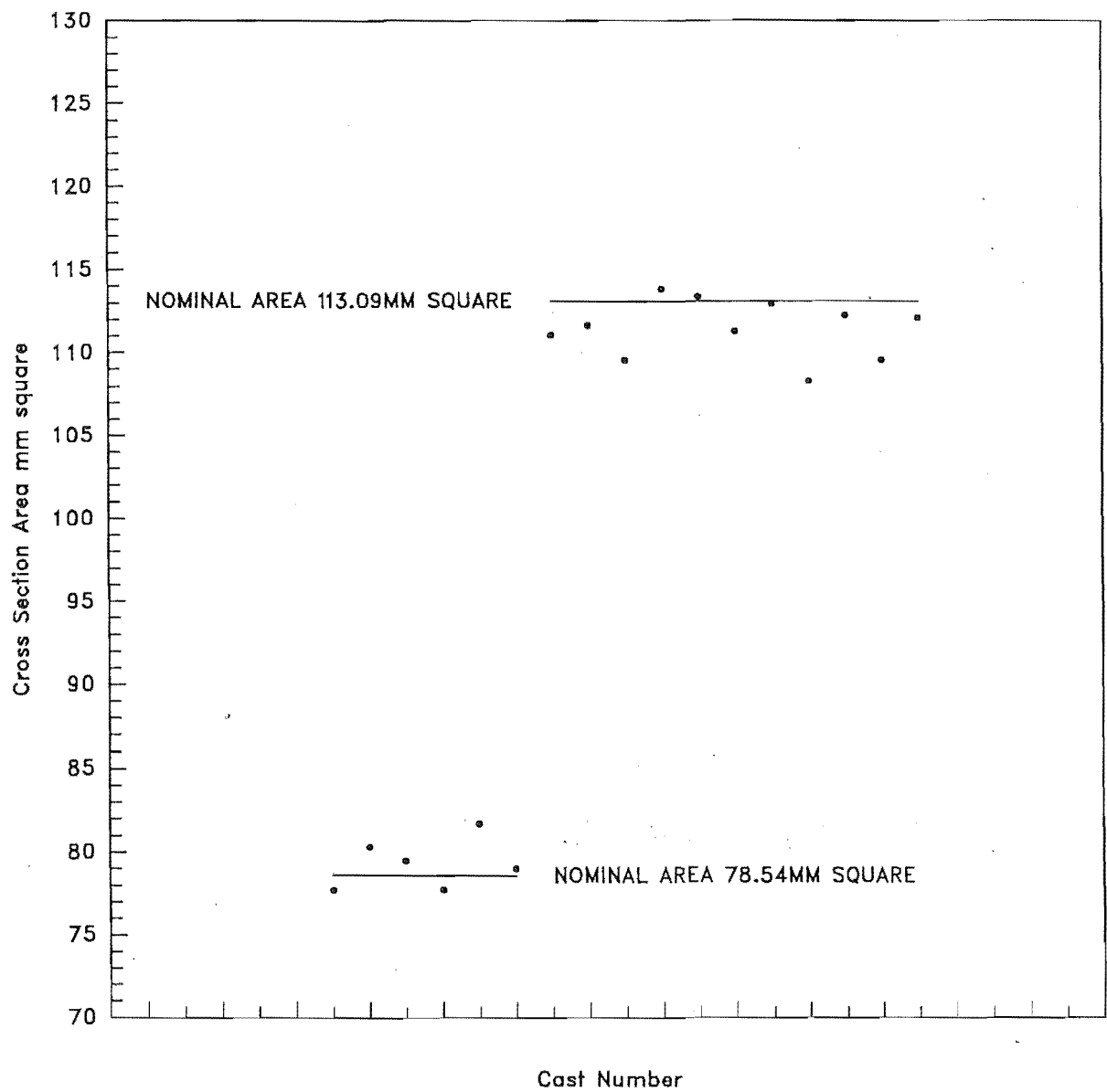


Figure 3.16: Variation of cross section areas of 10 mm and 12 mm lab deformed bars

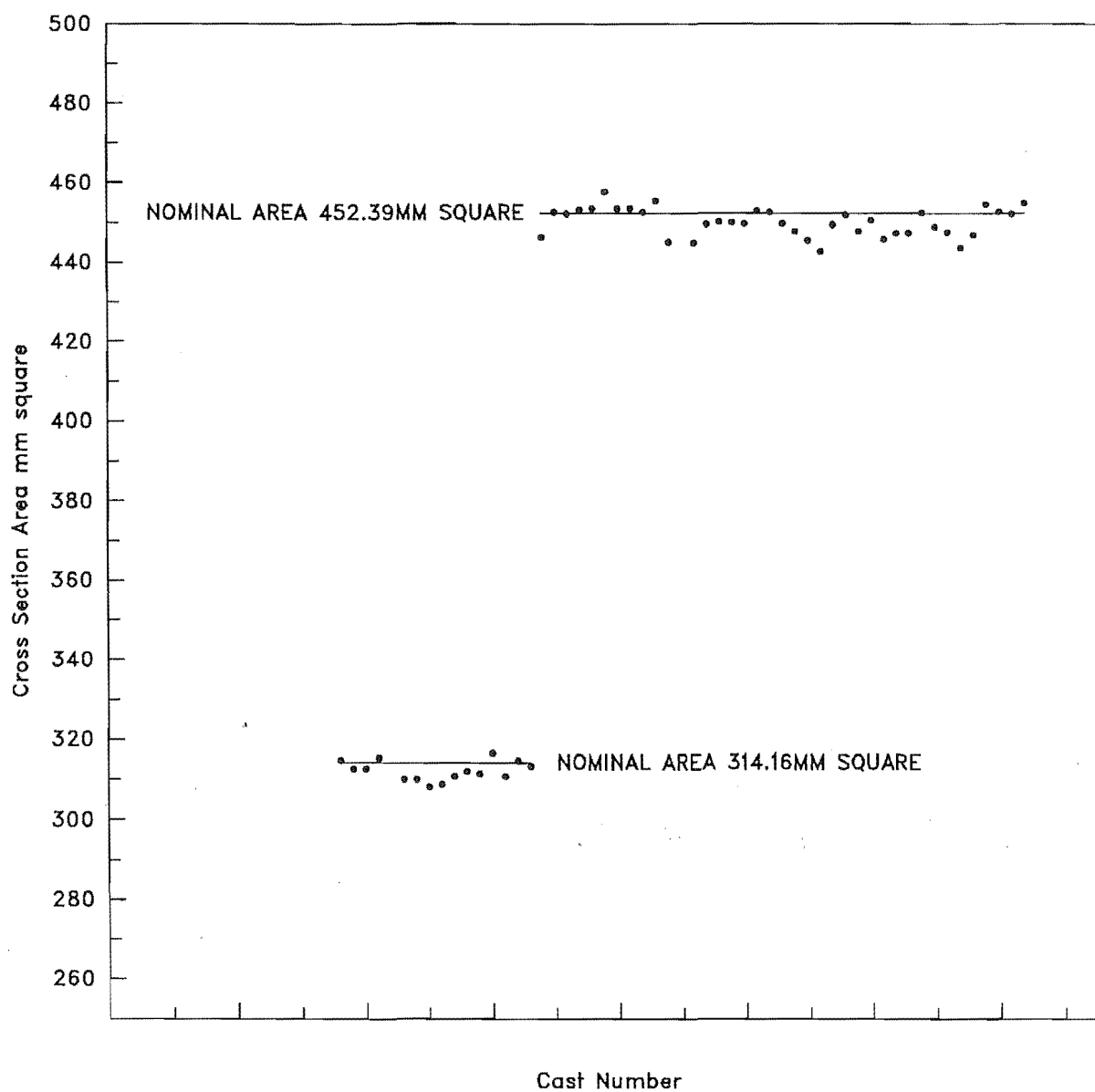
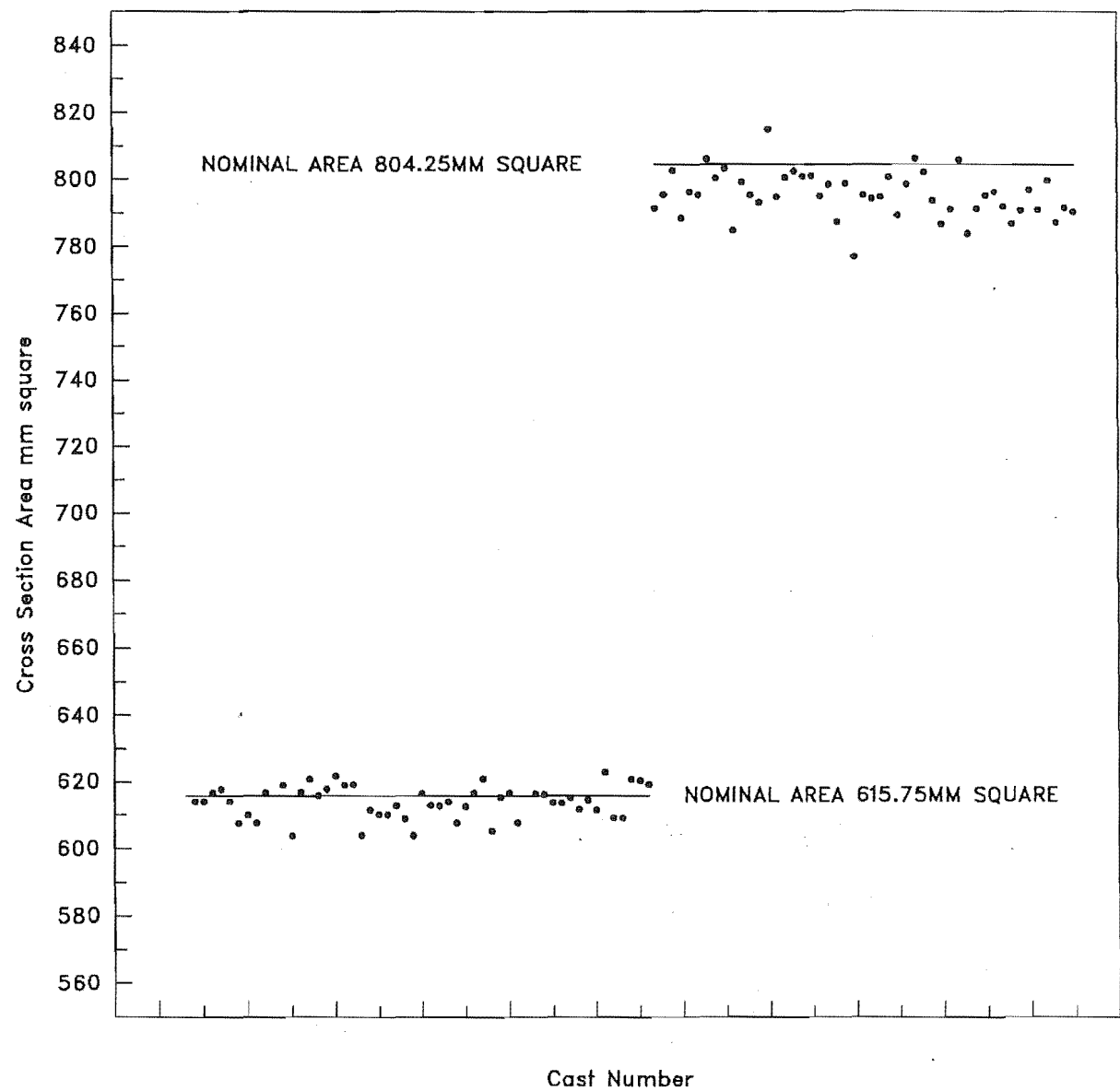


Figure 3.17: Variation of cross section areas of 20 mm and 24 mm lab deformed bars



sectional areas. This suggests that determination of stress based on effective cross-sectional area will result in a higher stress value. However, this contradicts the regression result shown in Figure 3.15. By considering all bars above 12 mm diameter (see Table 3.4), an average of approximately 1% in reduction of area can be obtained. This will correspond to an increase in stress of 1% if effective cross-sectional areas are used in the calculation of stress.

(2) Effect of test bar shape

As many as 57 deformed bars tested in the laboratory fractured outside the gauge length. All the fractures were located at the top machined end of the bars where the bar ribs were removed to avoid grip damage. This phenomenon could probably be due to misalignment of test pieces. Slipping of test bars would occur and this could affect the axiality of loading. In addition, any sudden reduction of area at the machined ends would correspond to a point of stress concentration. As a result, fracture would occur at these points at a lower applied stress.

However, it has been shown¹³ that the lower yield strength is relatively unaffected by test piece geometry and the testing technique. The relatively large distortion associated with the Luder's extension allows the test piece to accommodate itself to small amounts of non-axiality of loading, and the Luder's band is itself a stress concentration. Table 3.5 shows that there is only a marginal difference in mean values of lower yield strength between deformed bars which fractured outside the gauge length and those fracturing inside the gauge length.

Table 3.5: Comparison of mean lower yield strength of bars which fractured inside/outside the gauge length (G.L.)

Grade	Bars Fractured Inside G.L.		Bars Fractured Outside G.L.	
	Data Sets	Mean LYS, MPa	Data Sets	Mean LYS, MPa
300	35	311.4	20	308.9
430	88	433.0	37	428.6

(3) Effect of Strain Rate

It has been demonstrated¹³ that rapid loading can cause a significant increase in the lower yield strength of steel. Mander⁹ shows that the effect of a fast strain rate on the yield strength can be included by modifying the quasi-static value by a dynamic magnification factor as follows:-

$$(f_s)_{\text{dyn}} = D_s f_s \quad - \text{Eqn. 3.8}$$

where,

$(f_s)_{\text{dyn}}$ is the yield strength measured at a fast strain rate

f_s is the yield strength measured at quasi-static strain rate, assume strain rate of 0.00001/sec

D_s is a dynamic magnification factor.

The dynamic magnification of steel strength is assumed to be of the form of an equation suggested by Bodner and Symonds¹⁴.

$$D_s = d \left[1 + \left| \frac{\dot{\epsilon}}{\dot{\epsilon}_s} \right|^{\frac{1}{n}} \right] \quad - \text{Eqn. 3.9}$$

where,

d is a constant

$\dot{\epsilon}$ is the strain rate

$\dot{\epsilon}_s$ is an experimentally defined parameter equal to the rate of strain when the material strength doubles

n is a constant.

Regression analysis of the experimental data reported by the ACI committee 439¹⁵ carried out by Mander yielded values for the parameters d , $\dot{\epsilon}_s$ and n . The resulting dynamic magnification equation for low carbon steel under tensile loading was found to be

$$D_s = 0.953 \left[1 + \left| \frac{\dot{\epsilon}}{700} \right|^{\frac{1}{6}} \right] \quad - \text{Eqn. 3.10}$$

It is likely that production testing in a steel works will be carried out at a higher strain rate than is common in a teaching laboratory. Pacific Steel Ltd uses a higher strain rate in its tests than those carried out on the Baldwin universal testing machine in the Materials Laboratory. The strain rate used in the Satec testing machine to test the tensile specimens is also considerably higher than the rate used in the Baldwin universal testing machine. The discrepancy in lower yield strength of lab deformed and P.S. deformed and of machined specimen and lab deformed, as shown in Tables 3.2 and 3.3, is believed to be mainly attributed to different strain rates being employed in the tensile tests.

3.4 DISTRIBUTION OF TENSILE STRENGTH

Figures 3.19, 3.20 and 3.21 show the distributions of tensile strengths of Grade 300 reinforcing steel for different sets of data. The mean values are 489.5 MPa, 431.7 MPa and 464.1 MPa for machined specimens, lab deformed and P.S. deformed bars respectively. Distributions of tensile strengths for Grade 430 steel are shown in Figures 3.22, 3.23 and 3.24. The mean values are 633.8 MPa, 573 MPa and 606.8 MPa. Contributions from the "low carbon trial heats" samples can be seen at the lower 'tail' of the distributions. The tensile strengths of these samples fall in the range between 455 MPa and 565 MPa.

Unlike the lower yield strength, regression analysis carried out on machined specimen data and P.S. deformed data reveals that the tensile strengths of machined specimens are higher than the deformed bars tested by Pacific Steel Ltd, as shown in Figure 3.25. Regression analysis of two sets of data from deformed bars shows that the tensile strengths recorded by Pacific Steel Ltd are higher (see Figure 3.26).

Comparison of distributions of the tensile strengths of Grade 300 steel shows that the distribution produced from machined specimen data (Figure 3.19) is almost identical to the P.S. deformed distribution (Figure 3.21), but an increase in mean of 25.4 MPa is observed. However, the distribution of lab deformed data (Figure 3.20) is not seen to be comparable to the other two distributions. The same phenomenon is observed

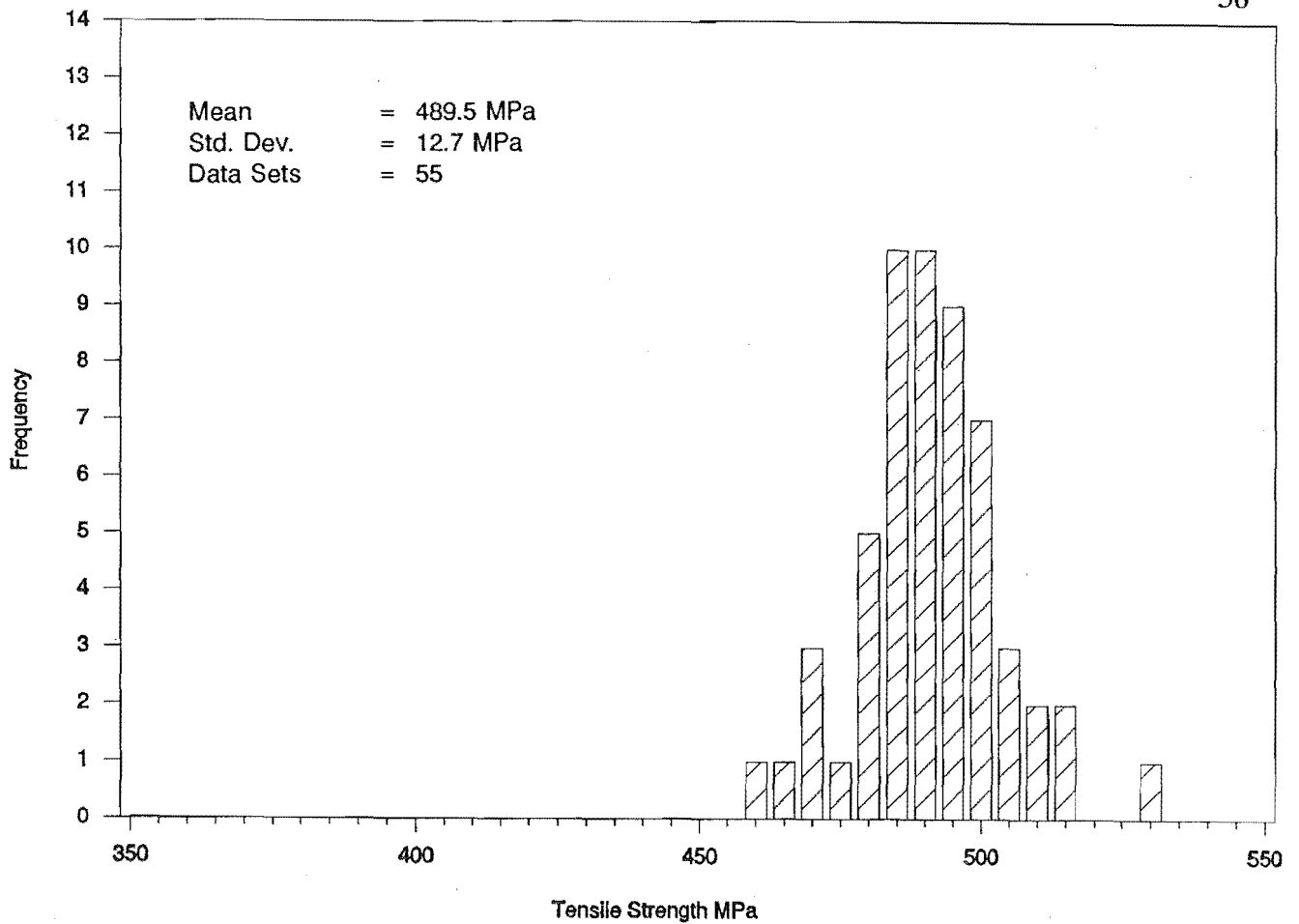


Figure 3.19: Distribution of tensile strength of Grade 300 machined specimen data

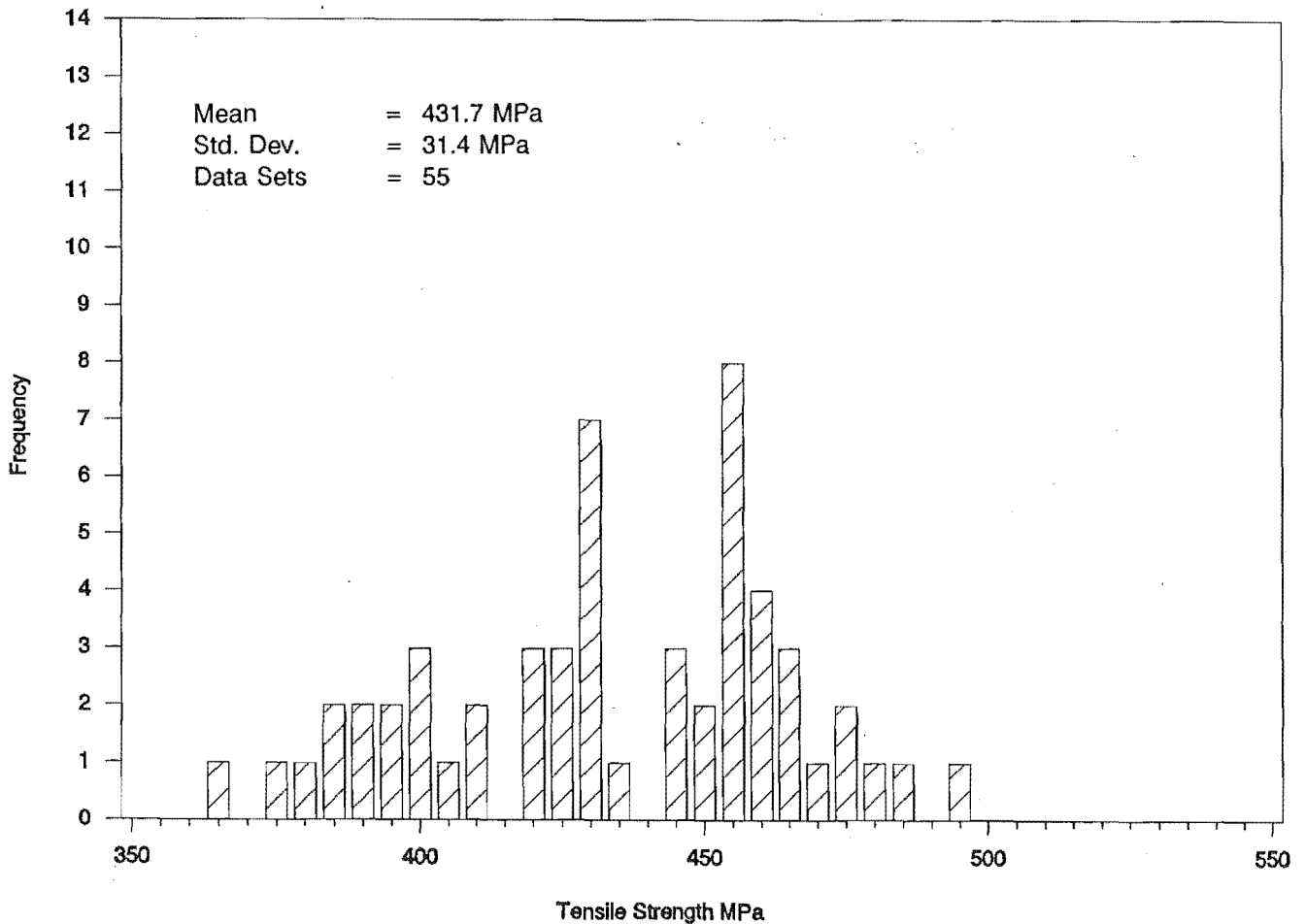


Figure 3.20: Distribution of tensile strength of Grade 300 lab deformed data

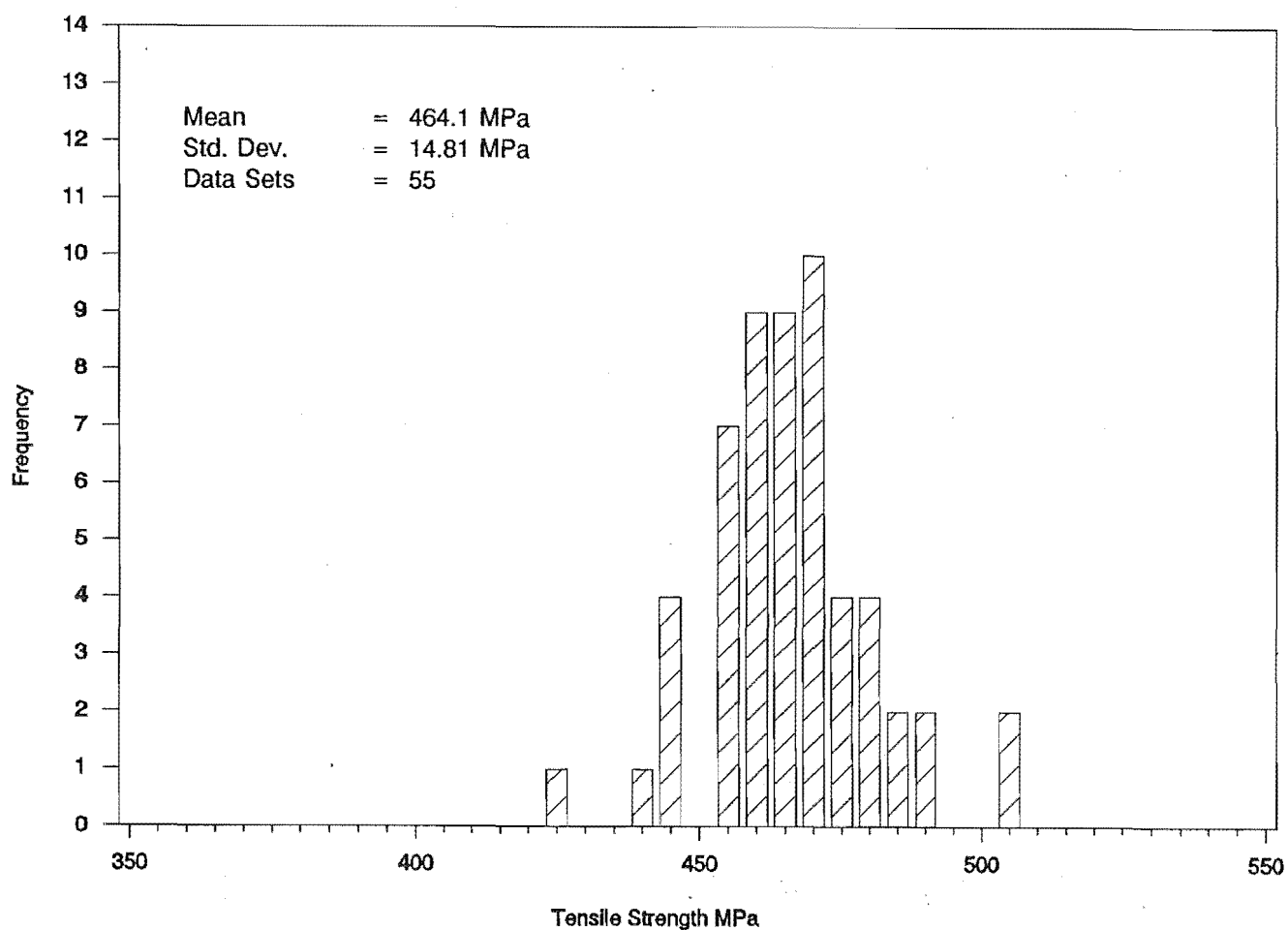


Figure 3.21: Distribution of tensile strength of Grade 300 P.S. deformed data

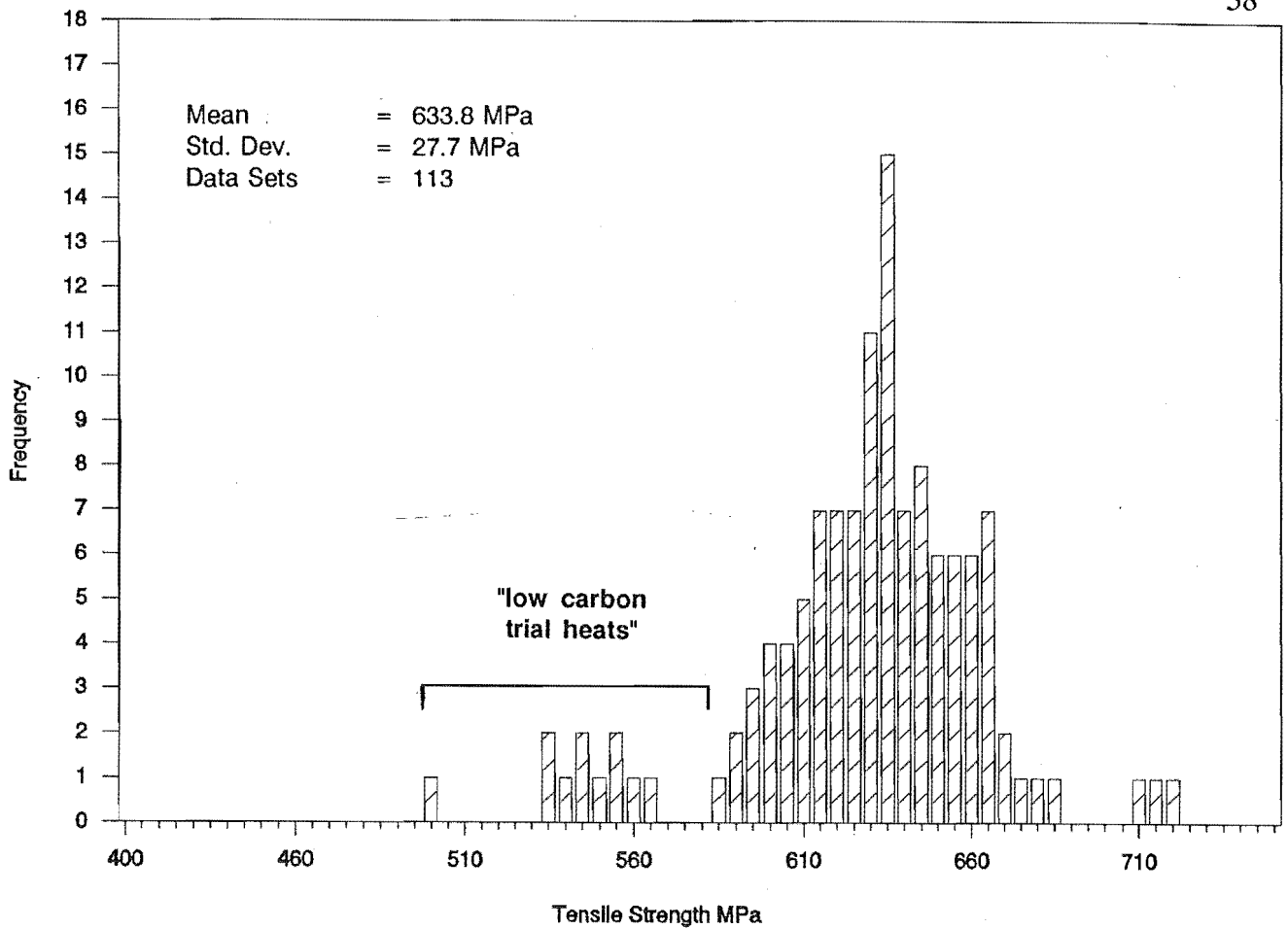


Figure 3.22: Distribution of tensile strength of Grade 430 machined specimen data

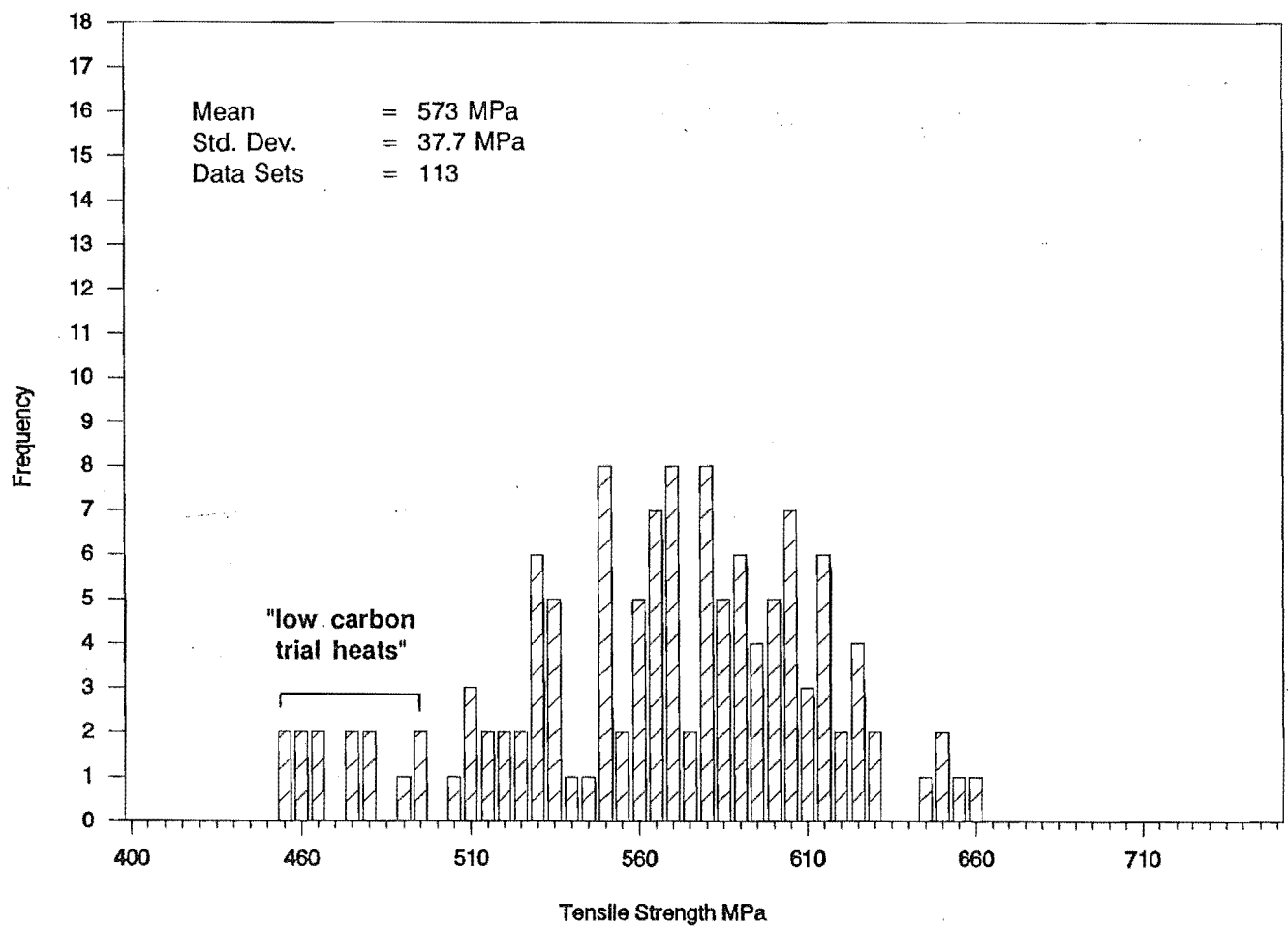


Figure 3.23: Distribution of tensile strength of Grade 430 lab deformed data

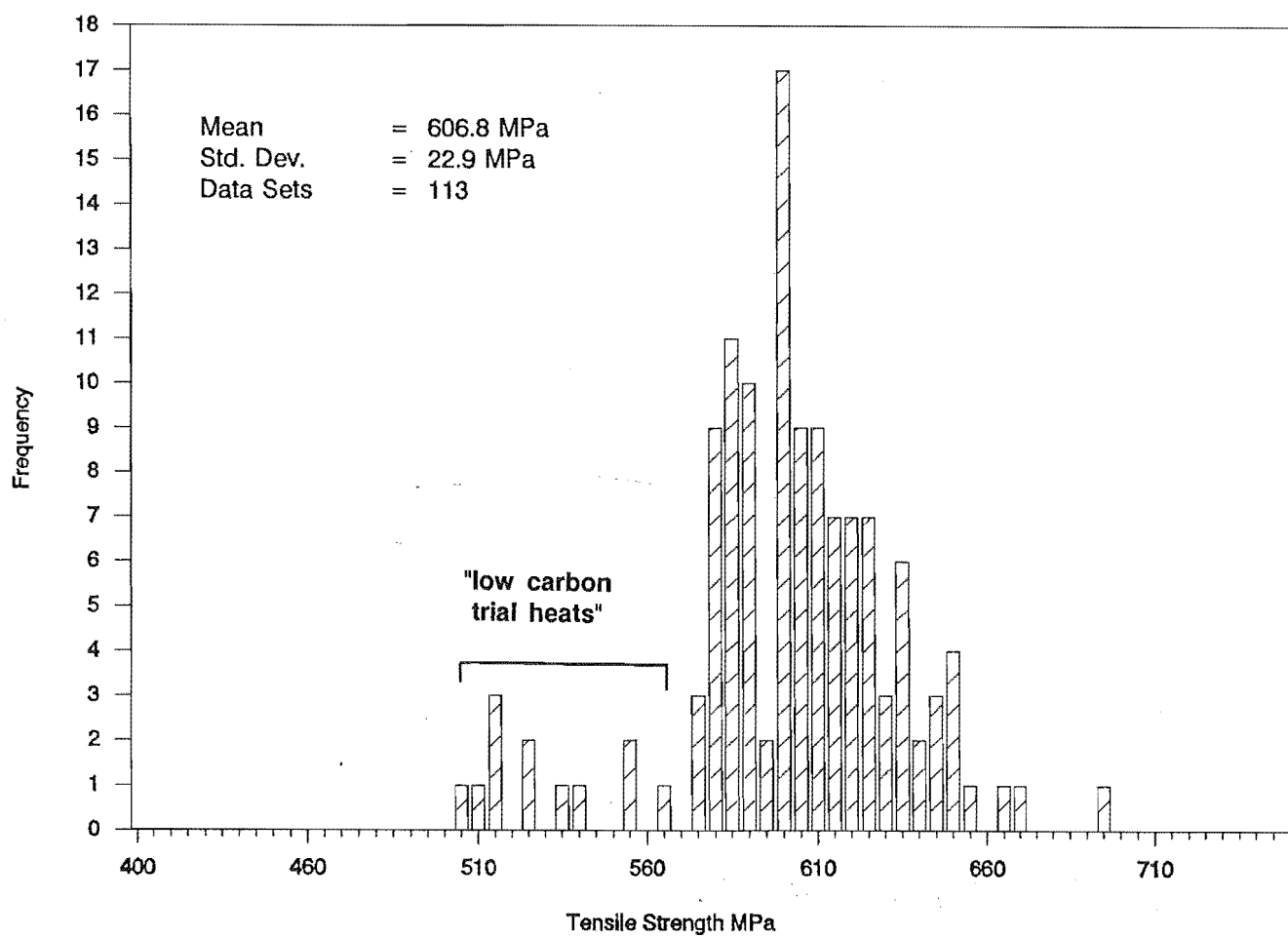


Figure 3.24: Distribution of tensile strength of Grade 430 P.S. deformed data

in comparing distributions of Grade 430 steel (Figures 3.22, 3.23 and 3.24). In both grades of steel, lab deformed data has the lowest mean tensile strength.

The regression line in Figure 3.25 is parallel to the expected correlation and a difference of approximately 25 MPa can be estimated. This figure is consistent with the difference in means of 25.4 MPa between Figures 3.19 and 3.21, and 27 MPa between Figures 3.22 and 3.24. The difference in the mean tensile strength between machined specimen data and P.S. deformed data is probably attributed to the geometry and condition of the test specimen. Unlike the good surface finish on the parallel length of a standard tensile specimen, defects on the surface and ribs of deformed bars could result in a series of stress concentrations and consequently lower the tensile strength.

Figure 3.26 shows that the tensile strengths of deformed bars recorded by Pacific Steel Ltd are generally greater than for those tested in the Materials Laboratory. A difference of 30 MPa is estimated from Figure 3.26. The difference in mean between P.S. deformed data and lab deformed data for Grade 300 and Grade 430 steels is 32.4 MPa (see Figures 3.20 and 3.21) and 33.8 MPa (see Figures 3.22 and 3.23) respectively. The difference is mainly due to the different strain rates used in the tensile tests, as Mander et al⁹ have found that it can be assumed that the strength of steel is increased by a fast strain rate by the same amount throughout the entire loading range.

Table 3.6 shows that lab deformed bars which fractured outside the gauge length have a significantly lower tensile strength. The mean tensile strength of lab deformed data is likely to be lowered by tensile strengths of those bars fracturing outside the gauge length.

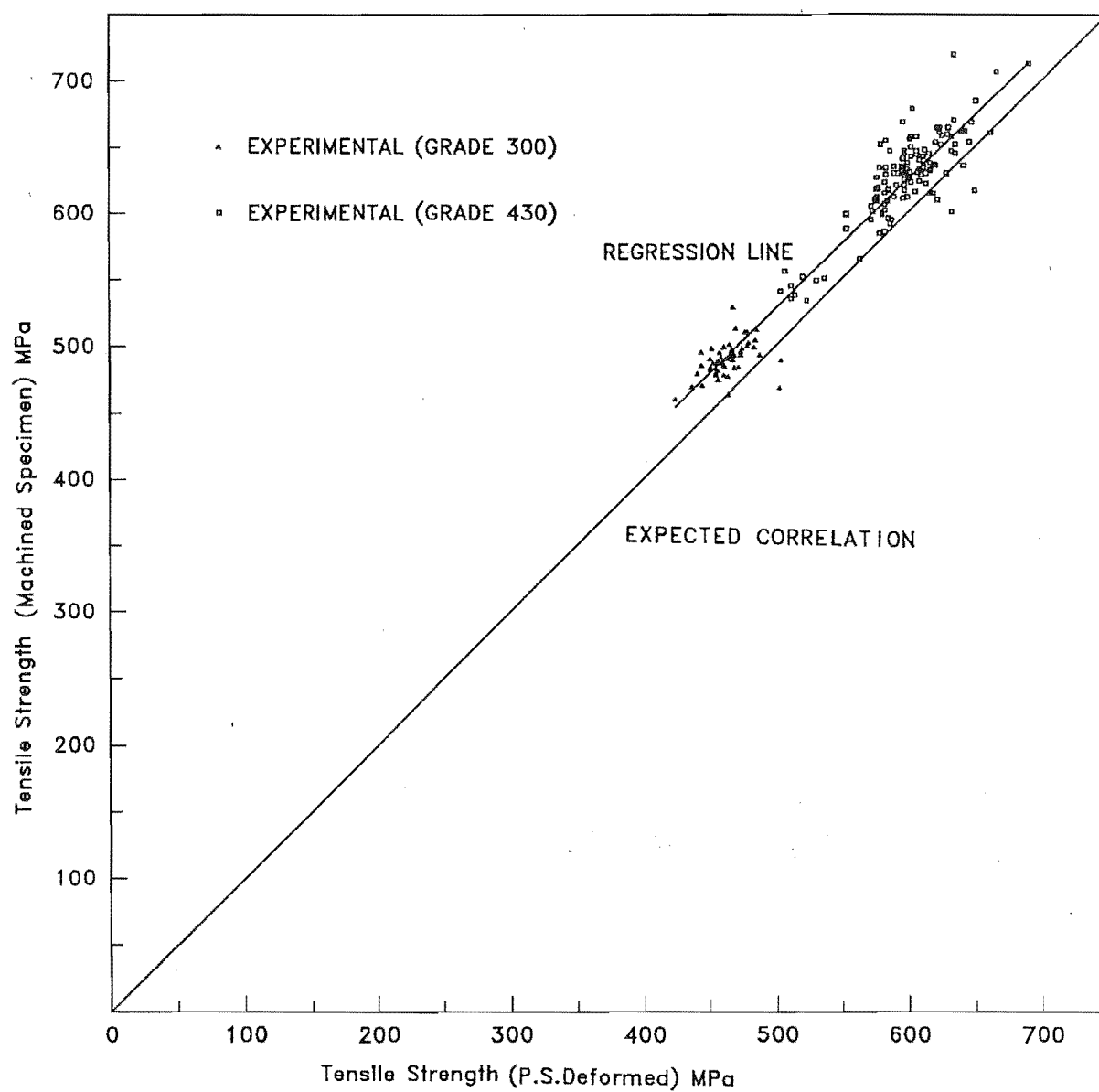


Figure 3.25: Graph of tensile strength of machined specimen vs P.S. deformed

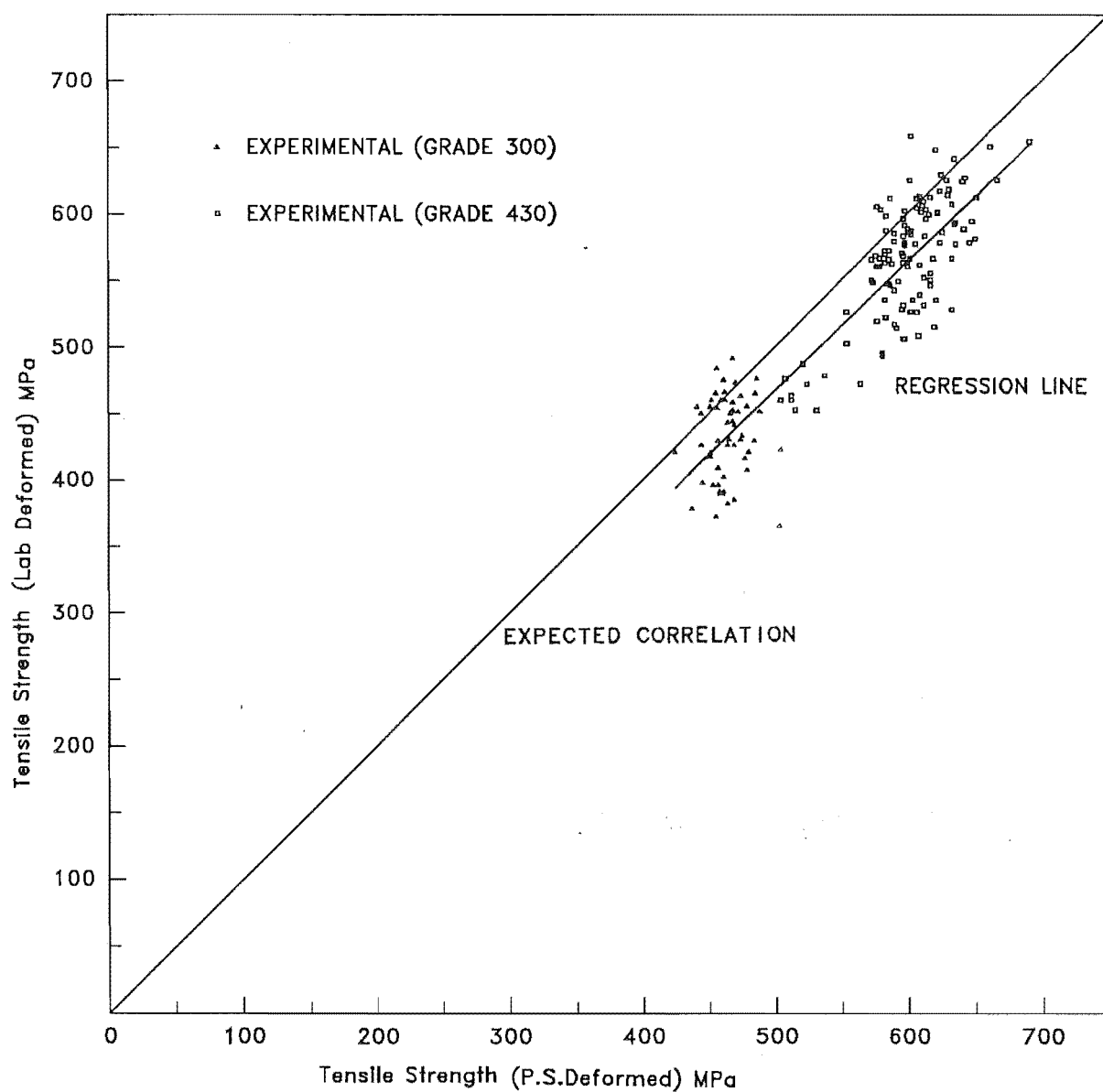


Figure 3.26: Graph of tensile strength of lab deformed vs P.S. deformed

Table 3.6: Comparison of mean tensile strength of bars which fractured inside/outside the gauge length (G.L.)

Grade	Bars Fractured Inside G.L.		Bars Fractured Outside G.L.	
	Data Sets	Mean TS, MPa	Data Sets	Mean TS, MPa
300	35	448.2	20	402.9
430	88	578.0	37	528.5

Table 3.7 summarises the statistical means and ranges of tensile strength for Grade 300 and Grade 430 reinforcing steels. Although there are differences in the mean tensile strength between different sets of data, all values tabulated in Table 3.7 have no difficulty in complying to the TS/YS ratio as specified in NZS 3402:1989. The specified minimum and maximum TS/YS ratios for Grade 300 and Grade 430 reinforcing steels are 1.15, 1.50 and 1.15, 1.40 respectively.

Table 3.7: Comparison of statistical means and ranges of tensile strength for Grade 300 and Grade 430 reinforcing steels

Source	Mean MPa	Standard Deviation MPa	Minimum MPa	Maximum MPa
Grade 300 Steel (Data Sets 55)				
Machined Specimen	489.5	12.74	460	529
Lab Deformed	431.7	31.39	365	491
P.S. Deformed	464.1	14.81	424	504
Grade 430 Steel (Data Sets 113)				
Machined Specimen	633.8	27.7	590	720
Lab Deformed	573.0	37.7	495	658
P.S. Deformed	606.8	22.9	575	691

3.5 DISTRIBUTION OF % ELONGATION AT FRACTURE

Figures 3.27 and 3.28 show the distributions of % elongation at fracture for Grade 300 reinforcing steel produced from machined specimen data and P.S. deformed data. There is no distribution for lab deformed data due to an incomplete set of results, because some deformed bars tested in the laboratory fractured outside the gauge length. Distributions of % elongation at fracture for Grade 430 reinforcing steel are shown in Figure 3.29 and 3.30. As can be seen from these figures, data points of "low carbon trial heats" samples fall in the range between 29% and 35%, at the higher 'tail' of the distributions.

Regression of these two sets of data yielded a regression line which does not agree with the expected correlation, as shown in Figure 3.31. There is also no indication of a consistent difference between the regression line and the expected correlation.

The difference in mean values between data produced from machined specimens (Figure 3.27) and data produced by Pacific Steel Ltd (Figure 3.28) is less than 1.7%, but the standard deviation of the distribution in Figure 3.28 is approximately twice that of Figure 3.27. For Grade 430 steel, the mean of the P.S. deformed data is lower by 4.6% than the machined specimen data but the distribution has a standard deviation twice that produced from machined specimen data (Figure 3.29). Generally, distributions of P.S. deformed data have a wider range as indicated by the higher standard deviation. This is because tensile testing of non-standard tensile specimens normally gives rise to greater variation in the results due to the fact that all deformed bars being tested would have slightly different dimensions and surface conditions. The regression line in Figure 3.31 is undoubtedly affected by the difference in the range of the two sets of data.

For both grades of steel, machined specimen data was found to have a higher mean % elongation at fracture than P.S. deformed data. This is probably because of the difference in the test piece geometry and condition.

As expected, the lower strength Grade 300 reinforcing steel was found to have better ductility than the higher strength Grade 430 steel. Table 3.8 shows the statistical

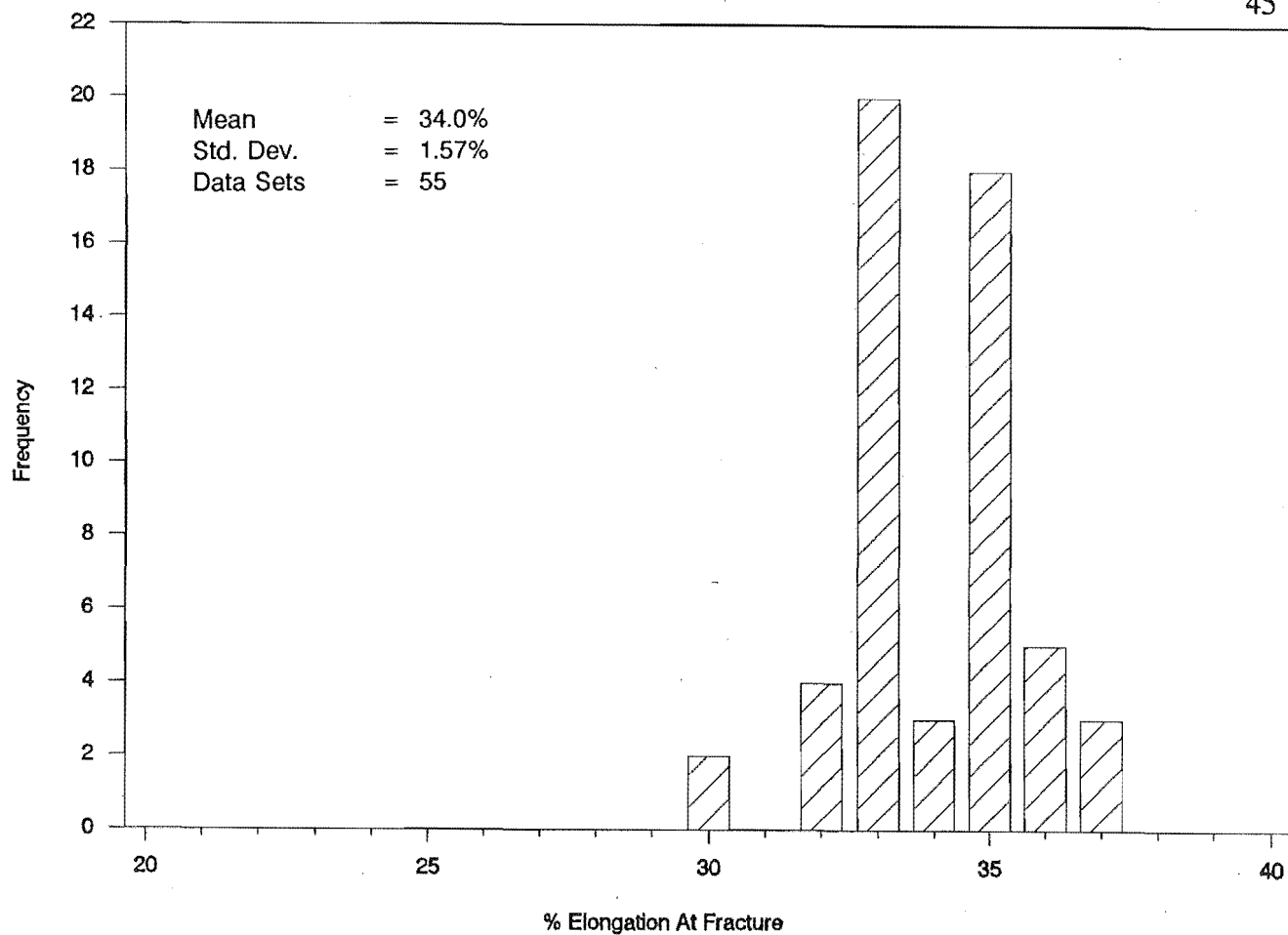


Figure 3.27: Distribution of % elongation at fracture of Grade 300 machined specimen data

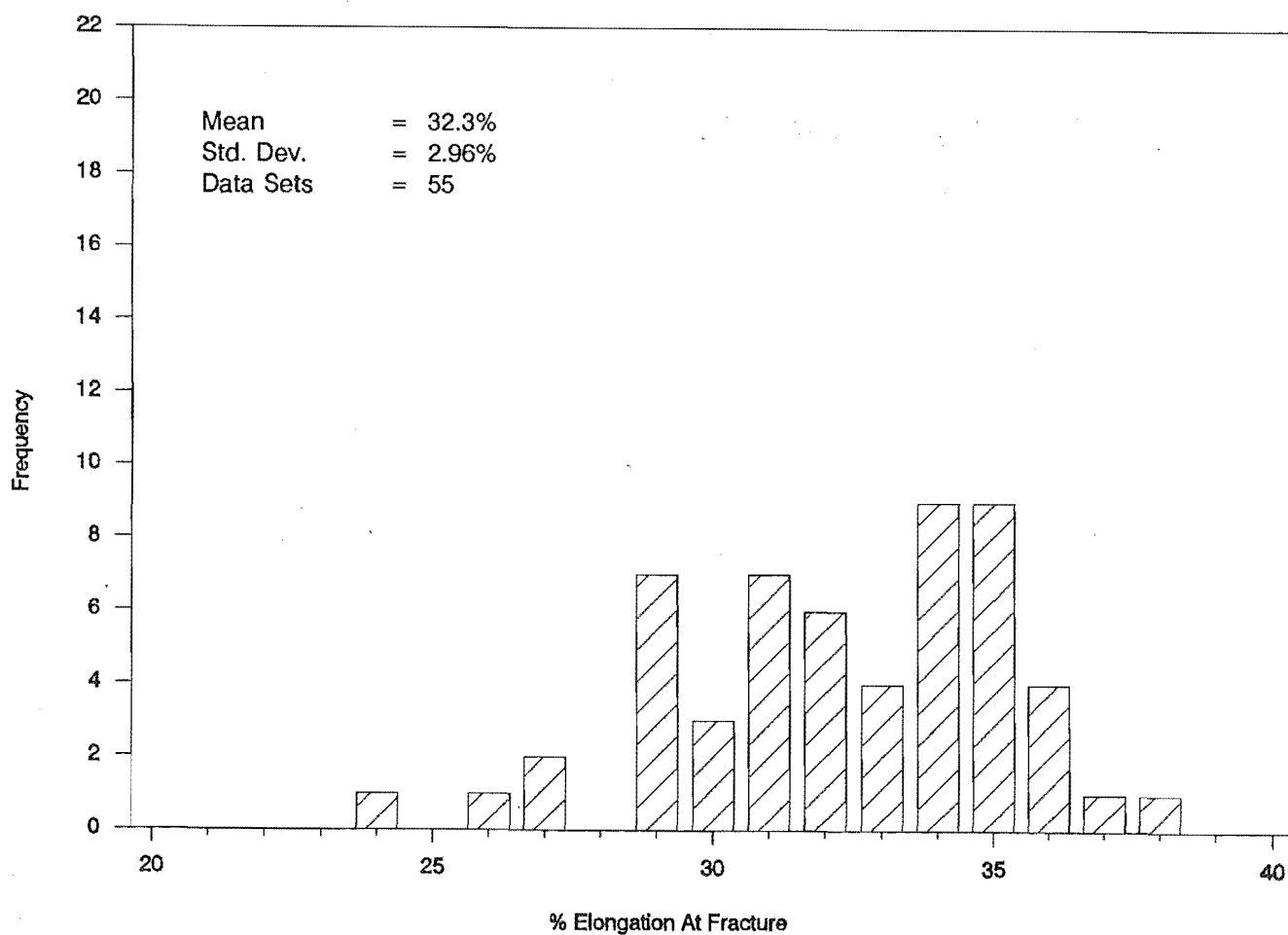


Figure 3.28: Distribution of % elongation at fracture of Grade 300 P.S. deformed data

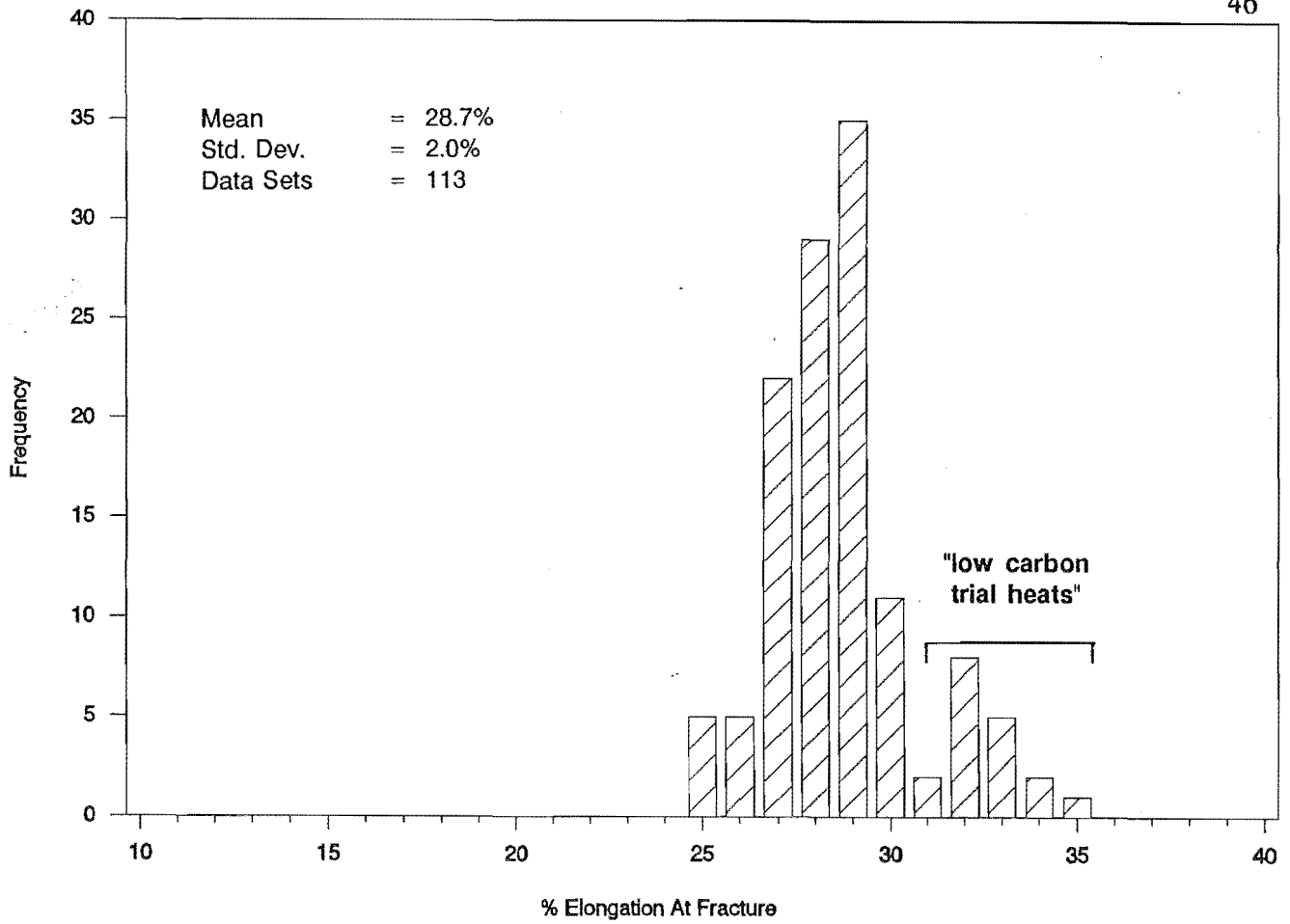


Figure 3.29: Distribution of % elongation at fracture of Grade 430 machined specimen data

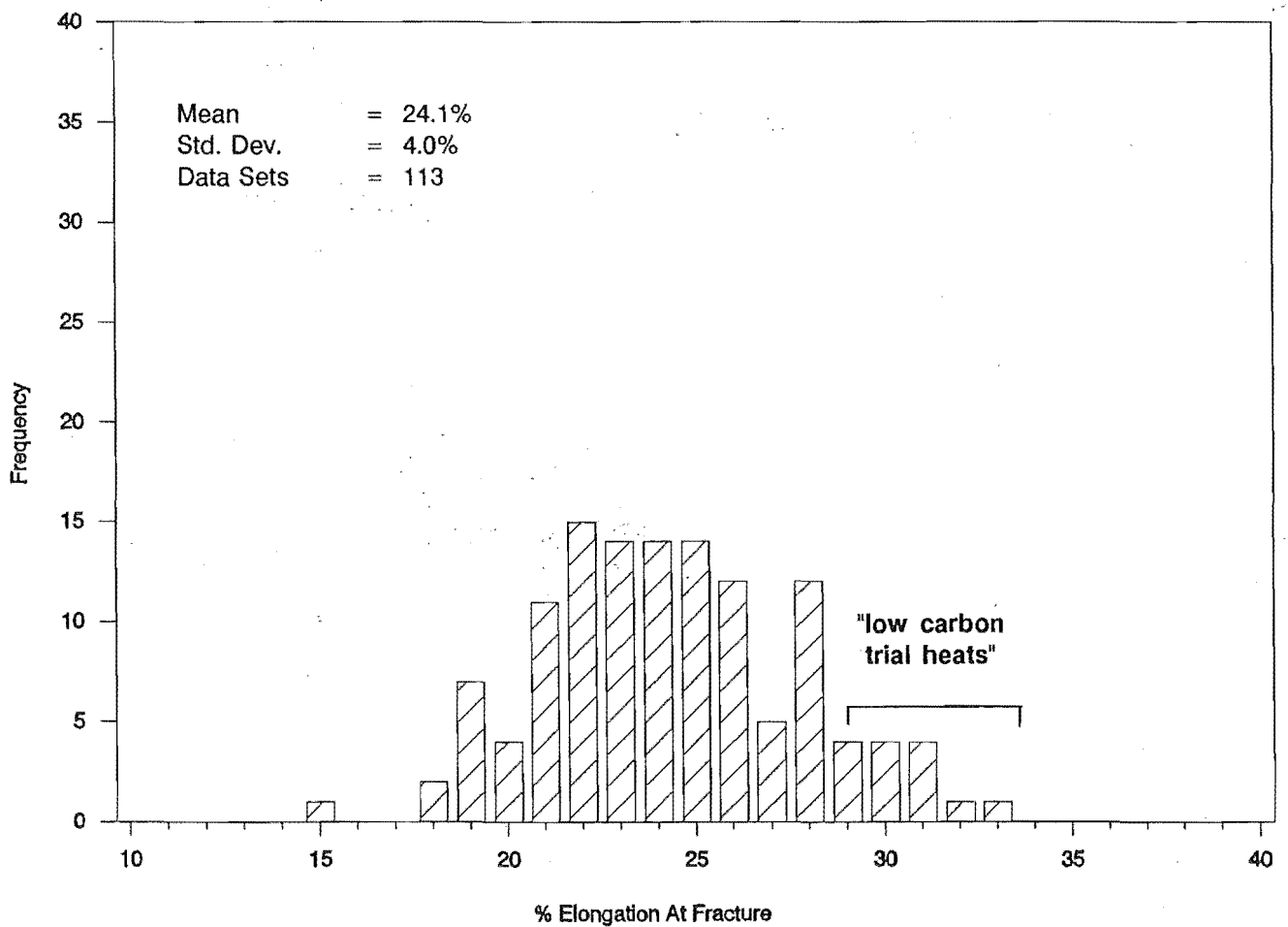


Figure 3.30: Distribution of % elongation at fracture of Grade 430 P.S. deformed data

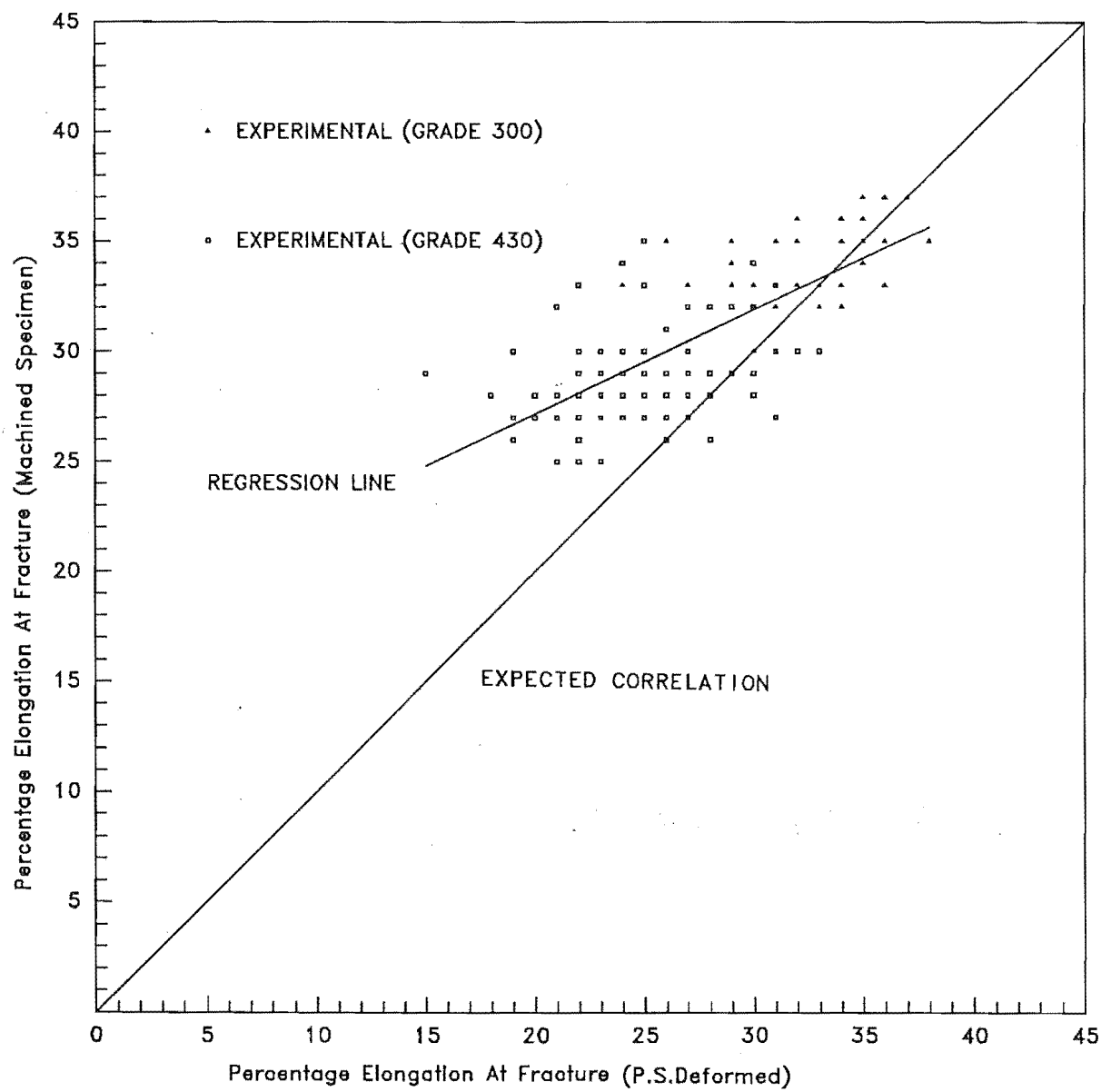


Figure 3.31: Graph of % elongation at fracture of machined specimen vs P.S. deformed

means and ranges of % elongation at fracture for Grade 300 and Grade 430 reinforcing steels. All the mean values shown in Table 3.8 are greater than the minimum elongation of 20% and 15% for grade 300 and Grade 430, specified in NZS 3402:1989.

Table 3.8: Statistical means and ranges of % elongation at fracture for Grade 300 and Grade 430 reinforcing steels

<i>Source</i>	<i>Mean</i> %	<i>Standard Deviation</i> %	<i>Minimum</i> %	<i>Maximum</i> %
Grade 300 Steel (Data Sets 55)				
Machined Specimen	34.0	1.57	30	37
P.S. Deformed	32.3	2.96	24	38
Grade 430 Steel (Data Sets 113)				
Machined Specimen	28.7	2.00	25	32
P.S. Deformed	24.1	4.00	15	28

3.6 DISTRIBUTION OF LUDER STRAIN

The distributions of Luder strain were produced from machined specimen data and lab deformed data only. Pacific Steel Ltd does not supply data on Luder strain. Figures 3.32 and 3.33 show the distributions of % Luder strains for Grade 300 steel. The mean Luder strains for machined specimen data and lab deformed data are 2.0% and 1.9% respectively. Distributions of % Luder strain for Grade 430 steel are shown in Figures 3.34 and 3.35. The mean values for both sets of data are consistent at 1.3%. Data points for the "low carbon trial heats" samples fall in the range between 1.4% and 2.1%, at the higher 'tail' of the distributions.

The regression analysis of these two sets of data yielded a regression line which is in good agreement with the expected correlation, as shown in Figure 3.36.

As shown in Figures 3.32 and 3.33, distributions produced from machined specimen data and lab deformed data can be seen to be closely comparable. The same

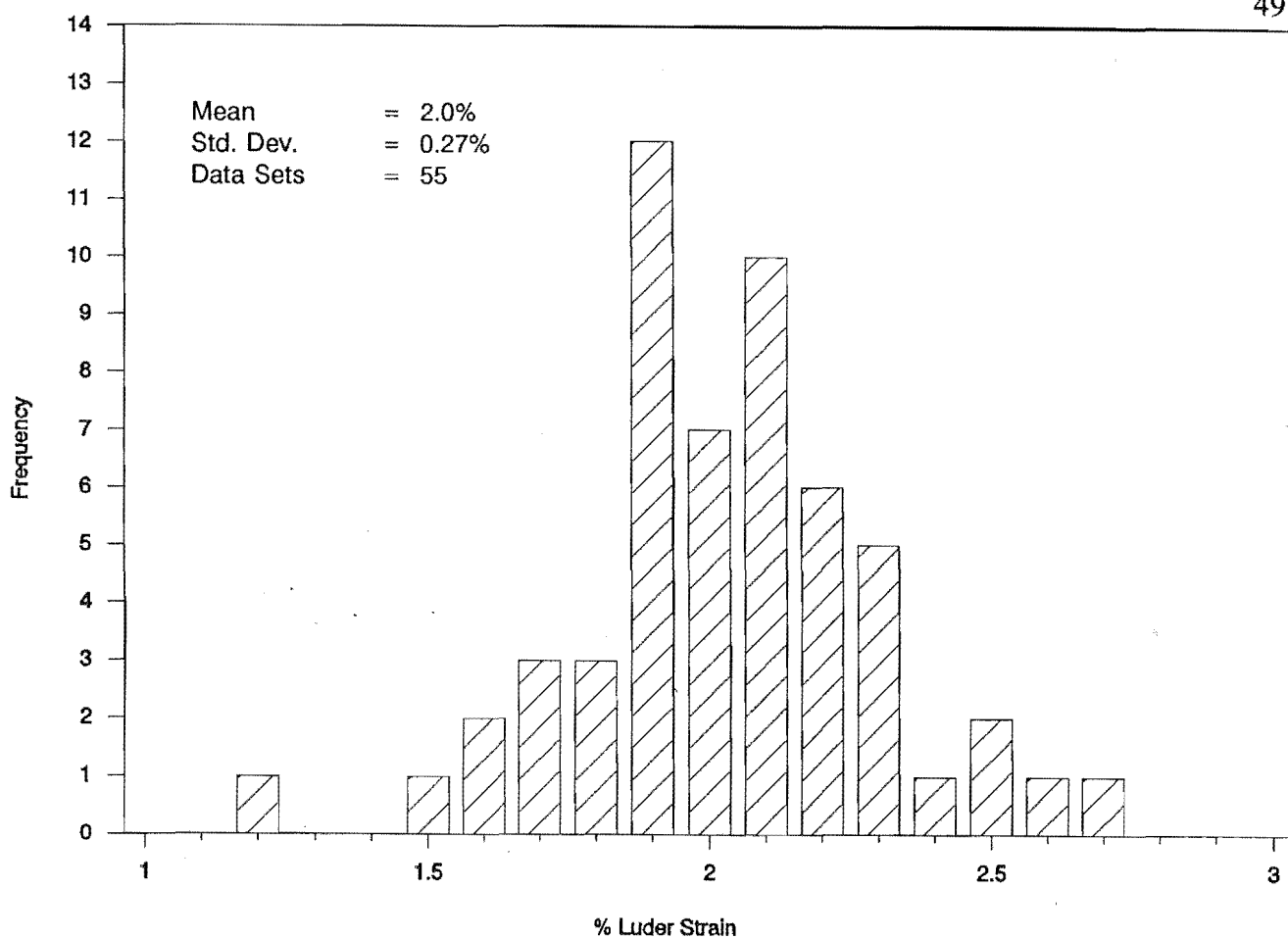


Figure 3.32: Distribution of % Luder strain of Grade 300 machined specimen data

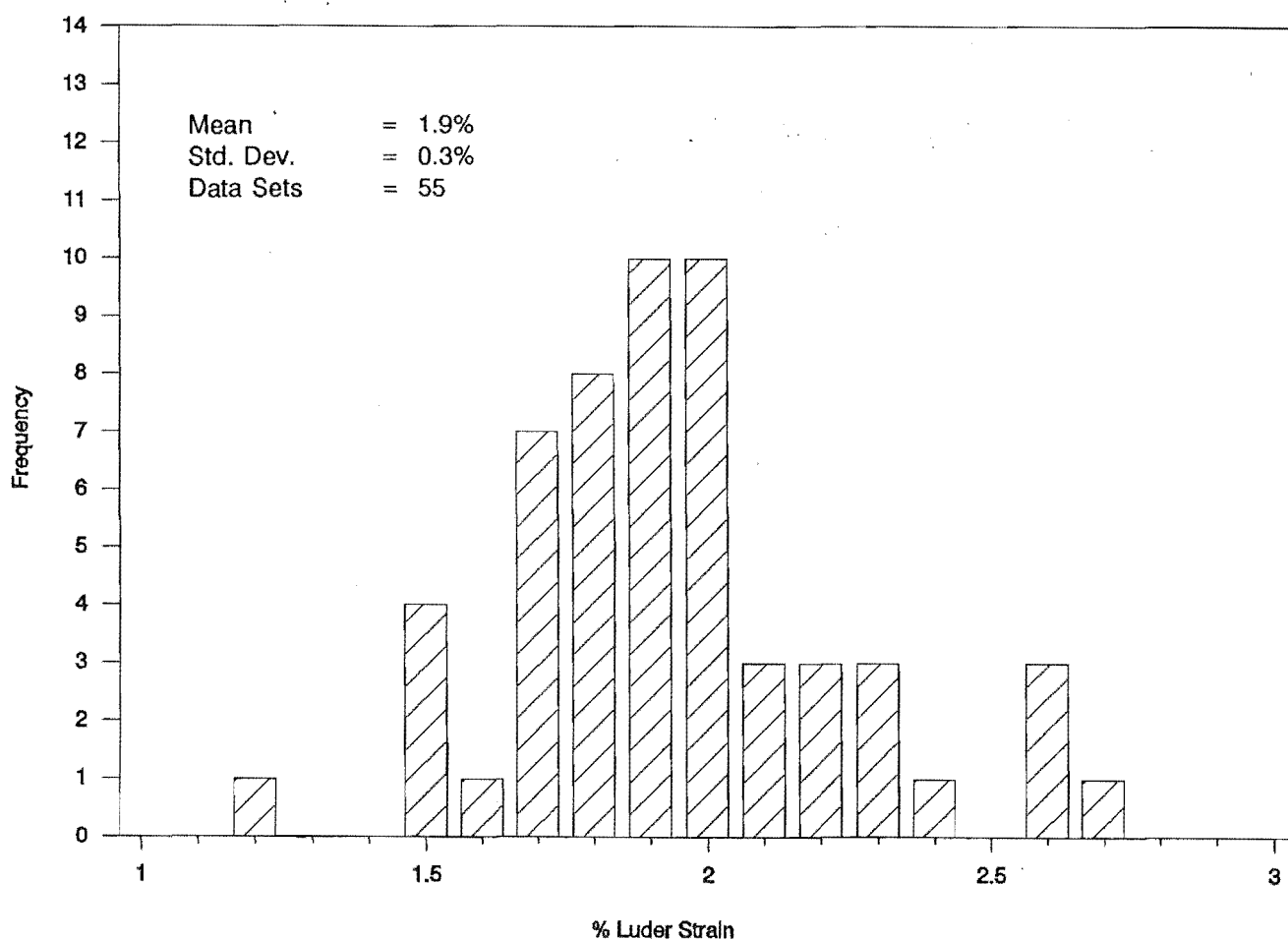


Figure 3.33: Distribution of % Luder strain of Grade 300 lab deformed data

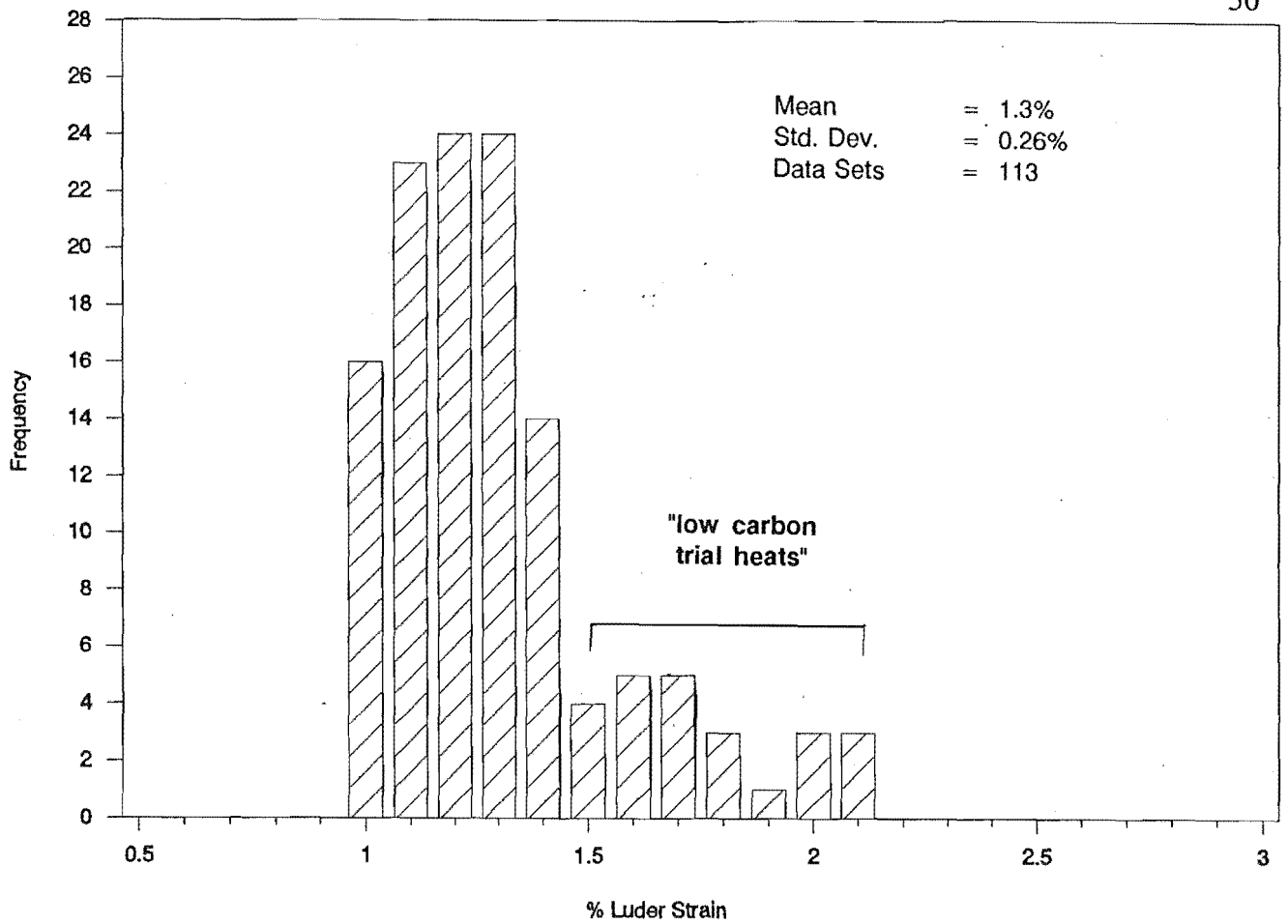


Figure 3.34: Distribution of % Luder strain of Grade 430 machined specimen data

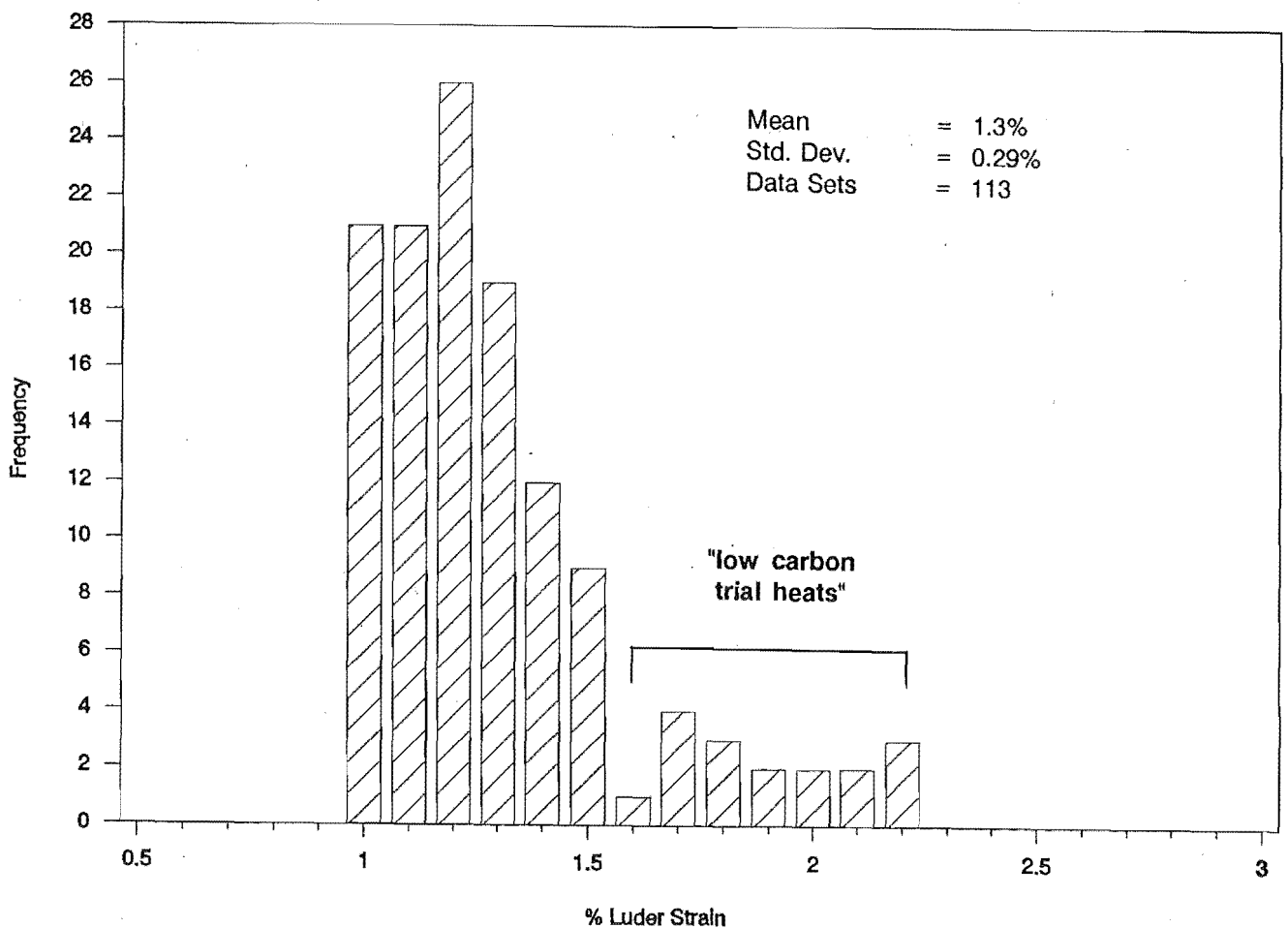


Figure 3.35: Distribution of % Luder strain of Grade 430 lab deformed data

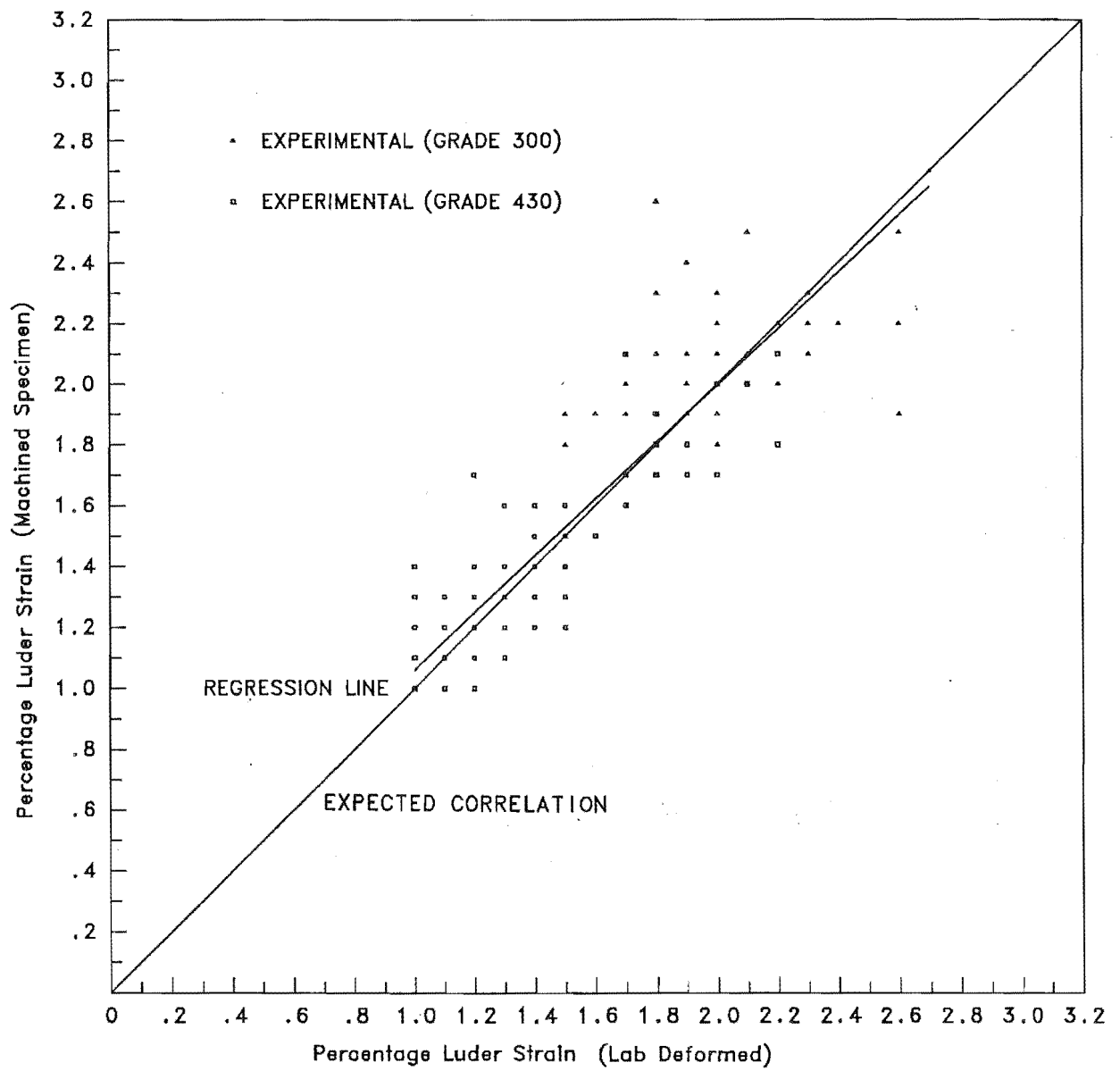


Figure 3.36: Graph of % Luder strain of machined specimen vs lab deformed

phenomenon is observed in Grade 430 steel, as shown in Figures 3.34 and 3.35. Good agreement in the mean values between the two sets of data of both grades of steel, and the regression result suggest that the length of Luder strain is not affected by the type of specimen being tested and the different strain rates being employed in the tensile tests. Distributions of % Luder strain for Grade 430 steel in Figures 3.34 and 3.35 are skewed to the right because of the contributions from the "low carbon trial heats" samples. The statistical means and ranges of % Luder strain of Grade 300 and Grade 430 reinforcing steels are shown in Table 3.9.

Table 3.9: Statistical means and ranges of % Luder strain for Grade 300 and Grade 430 reinforcing steels.

<i>Source</i>	<i>Mean</i> %	<i>Standard Deviation</i> %	<i>Minimum</i> %	<i>Maximum</i> %
Grade 300 Steel (Data Sets 55)				
Machined Specimen	2.0	0.27	1.2	2.7
Lab Deformed	1.9	0.30	1.2	2.7
Grade 430 Steel (Data Sets 113)				
Machined Specimen	1.3	0.26	1.0	1.7
Lab Deformed	1.3	0.29	1.0	1.7

Previous investigations^{17,18} have found that the mean % Luder strains of the old Grades 275 and 380 reinforcing steels were 2.2% and 0.97% respectively. Comparatively, Grade 300 has a slightly shorter Luder strain than Grade 275. However, the higher strength Grade 430 steel has a higher Luder strain than the previous Grade 380 steel. This improvement is very beneficial in the design of reinforced concrete structures. Grade 430 reinforcing steel can provide the required design strength while still having high Luder strain to accommodate the post-elastic deformation.

3.7 DISTRIBUTION OF STRAIN HARDENING EXPONENT AND COEFFICIENT

The distributions of strain hardening exponent and coefficient were produced from the machined specimen data only. Figures 3.37 and 3.38 show the distributions of the strain hardening exponent for Grade 300 and Grade 430 reinforcing steels. The Grade 300 data has a mean value of 0.258, and the mean n value for Grade 430 data is 0.2. It should be noted that n values for the "low carbon trial heats" samples fall in the range between 0.19 and 0.21. The contributions do not affect the distribution in Figure 3.38. The distributions of the strain hardening coefficient k for Grade 300 and Grade 430 steels are shown in Figures 3.39 and 3.40. The mean k values for Grade 300 and Grade 430 data are 968.5 MPa and 1094.2 MPa respectively. k values of the "low carbon trial heats" samples fall in the range between 910 MPa and 1000 MPa, at the lower 'tail' of the distribution in Figure 3.40. In both n and k distributions, data points which lie outside the normal range are probably due to errors in obtaining stress values from the strain hardening region of the stress-strain curves.

Comparison of Figures 3.37 and 3.38 reveals that n values for Grade 300 steel are greater than for Grade 430 steel. However, Grade 430 steel was found to have greater k values when compared to Grade 300 steel (see Figures 3.39 and 3.40). Table 3.10 shows the statistical means and ranges of strain hardening exponent and coefficient for Grade 300 and Grade 430 reinforcing steels.

Table 3.10: Statistical means and ranges of strain hardening exponent and coefficient for Grade 300 and Grade 430 reinforcing steels

<i>Grade</i>	<i>Mean</i>	<i>Standard Deviation</i>	<i>Minimum</i>	<i>Maximum</i>
Strain Hardening Exponent n				
300	0.258	0.027	0.151	0.299
430	0.2	0.017	0.152	0.29
Strain Hardening Coefficient k (MPa)				
300	968.5	72.9	748	1145
430	1094.2	67.8	1000	1278

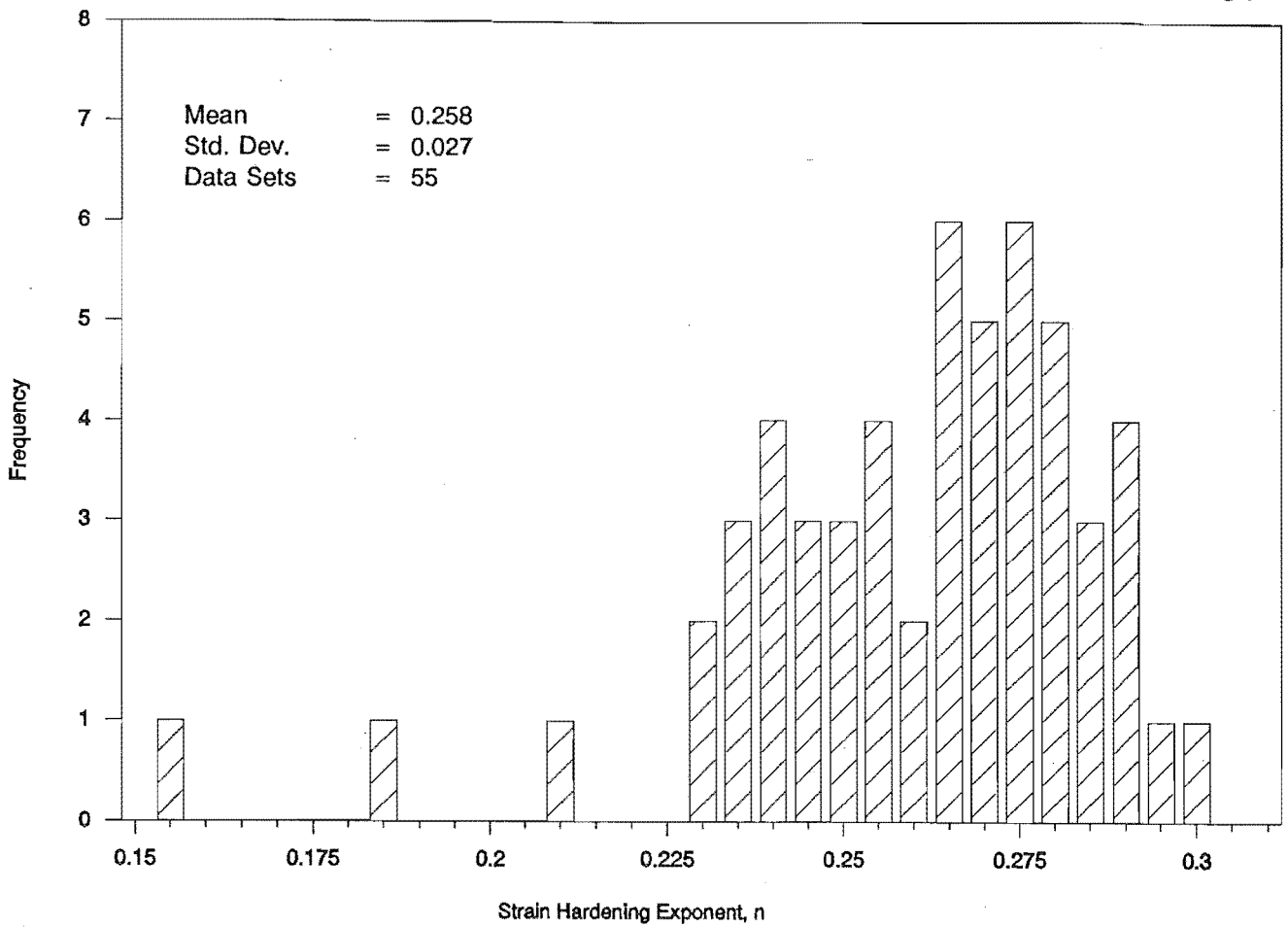


Figure 3.37: Distribution of strain hardening exponent of Grade 300 machined specimen data

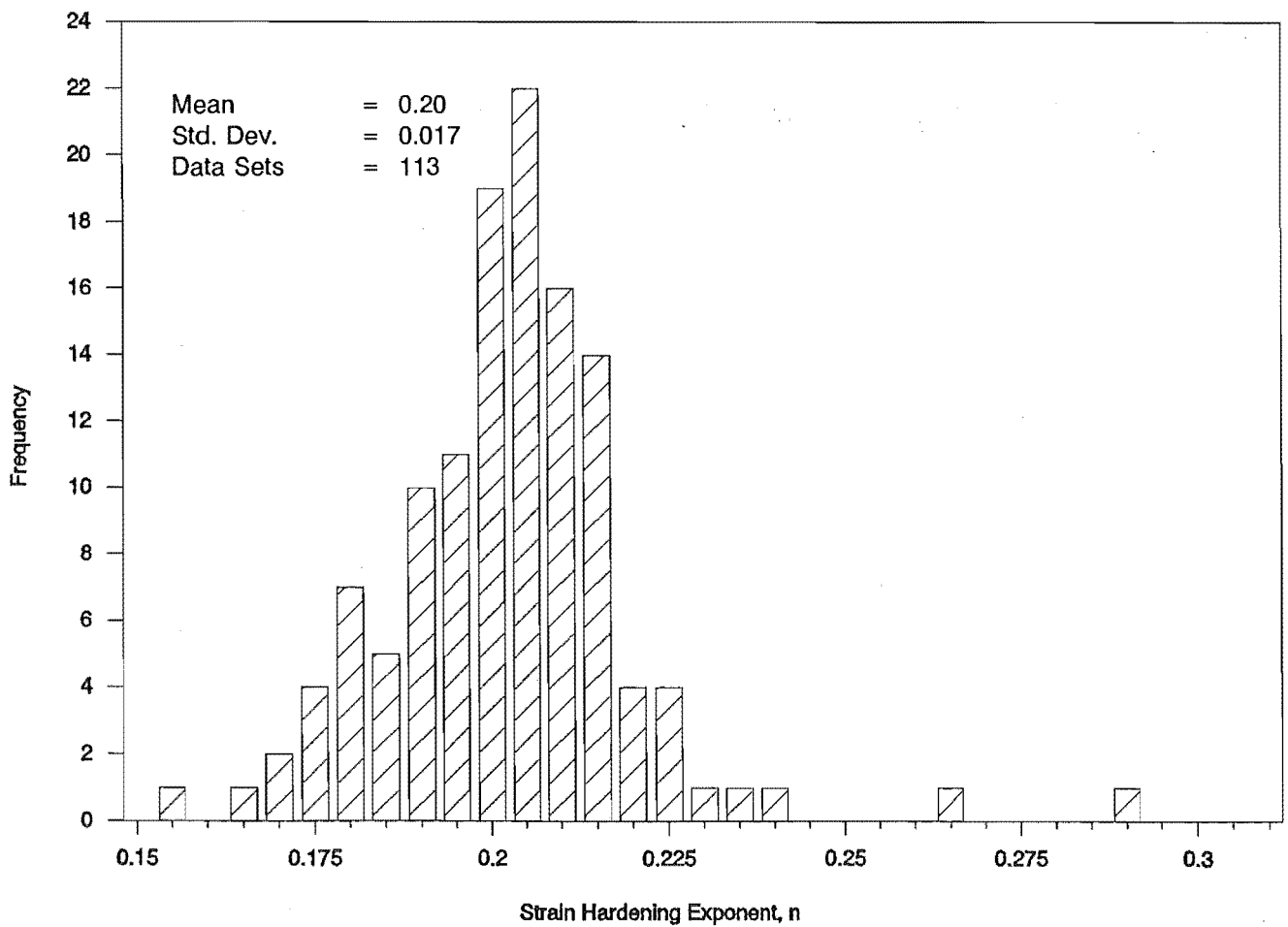


Figure 3.38: Distribution of strain hardening exponent of Grade 430 machined specimen data

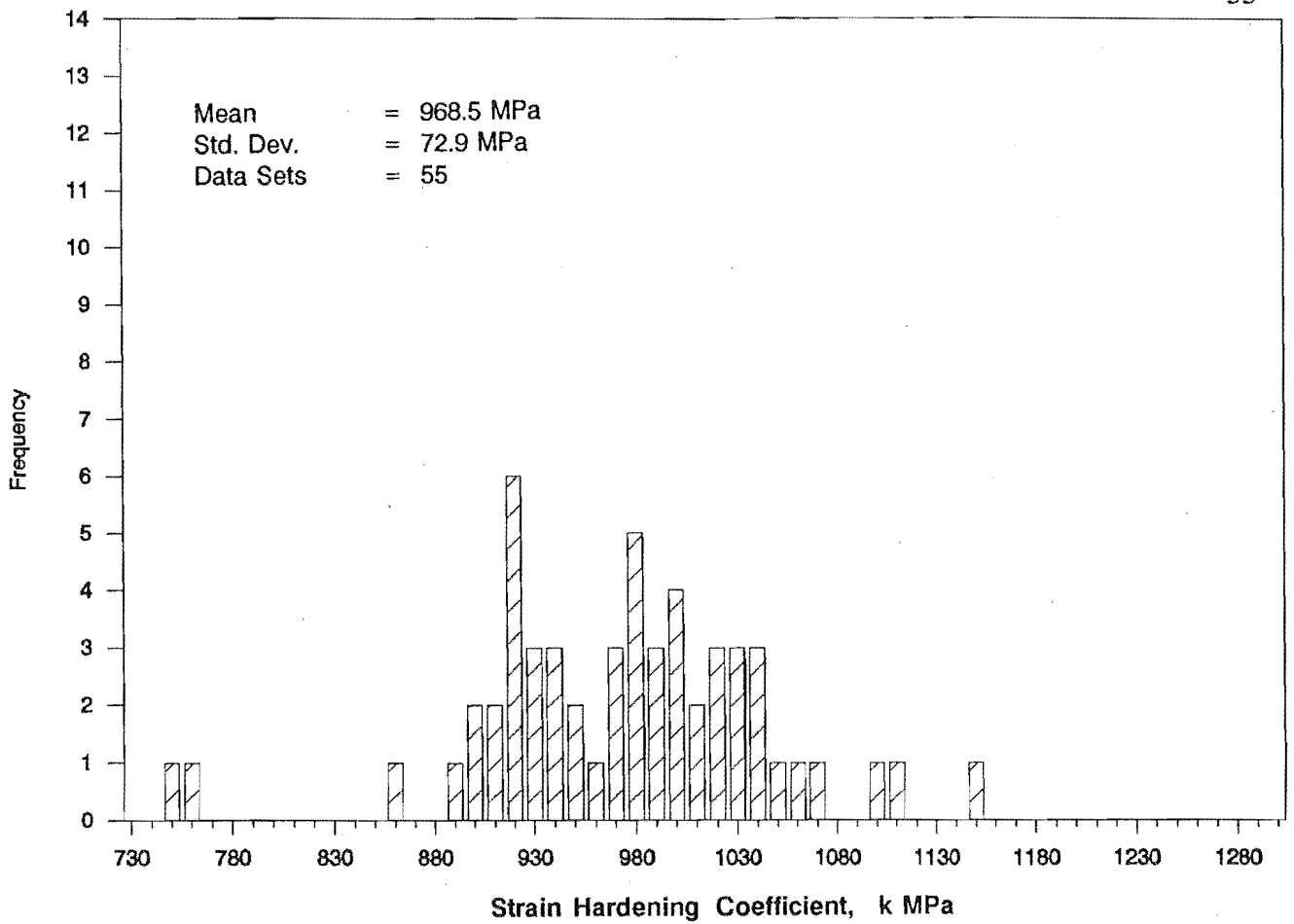


Figure 3.39: Distribution of strain hardening coefficient of Grade 300 machined specimen data

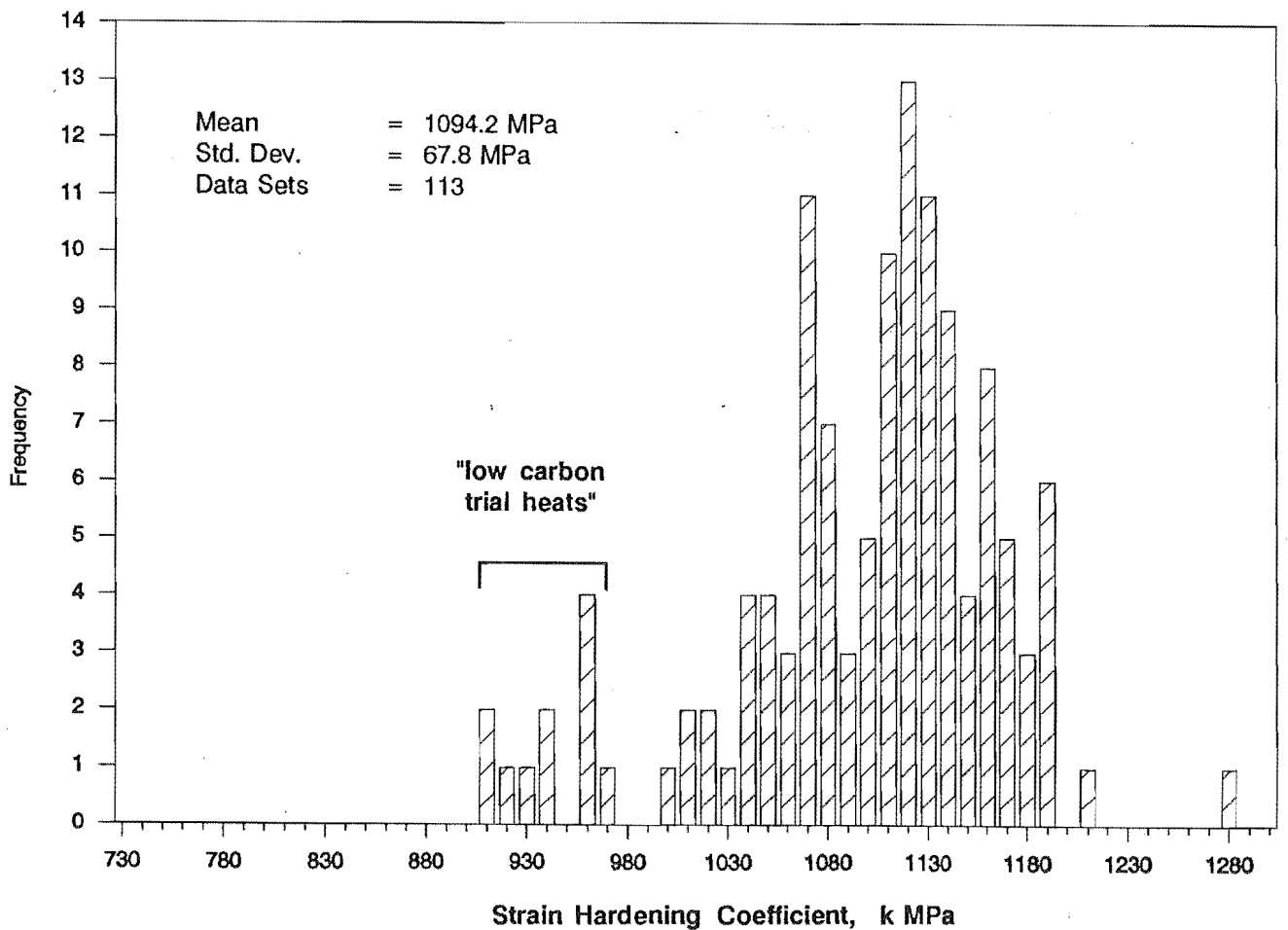


Figure 3.40: Distribution of strain hardening coefficient of Grade 430 machined specimen data

Generally, the constants n and k do not have individual significance. An important parameter which relates to them is the strain hardening rate and is defined by Equation 3.5 as $\frac{d\sigma}{d\epsilon} = nk(\epsilon)^{n-1}$. The strain hardening rate governs the rate of strength increase when a steel strain hardens. Thus, in the design of earthquake resisting structures, it is desirable to use reinforcing steel of low strain hardening rate to minimise the overstrength of plastic hinges.

The strain hardening rate at the commencement point of a strain hardening curve was determined based on the mean values of n and k (see Table 3.10) obtained in this study. In the calculation of strain hardening rates using Equation 3.5, strain corresponding to the linear elastic portion of the stress-strain curve is assumed to be negligible and the measured Luder strain is assumed to be the strain at the starting point of the strain hardening curve. Table 3.11 shows the comparison of the initial strain hardening rates between current and previous grades of reinforcing steel. The latter data is obtained from previous investigations^{17,18} where the strain hardening modulus is used to define the strain hardening curve.

Table 3.11: Comparison of strain hardening rates between current and previous grades of reinforcing steel

Grade	Mean n	Mean k MPa	Mean Luder Strain	Strain Hardening Rate, MPa
300	0.258	968.5	0.0200	4587
430	0.200	1094.2	0.0130	7099
275	-	-	0.0220	5266
380	-	-	0.0097	8979

Since the chemical composition of Grade 300 steel is generally similar to the previous Grade 275, ideally the strain hardening rates should be the same. However, as shown in Table 3.11, the strain hardening rate of Grade 300 steel is lower than that of Grade 275. The difference is 679 MPa, believed to be attributed to the different methods employed in defining the strain hardening curves. Despite a higher mean Luder strain, the strain hardening rate of Grade 430 steel is 1880 MPa lower than that of Grade 380. The resultant true strain hardening rates for Grade 300 and

Grade 430 reinforcing steels using n and k from Table 3.11 with Equation 3.5 is shown in Figure 3.41.

3.8 DISTRIBUTION OF STRAIN AGEING INDEX

In this study, three parameters measuring the strain ageing index were determined. These parameters are associated with the changes in tensile properties, namely ΔY , ΔU and ΔEl . Distributions of ΔY values produced from Grade 300 and Grade 430 data are shown in Figures 3.42 and 3.43. Figures 3.44 and 3.45 show the distributions of ΔU for Grade 300 and Grade 430 data. The distributions of ΔEl are respectively shown in Figures 3.46 and 3.47. In all cases, contributions from the "low carbon trial heats" samples cannot be distinguished as a separate cluster of data points.

Grade 430 steel has lower mean ΔY value than Grade 300. This is not unexpected since Grade 430 steel is micro-alloyed with approximately 0.04% vanadium. The presence of vanadium in the steel results in the formation of vanadium nitride precipitate, hence reducing the level of free nitrogen in the steel and consequently reducing the susceptibility of Grade 430 steel to strain ageing. The difference in mean ΔY values of 19.1 MPa between Grade 300 data (Figure 3.42) and Grade 430 data (Figure 3.43) is comparable to the result obtained by Pussegoda et al¹⁹ where 0.04% vanadium was found to be sufficient to reduce ΔY to approximately 15 MPa. Comparison of distributions of ΔU and ΔEl also reveals that strain ageing is significantly reduced in Grade 430 steel. The mean ΔU and ΔEl values for Grade 430 data were found to be approximately 55% of those for Grade 300 data. Table 3.12 shows the statistical means and ranges of ΔY , ΔU and ΔEl for Grade 300 and Grade 430 reinforcing steels.

In considering the effect of an increase in yield strength due to the strain ageing of reinforcing bar on the performance of plastic hinges, Grade 430 steel is preferable for use in reinforced concrete structures. Grade 430 micro-alloyed reinforcing steel has also been shown²⁰ to have a lower transition temperature compared to the plain carbon-manganese Grade 300 steel.

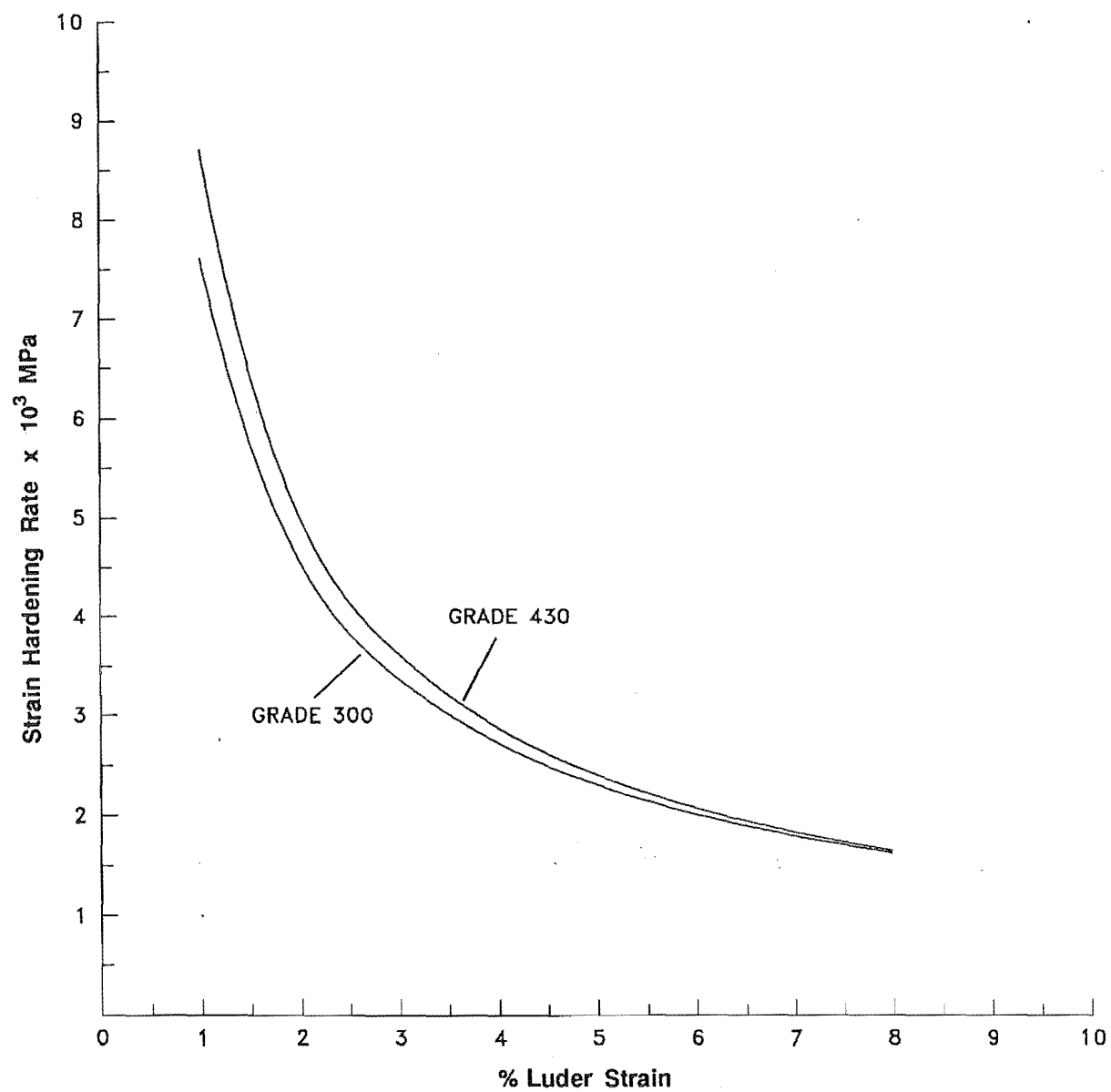


Figure 3.41: Mean strain hardening rate for Grade 300 and Grade 430 reinforcing steels

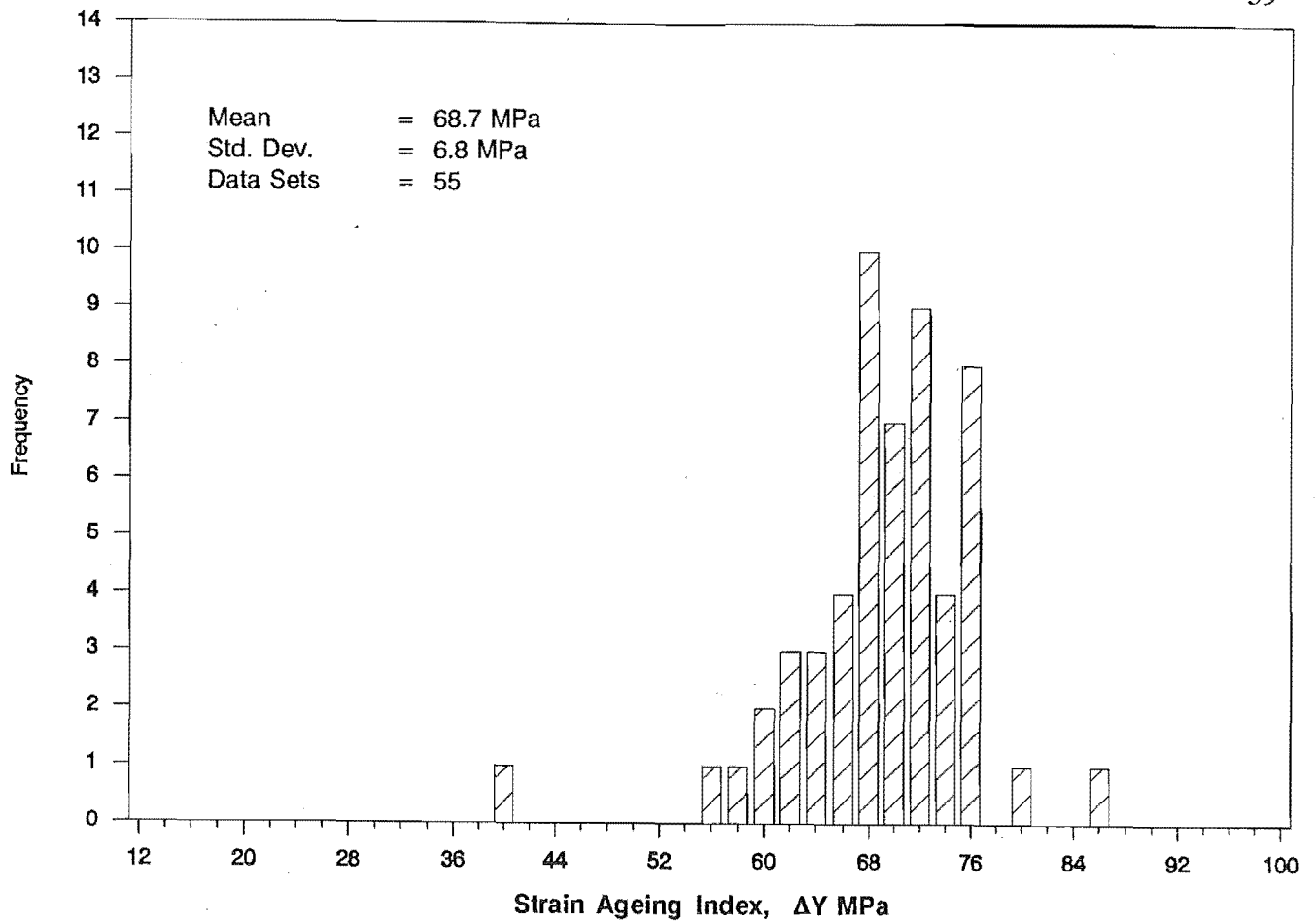


Figure 3.42: Distribution of strain ageing index ΔY of Grade 300 machined specimen data

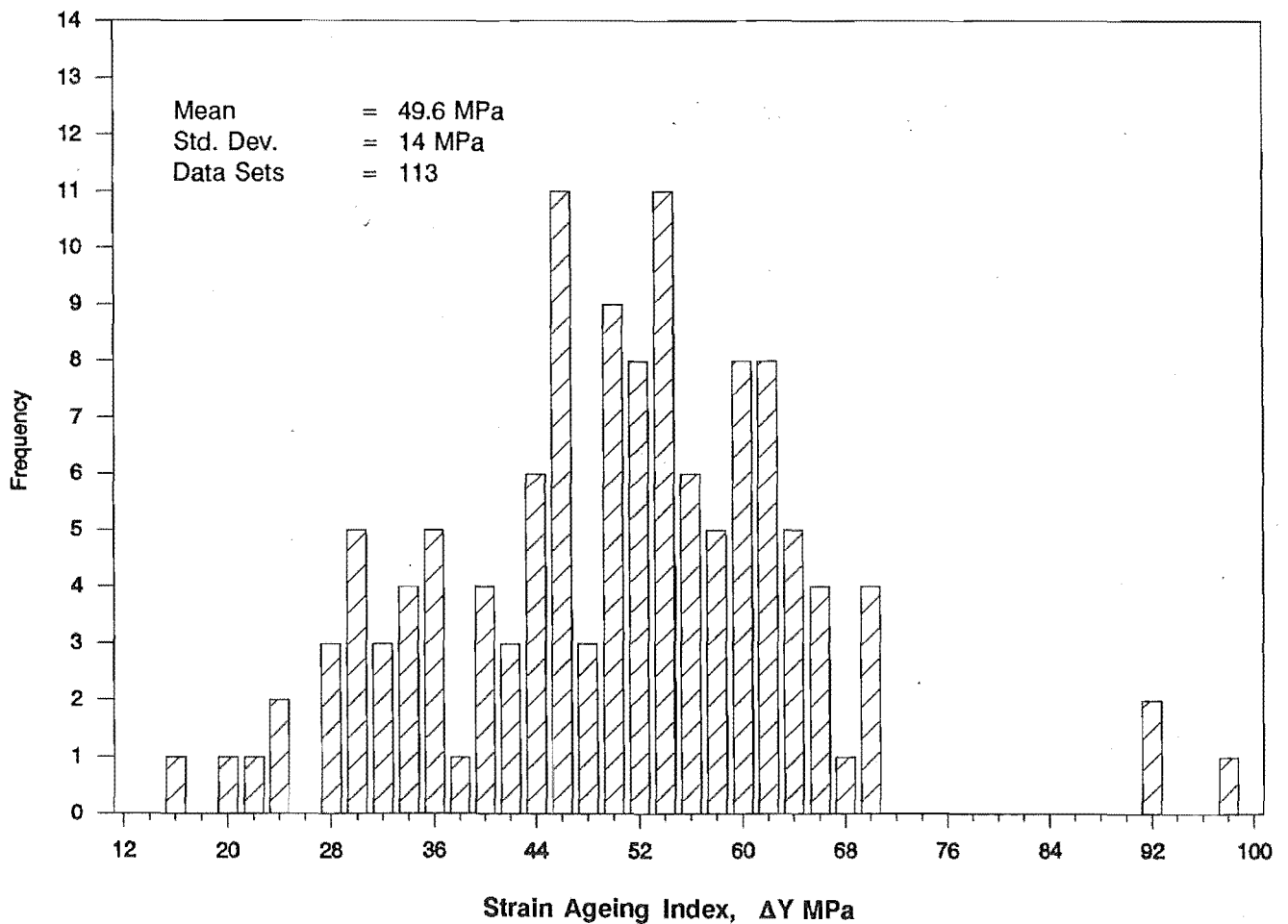


Figure 3.43: Distribution of strain ageing index ΔY of Grade 430 machined specimen data

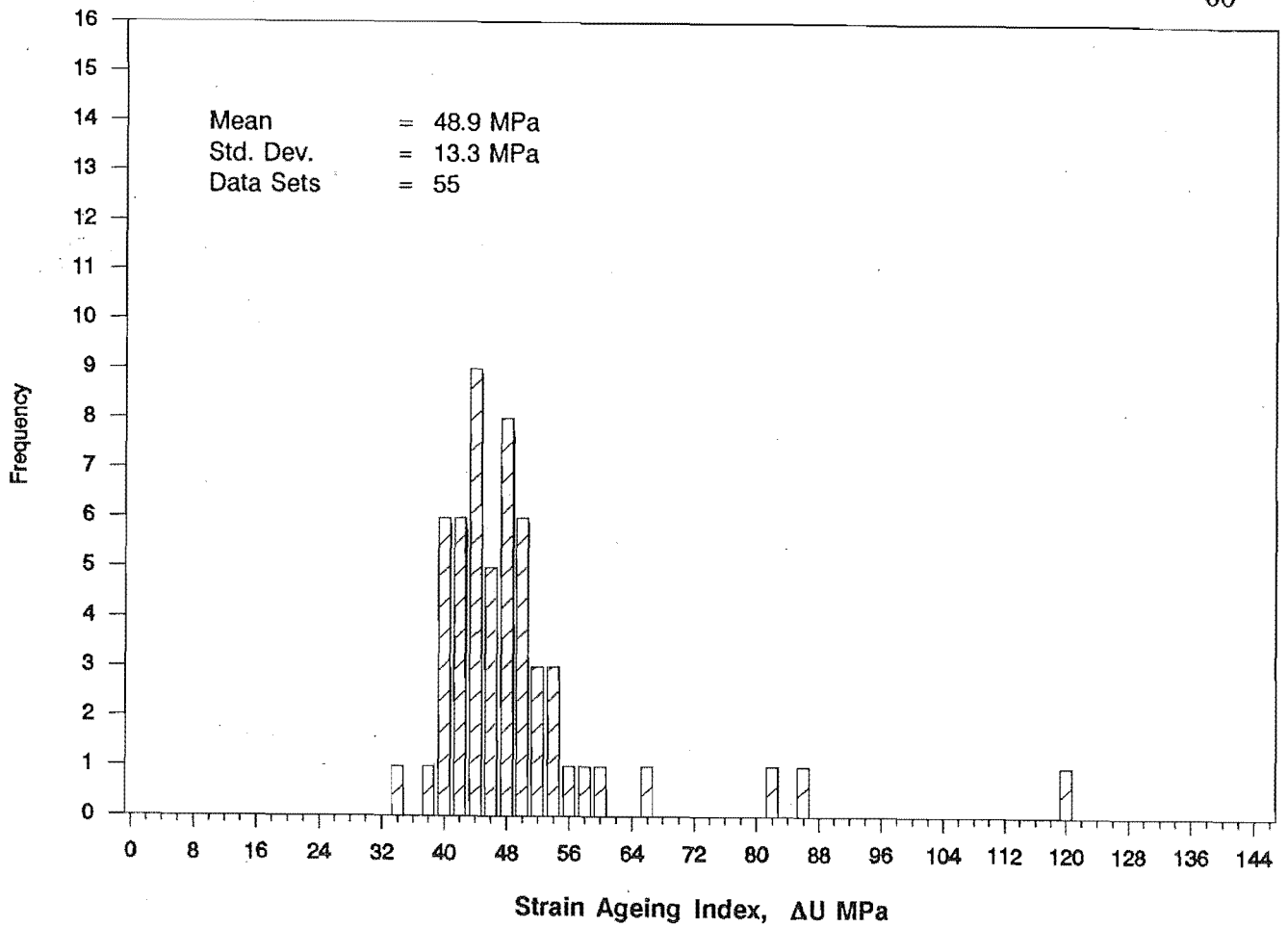


Figure 3.44: Distribution of strain ageing index ΔU of Grade 300 machined specimen data

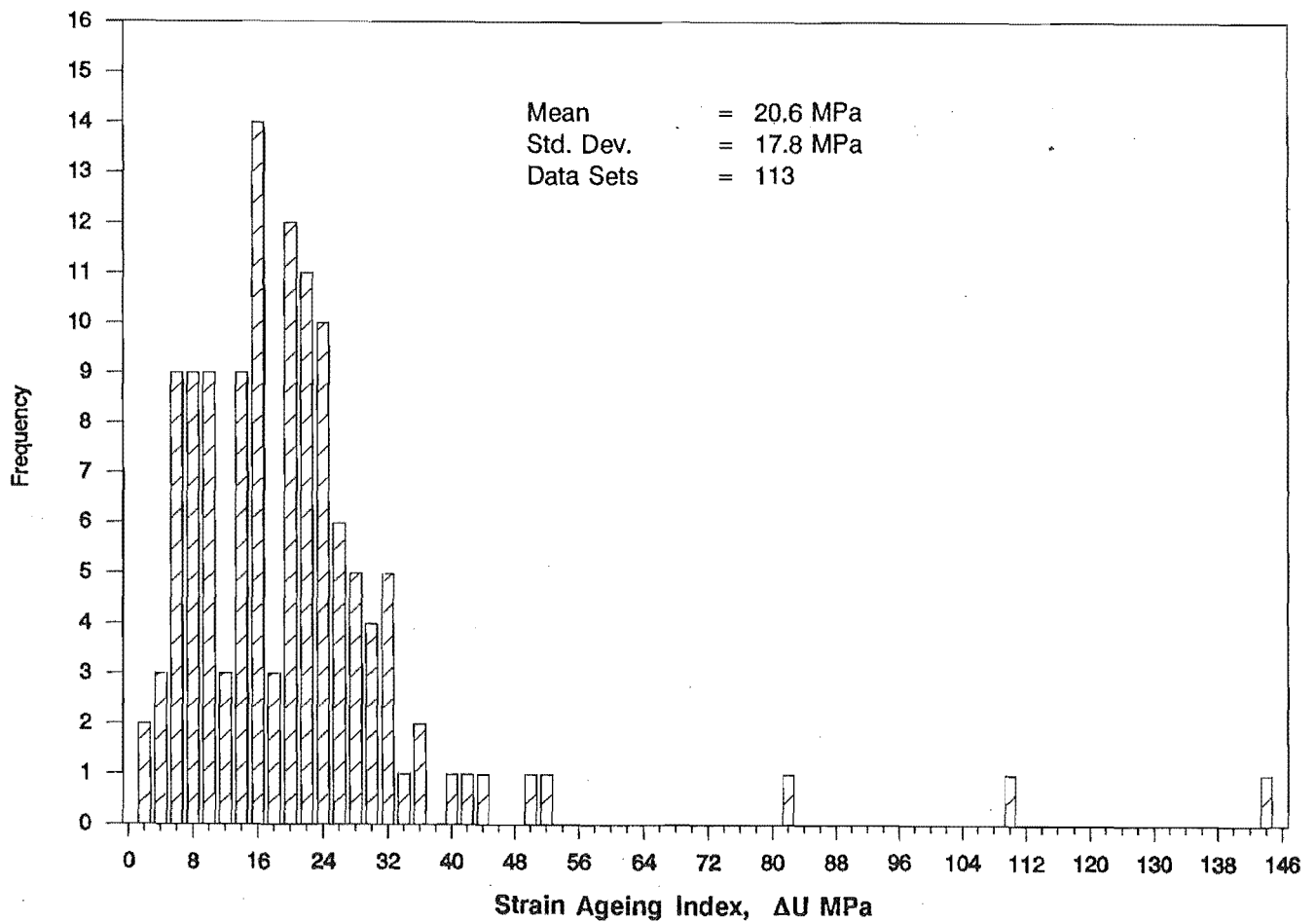


Figure 3.45: Distribution of strain ageing index ΔU of Grade 430 machined specimen data

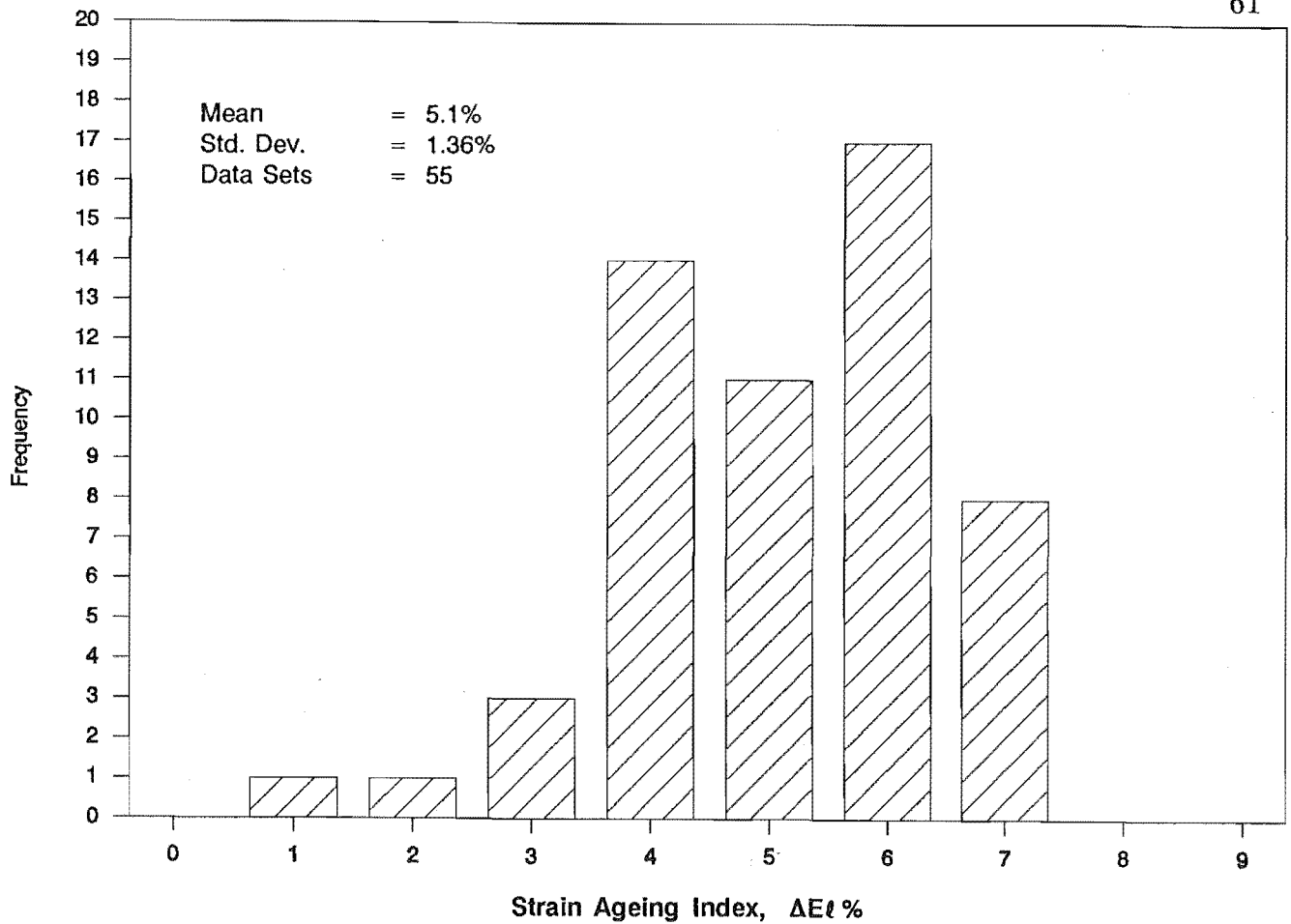


Figure 3.46: Distribution of strain ageing index $\Delta E\epsilon$ of Grade 300 machined specimen data

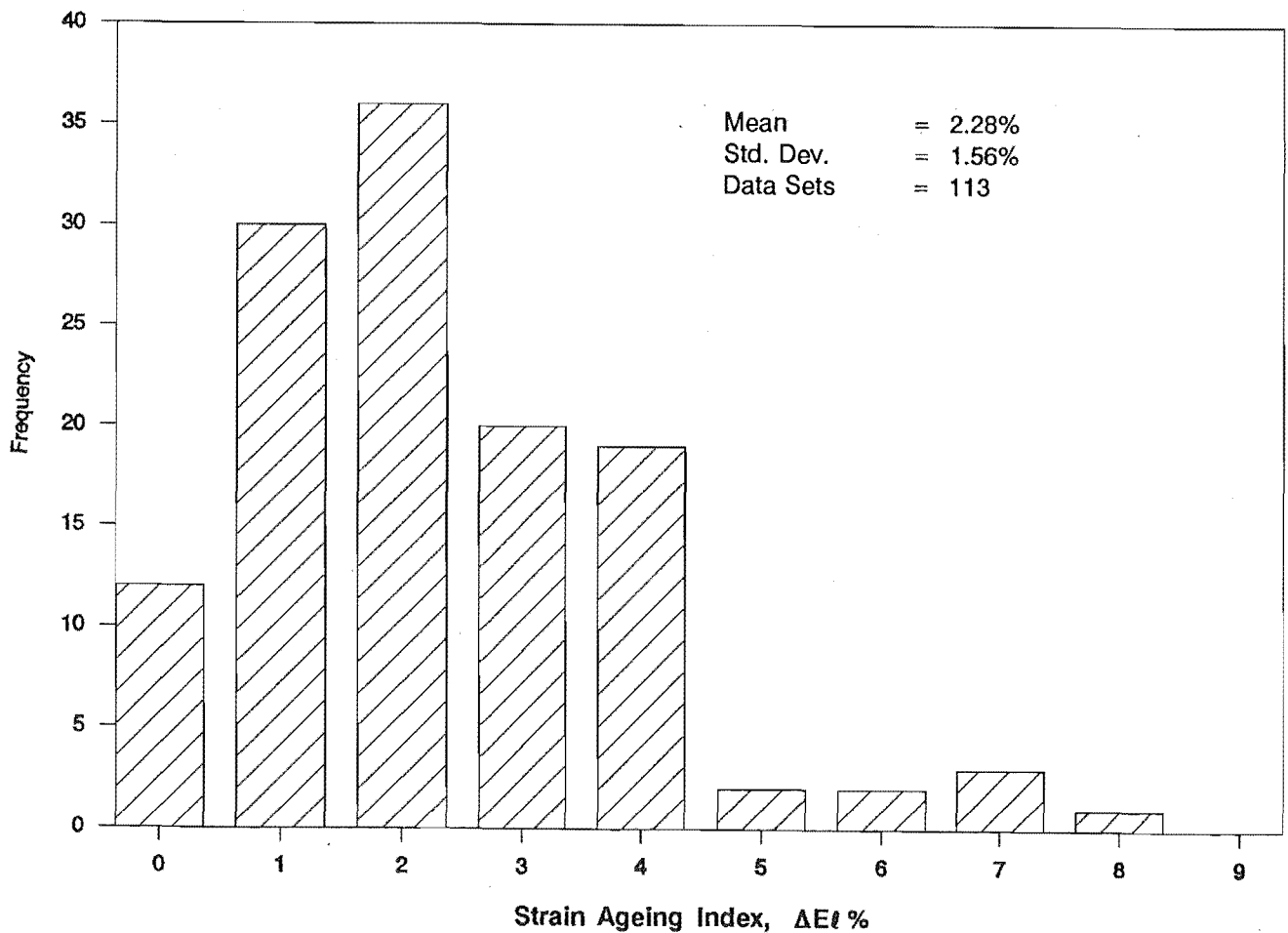


Figure 3.47: Distribution of strain ageing index $\Delta E\epsilon$ of Grade 430 machined specimen data

Table 3.12: Statistical means and ranges of ΔY , ΔU and ΔEI for Grade 300 and Grade 430 reinforcing steels

<i>Grade</i>	<i>Mean</i>	<i>Standard Deviation</i>	<i>Minimum</i>	<i>Maximum</i>
ΔY (MPa)				
300	68.7	6.8	40	86
430	49.6	14.0	15	97
ΔU (MPa)				
300	48.9	13.3	34	120
430	20.6	17.8	1	143
ΔEI (%)				
300	5.10	1.36	1	7
430	2.28	1.56	0	8

3.9 SPECIAL "LOW CARBON TRIAL HEATS"

In general, the "low carbon trial heats" samples were found to have properties quite similar to Grade 430 steel. However, results of lower yield strength and tensile strength for these samples fall in a range at the lower 'tail' of the distributions produced from Grade 430 data. On the other hand, the range of % elongation at fracture and % Luder strain of these samples was found to be at the higher 'tail' of the respective distributions. Comparatively, this steel has lower strength and higher ductility than Grade 430 because of its lower carbon content. It should be noted that the steel is micro-alloyed with vanadium and four different diameters of deformed bars were rolled from each cast number, and there is a slight difference in the carbon content between the three cast numbers of steel produced,.

The tensile results produced from different types of specimen of all the "low carbon trial heats" samples were used to investigate the significance of carbon content and bar size in the equations of lower yield strength and tensile strength obtained from the Multiple Linear Regression, which is discussed in Chapter 5.

3.10 SUMMARY

Variations in lower yield strength between different sets of data were found to be mainly caused by the different strain rates used in the tensile tests carried out at Pacific Steel Ltd and in the Materials Laboratory of the Mechanical Engineering Department. The type of test piece (i.e. machined specimen or deformed bar) also contributes to the variations, but the effect is more profound on the tensile strength and % elongation at fracture results. However, Luder strain results were found to be unaffected by these factors.

Tensile results obtained from mechanical tests of machined specimens were found to comply with the tensile properties as specified in Table 4 of NZS 3402:1989.

High strength Grade 430 reinforcing steel was found to have higher ductility and longer Luder strain than the previous Grade 380 steel. Also, the initial strain

hardening rate was found to be lower for Grade 430 steel. It is predicted that the flexural over-strength factor for Grade 430 steel will be lower than that for Grade 380 because of the improved properties.

Comparison of the strain ageing index between Grade 300 and Grade 430 steels reveals that Grade 430 reinforcing bars are less susceptible to strain ageing. The ΔY for Grade 430 steel is 50 MPa as compared to 70 MPa observed in Grade 300 steel. Strain ageing is reduced in Grade 430 steel because of the addition of approximately 0.04% vanadium. Previous investigations²⁰ have also shown that Grade 430 steel has better fracture toughness mainly attributed to the added vanadium. The statistical means and ranges of parameters measured in this study for Grade 300 and Grade 430 reinforcing steels are summarised in Tables 3.13 and 3.14.

Table 3.13 : Statistical means and ranges for parameters of Grade 300 reinforcing steel (Data Sets 55)

<i>Parameters</i>	<i>Mean</i>	<i>Standard Deviation</i>	<i>Minimum</i>	<i>Maximum</i>
Machined Specimen Data				
Lower Yield Strength (MPa)	339.8	11.90	314	373
Tensile Strength (MPa)	489.5	12.74	460	529
Elongation at Fracture (%)	34.0	1.57	30	37
Luder Strain (%)	2.0	0.27	1.2	2.7
n	0.258	0.027	0.151	0.299
k (MPa)	968.5	72.89	748	1145
ΔY (MPa)	68.7	6.79	40	86
ΔU (MPa)	48.9	13.26	34	120
ΔEI (%)	5.1	1.36	1	7
Lab Deformed Data				
Lower Yield Strength (MPa)	310.4	11.33	277	340
Tensile Strength (MPa)	431.7	31.39	365	491
Luder Strain (%)	1.9	0.30	1.2	2.7
Pacific Steel Deformed Data				
Lower Yield Strength (MPa)	329	13.00	300	372
Tensile Strength (MPa)	464.1	14.81	424	504
Elongation at Fracture (%)	32.3	2.96	24	38

Table 3.14: Statistical means and ranges for parameters of Grade 430 reinforcing steel (Data Sets 113)

<i>Parameters</i>	<i>Mean</i>	<i>Standard Deviation</i>	<i>Minimum</i>	<i>Maximum</i>
Machined Specimen Data				
Lower Yield Strength (MPa)	466.7	18.61	424	517
Tensile Strength (MPa)	633.8	27.7	490	720
Elongation at Fracture (%)	28.7	2.0	25	32
Luder Strain (%)	1.3	0.26	1	1.7
n	0.2	0.017	0.152	0.29
k (MPa)	1094.2	67.81	1000	1278
ΔY (MPa)	49.6	14.03	15	97
ΔU (MPa)	20.6	17.78	1	143
ΔEI (%)	2.28	1.56	0	8
Lab Deformed Data				
Lower Yield Strength (MPa)	438.3	26	393	502
Tensile Strength (MPa)	573	37.7	495	658
Luder Strain (%)	1.3	0.29	1	1.7
Pacific Steel Deformed Data				
Lower Yield Strength (MPa)	467.5	19.1	439	533
Tensile Strength (MPa)	606.8	22.9	575	691
Elongation at Fracture (%)	24.1	3.97	15	28

CHAPTER 4

MULTIPLE LINEAR REGRESSION^{21,22,23,24}

Regression analysis is a statistical technique for modelling and investigating the relationship between two or more variables. In general, there is a single dependent variable that is related to k independent variables, say x_1, x_2, \dots, x_k . The dependent variable y is a random variable, while the independent variables are assumed to be precisely known and are controllable by the experimenter. The relationship between these variables is characterised by a mathematical model called a regression equation.

The regression model involving only a single independent variable x is called the simple linear regression model and the regression equation is expressed as:

$$y = a + bx \quad \text{- Eqn. 4.1}$$

where

- y = estimated value of y for an observed value of x
- a = intercept, giving estimated value of y at $x = 0$
- b = slope of line, identical with regression coefficient

Equation 4.1 represents a linear regression model if the equation is a linear function of the unknown parameters a and b . This corresponds to a straight-line model in which data can be correlated by a straight line, called the regression line. The method of least squares is used to estimate parameters a and b so that the sum of squares of the deviations between the observations and the regression line (predicted value) is a minimum.

A regression model that involves more than one independent variable is called a multiple regression model. This analysis also assumes that the imprecision is associated with the dependent variable and the independent variables are the precise variables. In a manner directly analogous to that used for a simple linear regression,

in multiple linear regression, a dependent variable y may be expressed in terms of the independent variables as:

$$y = a + b_1x_1 + b_2x_2 + b_3x_3 + \dots + b_kx_k \quad \text{- Eqn. 4.2}$$

where b_1, b_2, \dots, b_k are the respective regression coefficients which are estimated using the least squares method. The term "linear" is used if the multiple regression model is linear in the parameters (b values).

Correlation coefficient (r) is a measure of the degree of relationship present between variables in a regression analysis. It is also an indication of the goodness of the fit of the regression line. The corresponding term for multiple regression is multiple correlation coefficient and is designated R .

A correlation of ± 1.0 indicates a perfect association between the variables whereas a correlation coefficient of 0.0 indicates a completely random relation. The correlation coefficient is a simple statistic for testing the significance of a simple two variables linear regression. However, in a multiple linear regression, the multiple correlation coefficient depends very much on the correlation between the independent variables. If there is a strong correlation between the independent variables, evidenced by a relatively large value of simple correlation coefficient, then the multiple correlation coefficient will not be much larger than the simple linear correlation coefficient with either variable separately. The multiple correlation coefficient only tells the overall multiple correlation irrespective of the inter-correlation that may exist between the independent variables.

Another way to test the significance of the multiple regression is by comparing the Variance ratio, F value with tables of Fisher's F at the corresponding degree of freedom. The F test tells the significance of the multiple regression at a particular probability level. Although this significance test is a test to determine the significance of a linear relationship between the dependent variable and the independent variables, it does not necessarily imply that the relationship found is an appropriate one.

Very often we are interested in testing the individual regression coefficients to evaluate the significance of the variables to the whole relation. Such tests would be useful in determining the value of each of the independent variables in the regression model. This is because the model might be more effective (signified by a higher multiple correlation coefficient and F value) with the inclusion of additional variables, or perhaps with the deletion of one or more of the variables already in the model.

The t-test is carried out by comparing the computed T value with t-test tables at (N-k-1) degrees of freedom. If the calculated value of t is below the tabulated value at the proper degree of freedom and at the significance level decided upon, then the variable could therefore be removed from the multiple regression. Adding an unimportant and insignificant variable to the regression model can actually decrease the usefulness of the model.

In a regression analysis, the regression line is only the best fit of line through all the data points so that the sum of squares of deviations between the observations and the regression line is a minimum. The estimated y values will lie exactly on the regression line but the actual y values will deviate from the line. The degree of deviation depends on the accuracy of the regression analysis. Normally, a confidence limit for the regression line is established to indicate the range that all the actual y values will lie. A confidence limit at a certain degree of confidence, say 95%, indicates the probability that all values of y lie in the listed interval is 0.95. In other words, we can assume that 95 out of every 100 results lie within these limits. The confidence limit for the regression line may be determined about y (mean) as $\pm t s$ where t is selected from the t-table at the proper degree of freedom at the desired probability level and s is the standard error of estimate.

Although multiple linear regression analysis is a very powerful technique, the significance of the analysis is a function of the selection of all the appropriate independent variables. Also, the analytical technique assumes linear relationships between dependent and independent variables. Finally, any correlation between variables defined as independent will result in uncertainty in the regression coefficients calculated and hence reduce the significance of the results. Sometimes

it is necessary to combine the variables in the regression analysis to account for any interaction between them. Although this will eliminate the inter-correlation problems between variables, it is not known which variable in the combining form is more significant to the regression analysis.

Multiple linear regression analysis reported here was carried out on the Mechanical Engineering Department Micro-Vax computer. The computer programme provides considerable diagnostic information for evaluating the regression equations. The programme also computes the statistical significance of each independent variable within the linear equation. Samples of the printout are shown in Tables 4.1 and 4.2. In the example shown in Table 4.1, comparison of the F value with Fisher's F tables²⁵ shows that the multiple regression is significant at the 1% probability level. The computed T values are compared with t-test tables²⁶ to determine the significance of the regression coefficients. From t-test tables for 50 degrees of freedom, the corresponding t values at the levels of significance are listed in Table 4.3.

Table 4.1: Multiple Linear Regression Printout 1

Dependent Variable (y)						
Variable No. 3 = Lower Yield Strength (MPa)						
Independent Variables (x)						
Variable No. 2 = bar diameter (mm)						
Variable No. 18 = % C						
Variable No. 23 = % Ni						
Variable No. 26 = % Cu						
Variable No.	Mean	Standard Deviation	Correlation X vs Y	Regression Coefficient (b)	Std. Error of Reg. Coef.	Computed T Value
2	25.45455	4.24185	- 0.27673	- 1.02129	0.39134	- 2.60970
18	0.18582	0.01931	0.02013	133.60536	85.36328	1.56514
23	0.10527	0.01359	0.34728	314.70746	122.59341	2.56708
26	0.38527	0.06292	0.11481	2.12197	26.71580	0.07943
Dependent						
3	339.78183	11.90346				
Intercept (a)		307.00443				
Multiple Correlation R		0.48076				
Std. Error of Estimate (s)		10.84707				
<u>ANALYSIS OF VARIANCE FOR THE REGRESSION</u>						
Source of Variation	Degrees of Freedom	Sum of Squares	Mean Squares	F Value		
Attributable to regression (k)	4	1768.43530	442.10883	3.75755		
Deviation from regression (N-k-1)	50	5882.94678	117.65894			
TOTAL	54	7651.38232				
From Fisher's Tables:	F 0.01,4,50	= 3.72*				
	F 0.005,4,50	= 4.23*				
* These are extrapolated values				∴ The regression is significant at 1%		

Table 4.2: Multiple Linear Regression Printout 2

Dependent Variable (y)

Variable No. 3 = Lower Yield Strength (MPa)

Independent Variables (x)

Variable No. 2 = bar diameter (mm)

Variable No. 18 = % C

Variable No. 23 = % Ni

Variable No.	Mean	Standard Deviation	Correlation X vs Y	Regression Coefficient (b)	Std. Error of Reg. Coef.	Computed T Value
2	25.45455	4.24185	- 0.27673	- 1.01584	0.38151	- 2.66269
18	0.18582	0.01931	0.02013	133.12459	84.31479	1.57890
23	0.10527	0.01359	0.34728	319.10635	108.29969	2.94651

Dependent

3 339.78183 11.90346

Intercept (a) 307.30948

Multiple Correlation R 0.48066

Std. Error of Estimate (s) 10.74088

ANALYSIS OF VARIANCE FOR THE REGRESSION

Source of Variation	Degrees of Freedom	Sum of Squares	Mean Squares	F Value
Attributable to regression (k)	3	1767.69312	589.23102	5.10747
Deviation from regression (N-k-1)	51	5883.68896	115.36645	
TOTAL	54	7651.38232		

From Fisher's Tables, F 0.005,3,51 = 4.80*
F 0.001,3,51 = 6.32*

* These are extrapolated values

∴ The regression is significant at 0.5%

Table 4.3: t values extracted from t-test tables

<i>Significance</i>	<i>t-test value</i>
50%	0.679
20%	1.299
10%	1.676
5%	2.009
2.5%	2.403
1%	2.678
0.5%	2.937

Comparison of computed T values in Table 4.1 with Table 4.3 shows that copper content has no significant effect on the lower yield strength. The correlation of carbon with lower yield strength is significant at the 20% probability level, whereas both diameter of the bar and nickel are significant at the 2.5% level. Table 4.2 shows that removing the insignificant variable (i.e. copper) from the multiple regression actually improves the overall significance of the regression to the 0.5% probability level. The computed T values for the independent variables are increased and nickel is found to have correlation with lower yield strength being significant at the 0.5% level.

In general, through a step by step elimination process of insignificant variables, the most statistically significant regression equation can be obtained. However, care should be taken in the elimination process when there is a possibility of strong inter-correlation between independent variables. This is because in some cases, the low computed T value of an independent variable is due to the strong correlation between this variable with others. Therefore, it is very helpful if the multiple linear regression computer programme does determine the correlation of one variable with respect to the others.

CHAPTER 5

MULTIPLE LINEAR REGRESSION ANALYSIS OF REINFORCING STEEL PROPERTIES

5.1 INTRODUCTION

Multiple linear regression analysis was used to study the effect of chemical composition on reinforcing bar properties. The properties investigated were as follows: lower yield strength, tensile strength, elongation at fracture, Luder strain, strain hardening exponent and coefficient, and the three strain ageing parameters ΔY , ΔU and ΔE_l . The data for these dependent properties was determined from mechanical tests of standard tensile specimen, conducted in the Materials Laboratory of the Department. The chemical composition, used as the independent variables, was obtained from analysis of each bar supplied by Pacific Steel Ltd. The regression analysis was carried out for various combinations of independent variables on the available data.

Separate regression analysis was performed on different groups of data with the first containing the 55 data sets for Grade 300 while the second has the 125 data sets associated with Grade 430. The third group was a combination of the grades containing 180 data sets. It should be noted that the data of 12 "low carbon trial heats" samples was included in the Grade 430 data group. The regression equations derived from the analysis of groups one and two were only applicable to Grade 300 and Grade 430 steels respectively. From the combined group, the resultant regression equations obtained can be used to predict the properties of general reinforcing steels within the overall range of chemical composition considered. Tables 5.1, 5.2 and 5.3 show the statistical means and ranges for the variables of the groups used in the multiple regression analysis.

Initially, multiple linear regression of bar properties was carried out against all the 11 chemical elements and the bar diameter. Using the significance of the resultant

computed t values, the insignificant independent variables were eliminated from further consideration. To determine whether inter-correlation occurred between the elements considered, as a function of property control used by the steel manufacturer, linear regression analysis was applied to specific combinations of independent variables (chemical elements). Most examples of appreciable inter-correlation occurring between elements were found insignificant in the multiple linear regression analysis. In the analysis of lower yield strength, the carbon equivalent ($CEQ = \% C + \frac{\% Mn}{6}$) was also used. Since no inter-correlation was found between carbon and manganese, this was considered unnecessary and carbon and manganese were subsequently treated as separate independent variables in the remaining analysis.

The results of multiple linear regression analysis for bar properties are presented in this chapter. The linear equations provide an indication of how the various bar properties were affected by the presence of the different elements and the bar diameter.

Table 5.1: Statistical means and ranges for variables of Grade 300 reinforcing steel examined by multiple linear regression (Date sets 55)

<i>Variable</i>	<i>Mean</i>	<i>Standard Deviation</i>	<i>Minimum</i>	<i>Maximum</i>
DEPENDENT VARIABLES				
Lower Yield Strength MPa	339.8	11.90	314	373
Tensile Strength MPa	489.5	12.70	460	529
Elongation at Fracture %	34.0	1.57	30	37
Luder Strain %	2.0	0.27	1.2	2.7
n	0.258	0.027	0.151	0.299
k	968.5	72.89	748	1145
ΔY MPa	68.7	6.80	40	86
ΔU MPa	48.96	13.26	34	120
ΔEI %	5.11	1.36	1	7
INDEPENDENT VARIABLES				
C %	0.1858	0.0193	0.15	0.24
Mn %	0.5651	0.0526	0.49	0.82
Si %	0.1564	0.0325	0.11	0.33
S %	0.0328	0.0075	0.019	0.044
P %	0.0236	0.0089	0.009	0.05
Ni %	0.1053	0.0136	0.09	0.16
Cr %	0.0938	0.0227	0.05	0.15
Mo %	0.0166	0.0026	0.011	0.023
Cu %	0.3853	0.0629	0.24	0.56
Sn %	0.0358	0.0055	0.02	0.056
V %	0.0027	0.0009	0.001	0.007
CEQ %	0.2935	0.0308	0.24	0.37

Table 5.2: Statistical means and ranges for variables of Grade 430 reinforcing steel examined by multiple linear regression (Data sets 125)

<i>Variable</i>	<i>Mean</i>	<i>Standard Deviation</i>	<i>Minimum</i>	<i>Maximum</i>
DEPENDENT VARIABLES				
Lower Yield Strength MPa	460.90	25.38	395	517
Tensile Strength MPa	626.10	35.87	496	720
Elongation at Fracture %	28.74	1.99	25	35
Luder Strain %	1.30	0.26	1.0	2.1
n	0.20	0.017	0.152	0.290
k MPa	1094.3	67.81	905	1278
ΔY MPa	49.6	14.03	15	97
ΔU MPa	20.60	17.78	1.0	143
ΔEI %	2.28	1.56	0	8.0
INDEPENDENT VARIABLES				
C %	0.2000	0.028	0.11	0.25
Mn %	1.2542	0.075	1.12	1.50
Si %	0.3265	0.0354	0.23	0.44
S %	0.0324	0.0065	0.011	0.047
P %	0.0254	0.0078	0.011	0.049
Ni %	0.1038	0.0150	0.08	0.16
Cr %	0.0983	0.0195	0.05	0.15
Mo %	0.0171	0.0035	0.011	0.027
Cu %	0.3861	0.0772	0.24	0.75
Sn %	0.0346	0.0045	0.026	0.049
V %	0.0403	0.0038	0.033	0.056
CEQ %	0.4255	0.0445	0.31	0.52

Table 5.3: Statistical means and ranges for variables of combined grades (Grade 300 and Grade 430) examined by multiple linear regression (Data sets 180)

<i>Variable</i>	<i>Mean</i>	<i>Standard Deviation</i>	<i>Minimum</i>	<i>Maximum</i>
DEPENDENT VARIABLES				
Lower Yield Strength MPa	423.9	60.15	314	517
Tensile Strength MPa	584.3	70.14	460	720
Elongation at Fracture %	30.4	3.07	25	37
Luder Strain %	1.53	0.43	1.0	2.7
n	0.218	0.034	0.151	0.299
k MPa	1055.8	90.34	748	1278
ΔY MPa	55.4	15.11	15	97
ΔU MPa	29.3	21.0	1.0	143
ΔEI %	3.14	1.99	0	8
INDEPENDENT VARIABLES				
C %	0.1956	0.0265	0.11	0.25
Mn %	1.0437	0.3256	0.49	1.50
Si %	0.2745	0.0858	0.11	0.44
S %	0.0325	0.0068	0.011	0.047
P %	0.0246	0.0082	0.009	0.05
Ni %	0.1043	0.0146	0.08	0.16
Cr %	0.0969	0.0206	0.05	0.15
Mo %	0.0169	0.0032	0.011	0.027
Cu %	0.3858	0.0730	0.24	0.75
Sn %	0.0350	0.0048	0.02	0.056
V %	0.0288	0.0176	0.001	0.056
CEQ %	0.3852	0.0734	0.24	0.52

5.2 THE REGRESSION OF LOWER YIELD STRENGTH

The regression analysis of the 55 sets of data for Grade 300 reinforcing steel yielded the following equation:-

$$\text{LYS (MPa)} = 133(\%C) - 1.0(d) + 319(\%Ni) + 307 \quad \text{- Eqn. 5.1}$$

(10%) (1%) (0.5%)

Equation 5.1 is significant at the 0.5% level, i.e. such a high degree of correlation will only occur by chance once in two hundred times. The significance levels of the regression coefficients are shown below the respective parameters. The parameter d is the nominal diameter of the reinforcing bar in mm.

On examination of Grade 430 steel, the 125 sets of data gave the following equation:-

$$\text{LYS(MPa)} = 523(\%C) + 105(\%Mn) - 0.97(d) + 43(\%Cu) + 750(\%V) + 203$$

(>0.00002%) (0.02%) (0.01%) (10%) (20%)

- Eqn. 5.2

The F-value (Variance ratio) of the equation is 31.58. Unfortunately, the highest significance level listed in the obtainable Fisher's F tables²⁵ is 0.1% with the corresponding F-value of 11.38 at 120 degrees of freedom. As a result, the exact significance level of Equation 5.2 cannot be established. The equation is therefore assumed to be significant at a level much greater than 0.1%. The carbon coefficient was found to be significant at a very high level, better than 0.00002% as indicated, which is the highest significance level listed in the t-test tables²⁶.

The analysis was repeated using the carbon equivalent ($\text{CEQ} = \%C + \frac{\%Mn}{6}$) to substitute for $\%C$ and $\%Mn$ and Equation 5.3 was obtained.

$$\text{LYS(MPa)} = 313(\text{CEQ}) - 1.10(d) + 80(\%Cu) + 1323(\%V) + 272 \quad \text{- Eqn. 5.3}$$

(>0.00002%) (0.001%) (0.05%) (0.5%)

Equation 5.3 is significant at a level greater than 0.1% (F-value is 34) and it can be seen that all parameters are more significant when compared to Equation 5.2. The regression coefficients for copper and vanadium are approximately twice those of Equation 5.2, whereas the regression coefficient for bar diameter and the constant of the equation are only slightly higher.

It was found that the %C and %Mn in Equation 5.2 contributed 236.3 MPa to the lower yield strength value, whereas the carbon equivalent in Equation 5.3 gave a contribution of 133.2 MPa, using calculations based on the mean values in Table 5.2. With these mean values and incorporating the bar diameter of 32 mm in Equations 5.2 and 5.3, lower yield strengths of 455.1 MPa and 454.2 MPa were predicted respectively. Therefore the difference in the apparent contributions of the carbon equivalent as opposed to the %C and %Mn is compensated by the regression coefficients of the other parameters.

In the regression of the Grade 430 data, carbon equivalent as the combined form of carbon and manganese can be used to substitute for them, since the two elements are respectively important and significant as shown in Equation 5.2. However, when carbon equivalent was used in the regression of the Grade 300 data, the variable was found to be very insignificant because there was no correlation with manganese in the analysis as shown in Equation 5.1.

The regression analysis of the 180 sets of the combined data yielded Equations 5.4 and 5.5.

$$\begin{aligned} \text{LYS(MPa)} = & 469(\%C) + 98(\%Mn) - 1.11(d) + 46(\%Cu) + 1253(\%V) + 205 \\ & (>0.00002\%) \quad (0.001\%) \quad (0.00005\%) \quad (1\%) \quad (0.2\%) \end{aligned}$$

- Eqn. 5.4

$$\begin{aligned} \text{LYS(MPa)} = & 281(\text{CEQ}) - 1.26(d) + 71(\%Cu) + 2226(\%V) + 256 \\ & (>0.00002\%) \quad (0.00002\%) \quad (0.01\%) \quad (>0.00002\%) \end{aligned}$$

- Eqn. 5.5

The above equations are very similar to Equation 5.2 and 5.3, with variations in the regression coefficients and appreciable improvements in the significance of these coefficients. In general, with the exception of vanadium, the regression coefficients of the remaining parameters and the constants of Equations 5.4 and 5.5 are of the same order of magnitude as those in Equations 5.2 and 5.3. The regression coefficients of copper and vanadium in Equation 5.4 are approximately twice those in Equation 5.5 and the coefficient of bar diameter and the constant are slightly higher. This phenomenon is very similar to that observed in Equations 5.2 and 5.3 for the Grade 430 data.

Generally, the equations obtained from the regression of the combined data can be seen to follow the trend of the Grade 430 equations. The 55 data sets of Grade 300 steel are less influential in contributing any significant parameter in the regression results. For instance, the significance of nickel has vanished in analysing the combined data. In this case, Grade 300 data was found mainly to affect the magnitude of the regression coefficients, particularly the vanadium coefficient.

Figures 5.1 and 5.2 respectively show the calculated lower yield strength (using Equation 5.4 and 5.5) plotted against the experimental lower yield strength and the 95% confidence limits of ± 31.2 MPa and ± 32.6 MPa. Grouping of the "low carbon trial heats" results can be seen in the lower strength range of Grade 430 data in Figures 5.1 and 5.2.

The significance levels of the parameters in equations for Grade 300 steel are much lower than those of equations for Grade 430 steel which in turn are lower than equations obtained from the combined data. This is mainly a function of the increasing number of data sets used in the analysis.

Although equations involving the carbon equivalent predict the same results and are as significant as the equations with separate carbon and manganese percentages, the latter equations are preferable because the significance of these individual elements can be assessed. It should be noted that the regression equations were obtained using statistical techniques based on the available data. As a result, the significance

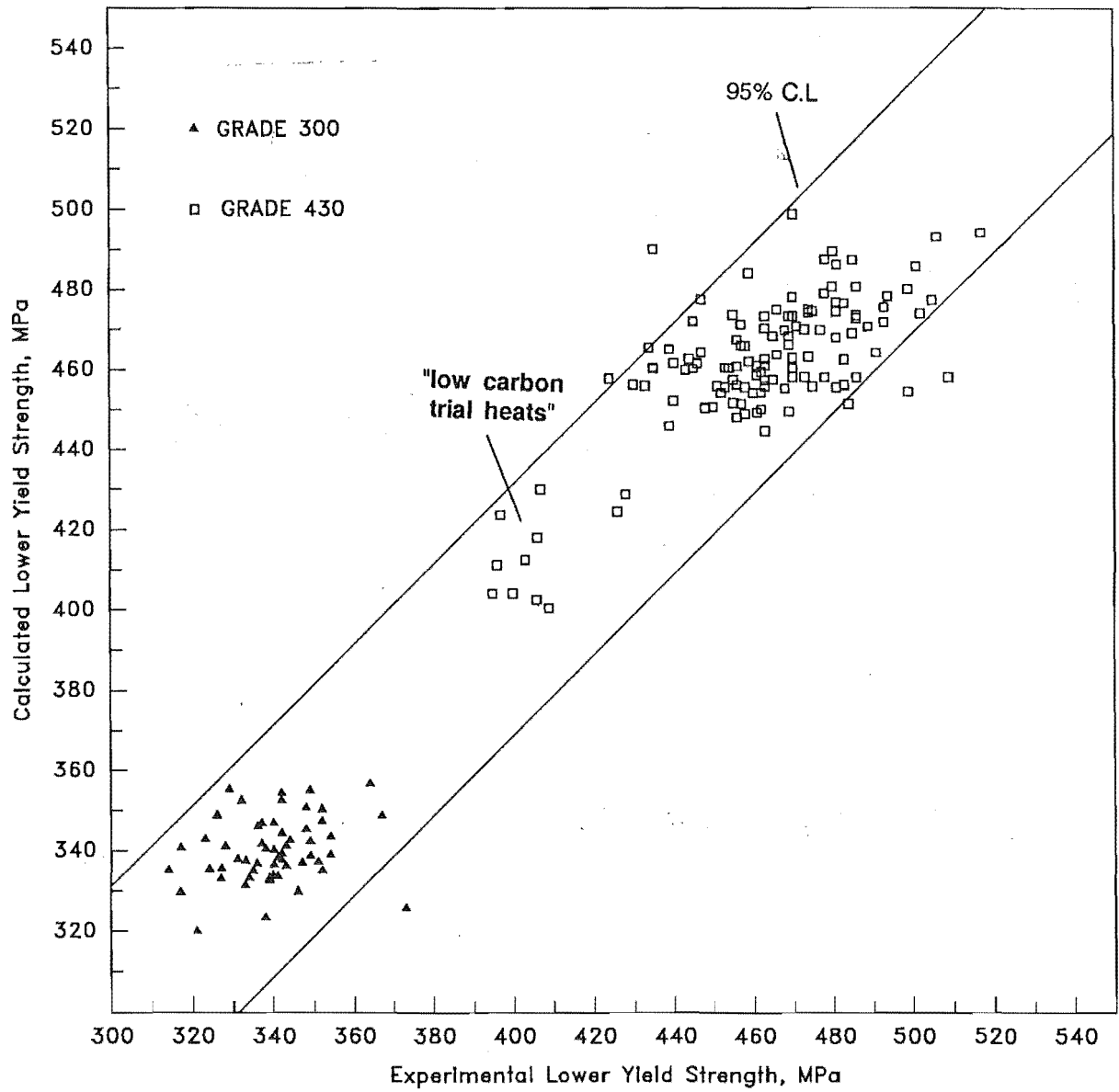


Figure 5.1: Calculated and observed lower yield strength for Grade 300 and Grade 430 reinforcing steels using Equation 5.4

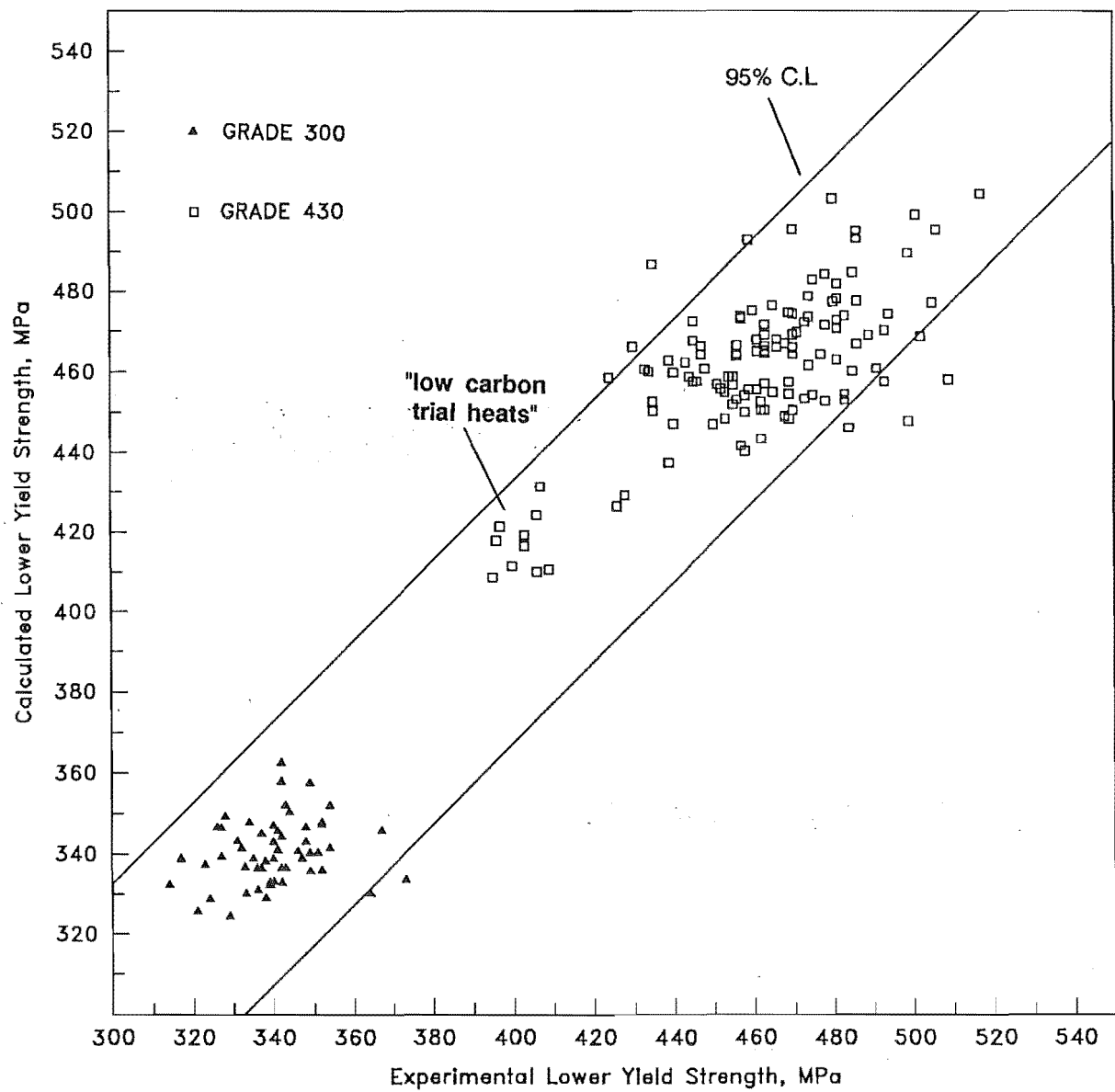


Figure 5.2: Calculated and observed lower yield strength for Grade 300 and Grade 430 reinforcing steels using Equation 5.5

of the coefficients is a function of the limited variation in specific elements in the regression analysis.

Examination of the regression equations reveals that all the parameters, with the exception of the bar diameter, have positive coefficients. This means that an increase in the values of these parameters results in an increase in the lower yield strength. However, increasing the bar diameter reduces the lower yield strength. The regression coefficient for bar diameter was found to be approximately constant.

The ferrite grain size is known^{27,28} to have a dominant influence on the lower yield strength of low carbon steels (i.e. reinforcing steels). While carbon and manganese content influence grain size, the major factor is cooling rate. It is believed that the bar diameter is related to the grain size. Since the surface area to volume ratio is inversely proportional to bar diameter, the smaller the bar diameter, the greater the cooling rate, assuming the energy transfer per unit surface area remains constant. Hence the smaller diameter bar would exhibit a finer ferrite grain size with an associated increase in lower yield strength. The same phenomenon, that decreasing the diameter of the bar on average increases the lower yield strength, was also reported by Sage²⁹. It was found²⁹ that a difference of about 30 MPa was produced by reducing the diameter from 30 mm to 18 mm in rolled bars with a base composition of 0.24%C, 1.25%Mn and 0.475%Si. The regression coefficient for bar diameter in Equation 5.4 predicts an increase of only 13 MPa. The discrepancy could be a function of differences in rolling practices used.

The grain size is also influenced by the rolling temperature and the reduction in cross-section imparted to the bar through the rolling passes. These factors affect the cooling rate and are known³⁰ to vary considerably within any one steel mill. Since grain size was not determined in this investigation, the bar diameter can be regarded as an indicator of grain size.

The effect of carbon content on the lower yield strength is related to the ferrite grain size³¹. Carbon is a strong austenite stabilizer and increasing the carbon content will increase the pearlite volume fraction as well as lowering the transformation temperature^{32,33} and consequently decreasing the ferrite grain size. The combination

of lower transformation temperature and increased carbon content will provide more nucleation sites during the transformation process with the grain size being further reduced. Since the mean carbon content of both grades of steel is approximately the same at 0.2%, ideally the strength increase due to carbon would be consistent. The discrepancy in the regression coefficients for carbon between Equations 5.1 and 5.2 could be a function of the inclusion of manganese in the analysis for Grade 430 as opposed to ignoring it for Grade 300.

Manganese increases the strength through its solid-solution strengthening effect, by refining the ferrite grain size and by increasing the volume fraction of pearlite³¹. The regression coefficient for manganese in Equation 5.2 shows that an increase of 11 MPa in lower yield strength can be expected for Grade 430 steel by increasing the manganese content in steel by 0.1%. However, there is no correlation with manganese in Equation 5.1. When manganese was included as a variable in the regression of Grade 300 data, the element proved to have very low significance. This could be a function of the confined range of manganese in the steel. The mean manganese content was found to be 0.56% with a standard deviation of 0.05%.

It is also probable that the variations caused by manganese are being masked by the effect of variations in nickel content, as nickel was found to be significant in Equation 5.1. Nickel is one of the residual elements present in the steel and has an ability in refining grain size which leads to an increase in strength and toughness. The increase in lower yield strength predicted by Equation 5.1 is equivalent to 22 MPa when increasing nickel from the data minimum (0.09%) to the maximum (0.16%).

Copper, rather than nickel, is the residual element found to be significant in the regression analysis of Grade 430 data. Equation 5.2 predicts that for every 0.1% increase in copper, the lower yield strength increases by 4.3 MPa. This figure compares well with the data extracted from a research report by Pui³⁴ where 0.1% copper was found to increase the lower yield strength by 4 MPa.

In the analysis, the strength increase due to nickel and copper corresponds well with the general consensus that steel of commercial heats made from scrap steel gives an

increased lower yield strength due to the hardening effect of the residual elements; chromium, copper and nickel.

The other important element to be considered is vanadium because of its relatively high positive regression coefficient. However, no correlation with vanadium was obtained in Grade 300 steel. This is not surprising when considering the mean vanadium content of 0.003% in the steel. The strengthening effect of vanadium is due to both grain refinement and precipitation hardening. Depending on the relative amounts of carbon and nitrogen in steel, the precipitating phase is predominantly either vanadium carbide or vanadium nitride. The precipitation strengthening effect depends on the degree of dispersion of the precipitated particles³³. Comparatively, vanadium nitrides have a lower solubility in ferrite and are more stable in resisting particle coarsening. For this reason, precipitation of vanadium nitrides rather than carbides gives a greater strengthening effect. These fine, second-phase vanadium nitride precipitates can further inhibit grain boundary movement and consequently lead to finer grain size. The effectiveness of vanadium can be further enhanced through an increased nitrogen content which would promote vanadium nitride precipitation. The work of Sage²⁹ revealed that by increasing the nitrogen content from 0.007% to 0.015%, the strength can be increased by about 50 MPa, regardless of vanadium content. Therefore, it is obvious that the interaction and relative amounts of vanadium and nitrogen are important.

The mean lower yield strength of 466.7 MPa for Grade 430 reinforcing steel compares well with the figure of 472 MPa obtained by Sage²⁹ from the 30 mm reinforcing bars with a composition of 0.24% C, 1.25% Mn, 0.45% Si, 0.05% V and 0.007% N. The regression coefficient for vanadium in Equation 5.2 predicts an increase of 75 MPa in lower yield strength for every increase of 0.1% vanadium. When compensating for the variation in the chemical composition, this figure shows reasonable agreement with the data extracted from the work of Pussegoda¹¹ where increasing the vanadium content to 0.1% in a steel of composition 0.21% C, 0.44% Mn, 0.18% Si, 0.036% S and 0.006% N was found to raise the lower yield strength by approximately 100 MPa.

Consider Equation 5.4 obtained from the regression of the combined data to predict the lower yield strength of Grade 300 and Grade 430 reinforcing steels. Since the carbon contents of the Grade 300 and Grade 430 steels are approximately constant at 0.2%, the observed increase in lower yield strength can be attributed to the increase in manganese and vanadium contents. The increase in the mean manganese content from 0.57% in the Grade 300 to 1.25% in the Grade 430 is responsible for 68 MPa of the predicted lower yield strength enhancement, while the addition of approximately 0.04% vanadium contributes 50 MPa.

To assess the effects of bar diameter and carbon content on lower yield strength, the composition of each cast number of the "low carbon trial heats" in Table A.3 was substituted in Equation 5.2 to predict the lower yield strength for different bar sizes. Figure 5.3 shows the calculated lower yield strength and the experimental lower yield strength plotted against four different bar diameters from these samples. As shown in Figure 5.3, the predicted lines do not correspond well with the experimental data. This is mainly because there are too few experimental points to clearly reveal the predicted trend. Equation 5.2 was statistically obtained from the regression of a reasonably large number of data sets, therefore the prediction only represents the general trend of a large sample size.

5.3 THE REGRESSION OF TENSILE STRENGTH

The regression of tensile strength against the chemical composition using the 55 sets of data for Grade 300 steel yielded the following equation:-

$$\text{TS(MPa)} = 264(\%C) + 103(\%Si) + 424 \quad \text{- Eqn. 5.6}$$

(0.2%) (5%)

The regression equation produced by the Grade 430 data is:

$$\text{TS(MPa)} = 695(\%C) + 141(\%Mn) - 0.87(d) + 66(\%Cu) + 768(\%V) + 277$$

(>0.00002%) (0.2%) (2%) (10%) (20%)

- Eqn. 5.7

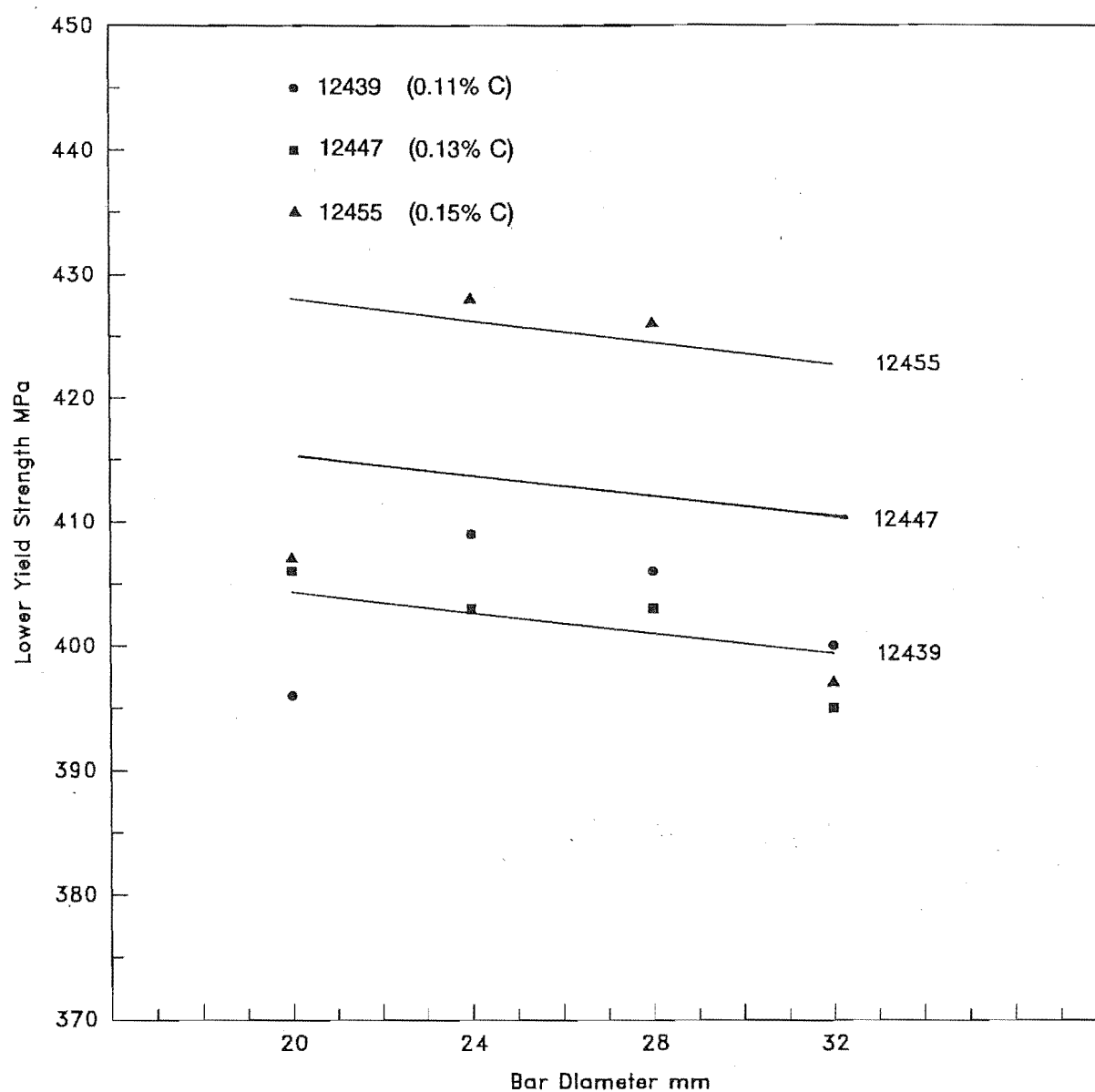


Figure 5.3: Calculated and observed lower yield strength for "low carbon trial heats" using Equation 5.2

When the regression was carried out on the 180 sets of the combined data, Equation 5.8 was obtained.

$$\text{TS(MPa)} = 659(\%C) + 131(\%Mn) - 0.92(d) + 62(\%Cu) + 992(\%V) + 290$$

(>0.00002%) (0.005%) (0.2%) (2%) (10%)

- Eqn. 5.8

Equations 5.7 and 5.8 are significant at a level much greater than 0.1%. Both equations are very similar with only minor alterations in the regression coefficient. As seen earlier in the case of the lower yield strength equations, Equation 5.8 is mainly influenced by Grade 430 data. Figure 5.4 shows the tensile strength calculated from Equation 5.8 plotted against the experimental tensile strength, with the 95% confidence limits of ± 45 MPa. As expected, grouping of the "low carbon trial heats" data can be seen in the lower strength range of Grade 430 data from Figure 5.4.

Equations 5.7 and 5.8 show the adverse effect of increasing bar diameter on tensile strength. However, bar diameter was found to be significant only at the 50% level for Grade 300 steel and was dropped from the analysis. The bar diameter would affect the tensile strength in the same way as it does on the lower yield strength, but at a lower magnitude as revealed by the lower regression coefficient for bar diameter in Equations 5.7 and 5.8. This is because bar diameter is related to ferrite grain size and generally ferrite grain size has less effect on tensile strength than it does on the lower yield strength³⁵.

Carbon was found to be the most significant parameter in Equations 5.7 and 5.8, followed by manganese. Carbon and manganese were found in the regression equations associated with tensile strength in most of the published reports^{27,30,31}. The absence of correlation with manganese in Equation 5.6 is probably due to the narrow range of manganese in the steel data. Increasing carbon and manganese is known to raise the tensile strength³¹. The strengthening mechanism is basically similar to that for the lower yield strength. The discrepancy in the regression coefficients for carbon between Equations 5.6 and 5.7 is probably a result of the small sample size for Grade 300 and limited range of carbon contents.

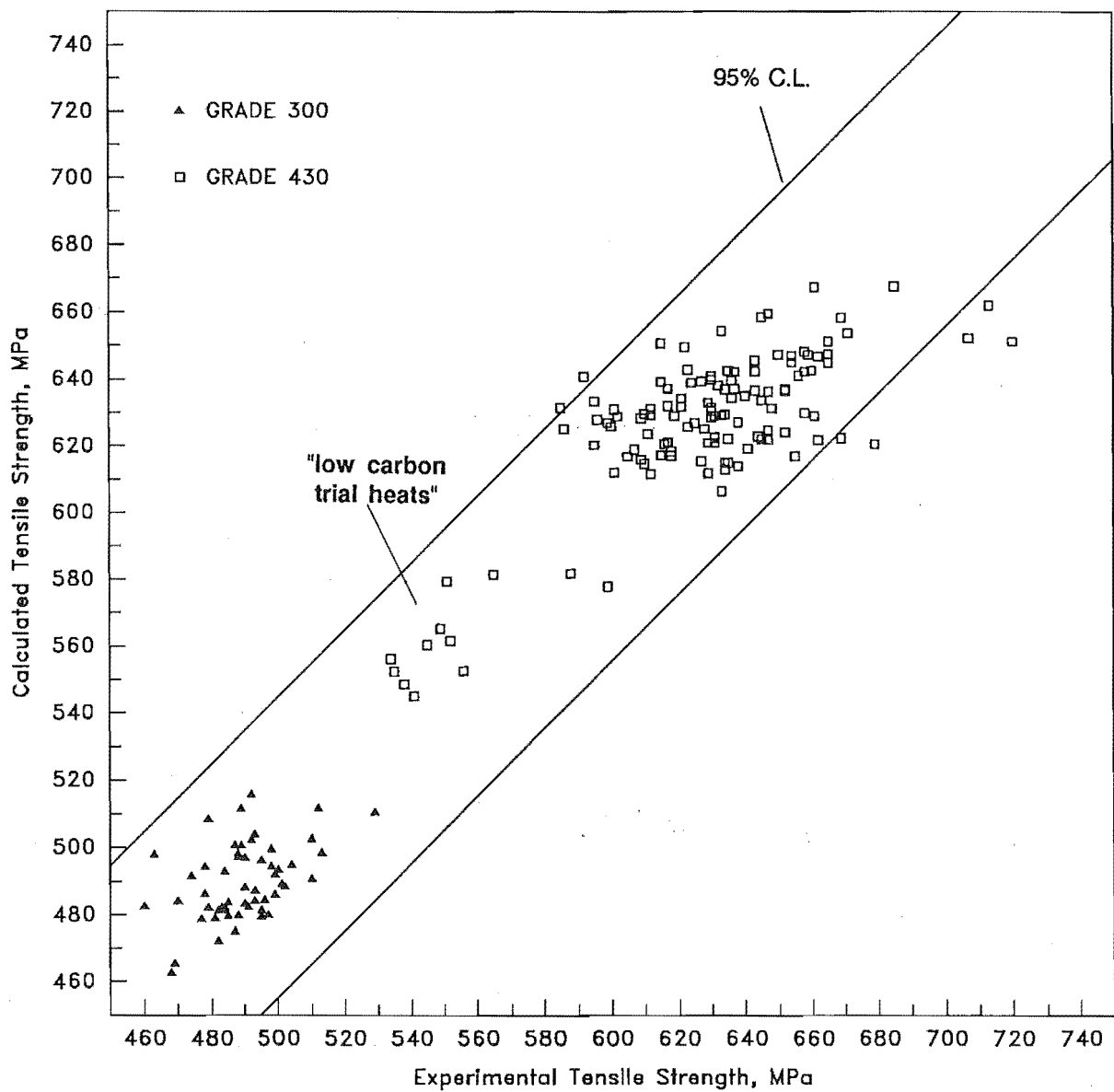


Figure 5.4: Calculated and observed tensile strength for Grade 300 and Grade 430 reinforcing steels using Equation 5.8

The regression coefficient for manganese in Equation 5.8 corresponds to an increase in tensile strengths of 74 MPa and 164 MPa when considering the mean manganese content of Grade 300 and Grade 430 steels respectively. The variation in manganese content is partly responsible for the observed increase in tensile strength of Grade 430 steel.

Silicon was found to be significant in the analysis of Grade 300 data (see Equation 5.6). However, there was no correlation with silicon in the regression of Grade 430 and the combined data, as shown in Equations 5.7 and 5.8. It could be due to the narrow range of the silicon content as the ratio of standard deviation to mean for silicon in Grade 300 is 0.2 while it is 0.1 in Grade 430. It is also probable that the significance of silicon is being masked by the considerable contribution from the variation of manganese. Silicon is known^{36,37} to improve strength through substitutional solution hardening mechanism and by inhibiting grain growth. Anya et al³⁸ showed that the increase in strength of steels containing up to 0.78% Si can also be attributed to the reduction of the interlamellar spacing of the cementite in the pearlite colonies, caused by the precipitation of α - Si_3N_4 . This microstructural feature has been observed in steels containing 0.13% C and 0.31% - 0.78% Si³⁸. The regression coefficient for silicon in Equation 5.6 corresponds to 16 MPa when considering the mean silicon content of 0.16% for Grade 300 steel.

As shown in Equations 5.7 and 5.8, there is a noticeable general increase in tensile strength with increasing copper content. For every 0.1% increase in copper, the tensile strength is predicted to increase by approximately 7 MPa. This increase is however 2.4 times less than the figure extracted from the work of Pui³⁴. The persistent correlation of copper and tensile strength in both cases has been beneficial. However, the presence of copper in reinforcing bars has been found³⁴ to have a detrimental effect on surface cracking at high temperature, leading to poor hot-workability.

Equations 5.7 and 5.8 reveal the correlation of vanadium with tensile strength. The increase of 8 MPa for every increase of 0.01% vanadium predicted by Equation 5.7 shows good agreement with Pussegoda's results¹¹, where tensile strengths of 0.2% C, 0.44% Mn, 0.17% Si and 0.006% N steels were found to increase linearly with

vanadium content, with an increase of 0.01% vanadium corresponding to an increase of approximately 10 MPa in tensile strength. Vanadium gives rise to an increase in tensile strength by the same mechanism which affects the lower yield strength, i.e. through precipitation hardening as well as grain refinement. The addition of 0.04% vanadium in Grade 430 steel also contributes to the observed increase in tensile strength of the steel.

Figure 5.5 shows the predicted tensile strengths from Equation 5.7 and the experimental tensile strengths of the "low carbon trial heats" samples plotted against bar diameter. As in the case of lower yield strength (see Figure 5.3), the experimental points do not correspond with the predicted results. The adverse effect of bar diameter on tensile strength is not clearly revealed mainly because there are too few experimental points. However, samples of higher carbon content can be seen to have higher tensile strength.

5.4 THE REGRESSION OF ELONGATION AT FRACTURE

The regression analysis carried out on data sets of Grade 300 and Grade 430 reinforcing steels yielded Equations 5.9 and 5.10 respectively:

$$\text{Elongation at Fracture}(\%) = 46 - 28(\%C) - 0.18(d) - 4.8(\%Cu) \\ (0.2\%) \quad (0.005\%) \quad (10\%) \quad - \text{Eqn. 5.9}$$

$$\text{Elongation at Fracture}(\%) = 44.4 - 28(\%C) - 4.6(\%Mn) - 0.10(d) - 96(\%Mo) \\ (>0.00002\%) \quad (2\%) \quad (0.001\%) \quad (2\%) \\ - \text{Eqn. 5.10}$$

The F-value for the equations were found to be 22 and 24 respectively, therefore, these equations are assumed to be significant at a level much greater than 0.1%.

From the regression of the combined data, an equation similar to Equation 5.10, but with an additional term for vanadium was obtained.

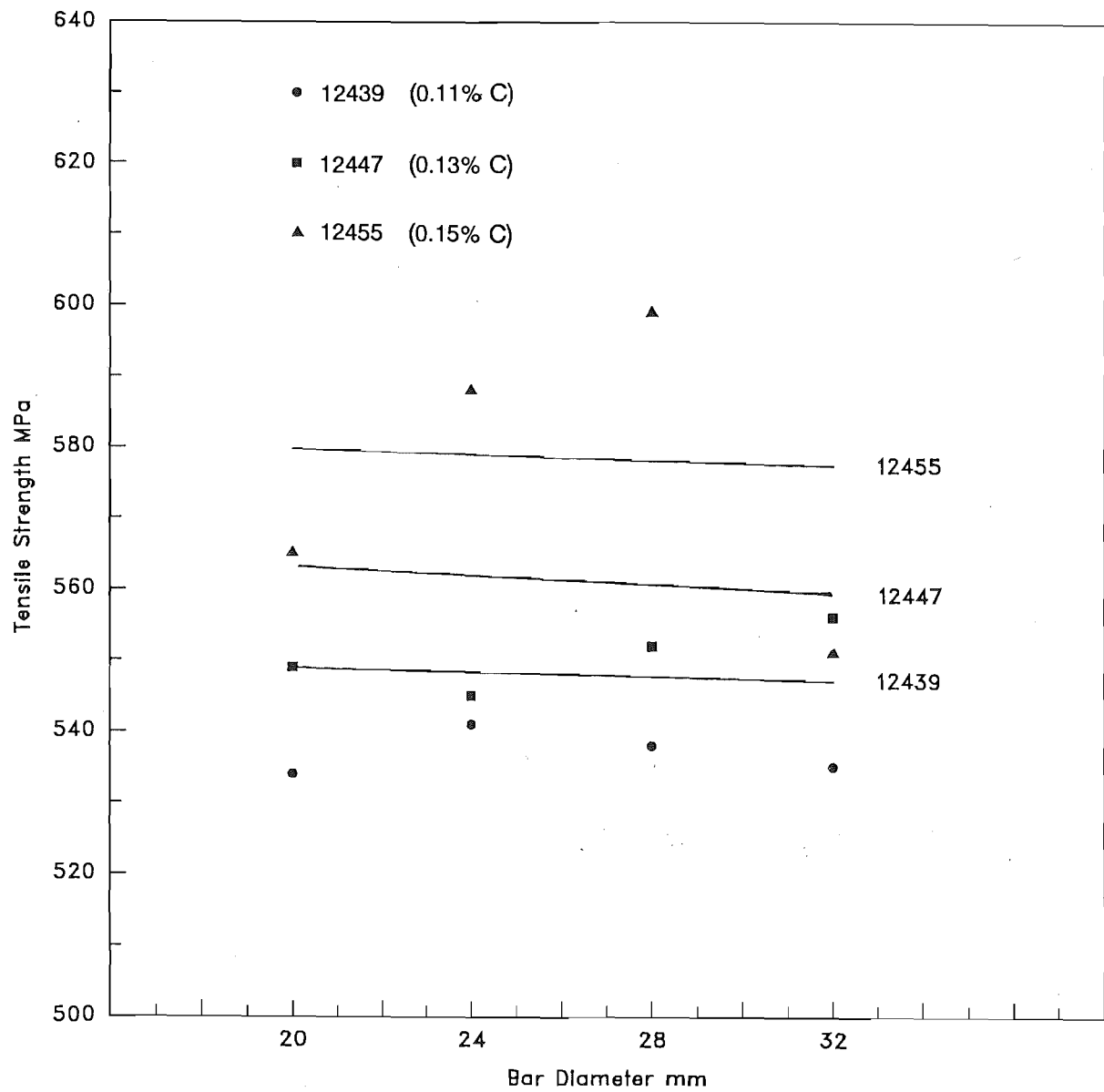


Figure 5.5: Calculated and observed tensile strength for "low carbon trial heats" using Equation 5.7

$$\begin{aligned}
 \text{Elongation at Fracture}(\%) = & 46 - 30(\%C) - 3.9(\%Mn) - 0.12(d) - 66(\%Mo) \\
 & (>0.00002\%) \quad (5\%) \quad (>0.00002\%) \quad (5\%) \\
 & - 54(\%V) \quad (20\%) \quad \quad \quad - \text{Eqn. 5.11}
 \end{aligned}$$

Equation 5.11 was also found to be significant at a level much greater than 0.1%. Although vanadium is only significant at the 20% level, the important thing to note is that the sign of the coefficient is consistent with other terms. Figure 5.6 shows the calculated % elongation at fracture from Equation 5.11 plotted against the experimental data, with the lines representing the 95% confidence limits of $\pm 2.8\%$. The vertical distribution of data in Figure 5.6 is because the calculated values were not rounded off to whole numbers as the experimental values were.

The regression coefficient for carbon in Equations 5.9 and 5.10 is the same. However, there is no correlation with manganese and molybdenum in Equation 5.9, instead copper was found to be significant. As previously mentioned, the difference between Equations 5.9 and 5.10 was considered to be influenced by the small data sets and limited range of variables available for the Grade 300 steel. In the analysis, it was found that there is no inter-correlation between copper and molybdenum.

The % elongation at fracture is a measure of the ductility of the metal. All parameters in Equations 5.9, 5.10 and 5.11 have negative regression coefficients meaning they decrease the ductility of the steel. This suggests that pure iron would have the maximum possible ductility and addition of alloys reduce the ductility.

It has been generally observed that high-strength high-carbon steels have a smaller elongation at fracture than lower-strength low-carbon steels. Comparison with the equations for the lower yield strength (Equations 5.1, 5.2 and 5.4) show that for this analysis, elements which improve the yield strength have an adverse effect on ductility. For instance, increasing carbon content was found to improve the strength and reduce the ductility. The effect of increasing carbon content on ductility is considered to be a function of the increased pearlite content and the amount of the associated brittle cementite.

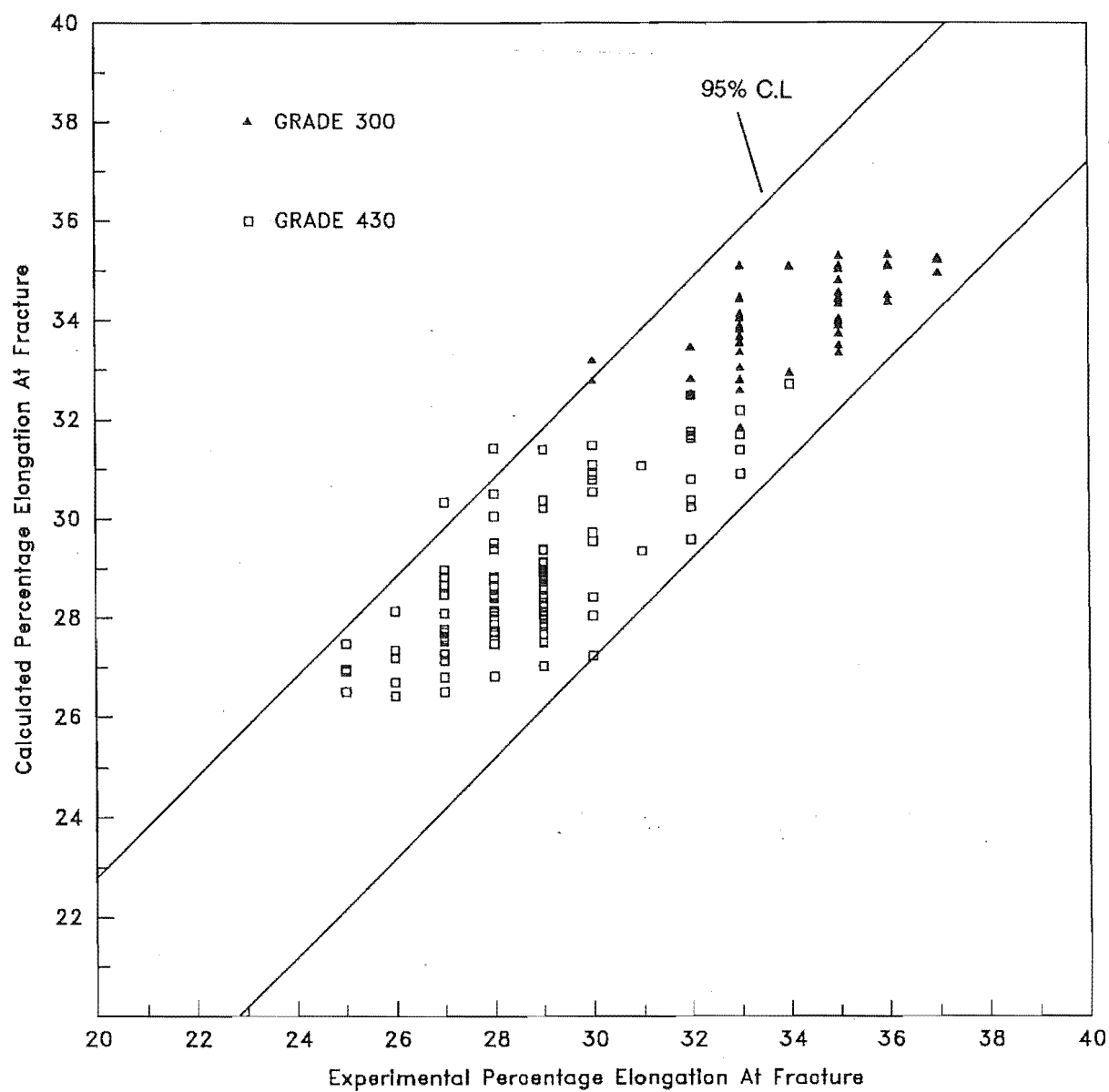


Figure 5.6: Calculated and observed % elongation at fracture for Grade 300 and Grade 430 reinforcing steels using Equation 5.11

Increasing pearlite content gives rise to a reduction of the interlamellar spacings. This results in a higher rate of strain hardening and hence reduces ductility. Elements such as manganese can also alter the proportion of pearlite by changing the eutectoid composition, or by depressing the transformation temperature⁴⁰, at any given cooling rate, thereby increasing the volume fraction of pearlite and modifying the interlamellar spacings.

The regression coefficients for copper and molybdenum in Equations 5.9 and 5.10 correspond to reductions of 1.8% and 1.6% in elongation at fracture, when considering the mean copper and molybdenum contents in Grade 300 and Grade 430 steels respectively. However, these reductions are relatively small when compared to the mean % elongation at fracture of 34% and 29% for Grade 300 and Grade 430 steels.

The addition of vanadium in steels was found to decrease the ductility as revealed in Equation 5.11. The same phenomenon was also observed by Sage²⁹. In his work, a reduction of 9% in elongation at fracture was recorded in 30 mm reinforcing bars of steels with a composition of 0.24% C, 1.25% Mn and 0.48% Si when the vanadium content was increased to 0.18%. The regression coefficient for vanadium in Equation 5.11 gives a reduction of 9.7% when increasing vanadium to 0.18%. In this particular case, addition of 0.04% vanadium in Grade 430 steel reduces the elongation at fracture by 2.1%.

Equations 5.9, 5.10 and 5.11 reveal that smaller diameter bars have longer % elongation at fracture. A reduction of approximately 2% in elongation is predicted from Equation 5.10 when increasing bar diameter from 10 mm to 32 mm. The reduction is small when compared to the total elongation of 34% and 28.7% for Grade 300 and Grade 430 steels.

5.5 THE REGRESSION OF LUDER STRAIN

There are a limited number of research publications available on the range of Luder strain in reinforcing steels, and the factors affecting this property. The length of the Luder strain is generally known to be a function of the strength of the material. As for the elongation at fracture, a shorter Luder strain is observed in high-strength high-carbon steels, when compared with that for lower-strength low carbon steels. This general phenomenon agrees with the result for Grade 300 steel which has a longer Luder strain than Grade 430 steel.

The regression of the 55 sets of data of Grade 300 steel yielded Equation 5.12 which was found to be significant at the 2.5% level.

$$\text{LS}(\%) = 2.53 - 0.02(d) \quad - \text{Eqn. 5.12}$$

(5%)

Equation 5.12 suggests that Luder strain of Grade 300 steel is only affected by the bar diameter. Equations 5.13 and 5.14 produced from the regression of Grade 430 data and the combined data show a consistency of magnitude and sign of the coefficient for bar diameter.

$$\text{LS}(\%) = 3.0 - 1.8(\%C) - 0.64(\%Mn) - 0.02(d) \quad - \text{Eqn. 5.13}$$

(1%) (2%) (0.1%)

$$\text{LS}(\%) = 3.4 - 1.53(\%C) - 0.98(\%Mn) - 0.02(d) \quad - \text{Eqn. 5.14}$$

(5%) (0.1%) (0.02%)

Figure 5.7 shows the calculated % Luder strain from Equation 5.14 plotted against the experimental data, with the 95% confidence limits being $\pm 0.45\%$. An equation similar to Equation 5.14 but with an additional vanadium term was also obtained from the regression of the combined data.

$$\text{LS}(\%) = 3.16 - 1.33(\%C) - 0.62(\%Mn) - 0.02(d) - 6.92(\%V) \quad - \text{Eqn. 5.15}$$

(10%) (5%) (0.02%) (50%)

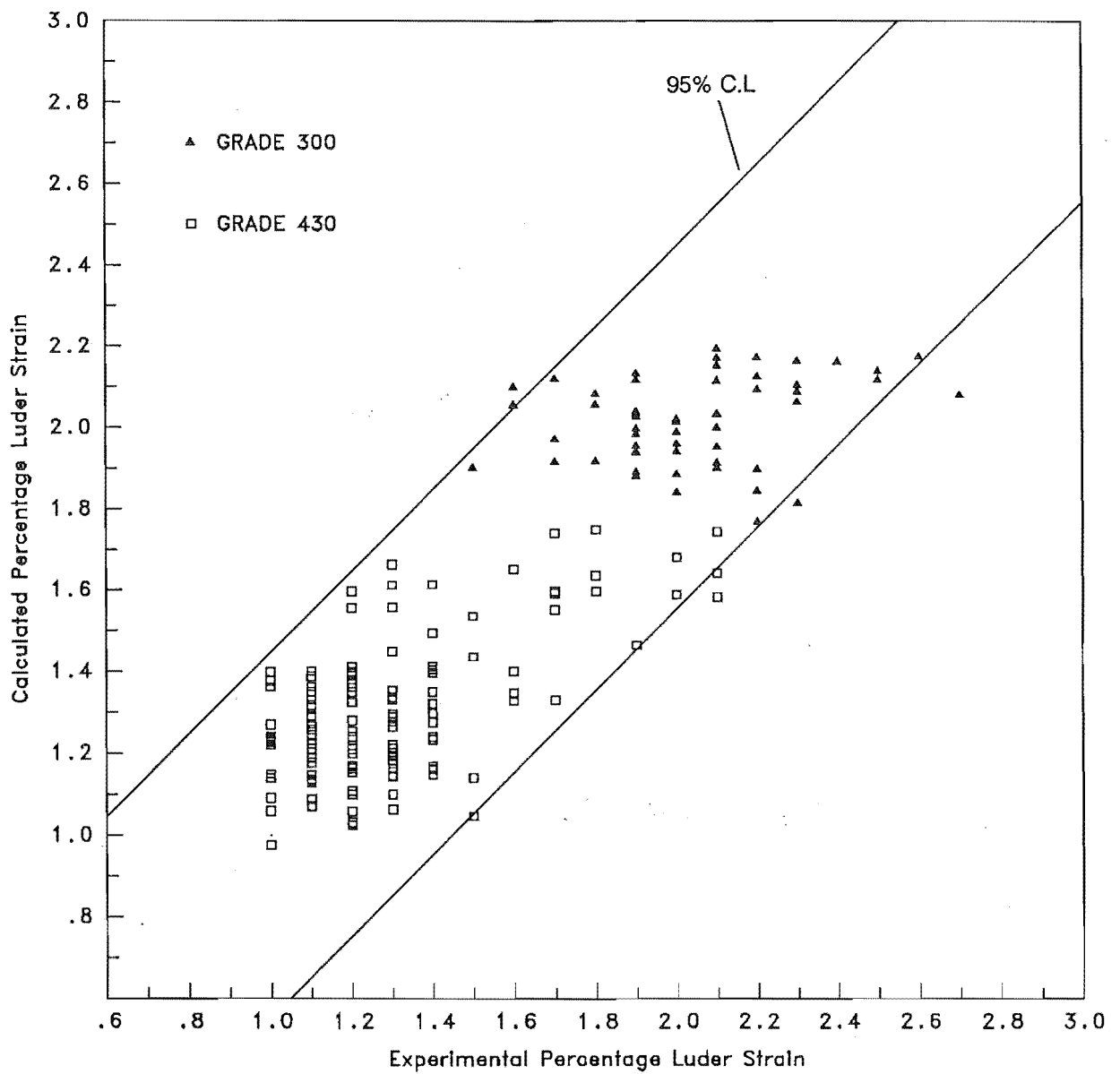


Figure 5.7: Calculated and observed % Luder strain for Grade 300 and Grade 430 reinforcing steels using Equation 5.14

Erasmus³⁰ suggested that Luder strain is influenced by the same microstructural and composition variables as affect the lower yield strength. Comparison of Equations 5.4 and 5.14 confirms this suggestion. Carbon, manganese and bar diameter are common parameters found in almost all the regression equations discussed. In the analysis, carbon and manganese were found to improve the strength but decrease the ductility and the Luder strain.

Luder strain has been regarded⁴¹ as the discontinuous strain required prior to uniform work hardening, i.e. strain preceding the normal smooth work-hardening curve. Therefore, the extent of Luder strain depends on the amount of work-hardening required to support the applied load. Since the increasing carbon and manganese contents decrease the Luder strain, the pearlite must be considered to have a major effect. The associated increase in pearlite content combined with a finer interlamellar spacing would result in a higher rate of strain hardening, hence reducing the Luder strain. The shorter mean Luder strain of Grade 430 is believed to be mainly attributed to the higher manganese content (approximately 2.2 times greater than Grade 300 steel) in the steel.

Since grain size is related to bar diameter, Equations 5.12, 5.13 and 5.14 predict that Luder strain increases with decreasing grain size (i.e. smaller bar). The prediction is consistent with the study of Evans⁴² where the variation of Luder strain was found to be linear with the reciprocal of the square root grain size ($d^{-1/2}$) for a limited range of grain sizes (8 μm - 25 μm). Although there is a strong correlation with bar diameter in the equations, the regression coefficient is relatively small. It is unfortunate that the grain size dependency cannot be assessed due to the lack of data.

In the work of Pussegoda¹¹, addition of vanadium to 0.24% C steels was found to have little effect on Luder strain. A slight decrease of approximately 0.06% in Luder strain with a 0.01% increase in vanadium content was observed. In the regression analysis, vanadium was found to be relatively insignificant, at the 50% level (see Equation 5.15). A slightly higher reduction of 0.07% in Luder strain for every 0.01% increase in vanadium was predicted from Equation 5.15. The Luder strain is little affected by vanadium, thus the ability of steels when micro-alloyed with vanadium

(i.e. Grade 430 reinforcing steel) to satisfactorily form plastic hinges during severe seismic loading is not adversely affected.

5.6 THE REGRESSION OF STRAIN HARDENING EXPONENT AND COEFFICIENT

The preferred regression equations for strain hardening exponent, n , produced by Grade 300, Grade 430 and the combined data are:-

$$n = 0.085(\%C) + 0.166(\%Si) + 0.216 \quad - \text{Eqn. 5.16}$$

(20%) (10%)

$$n = 0.073(\%C) - 1.31(\%V) + 0.24 \quad - \text{Eqn. 5.17}$$

(10%) (0.2%)

$$n = 0.07(\%C) - 1.55(\%V) + 0.25 \quad - \text{Eqn. 5.18}$$

(10%) (0.01%)

The equations are respectively significant at 25%, 1% and greater than 0.1% levels. Figure 5.8 shows the calculated n values from Equation 5.18 plotted against the experimental n values. Also shown are lines representing the 95% confidence limits of ± 0.04 . As can be seen in Figure 5.8, there is very limited variation in the calculated n values for Grade 300 steel. This is because the range of vanadium in Grade 300 steel is too small to enable the vanadium term in Equation 5.18 to make any contribution to the predicted results.

The regression equations relating to the strain hardening coefficient, k , obtained from Grade 300 data, Grade 430 and the combined data are as follows:-

$$k(\text{MPa}) = 1345(\%C) + 719 \quad - \text{Eqn. 5.19}$$

(1%)

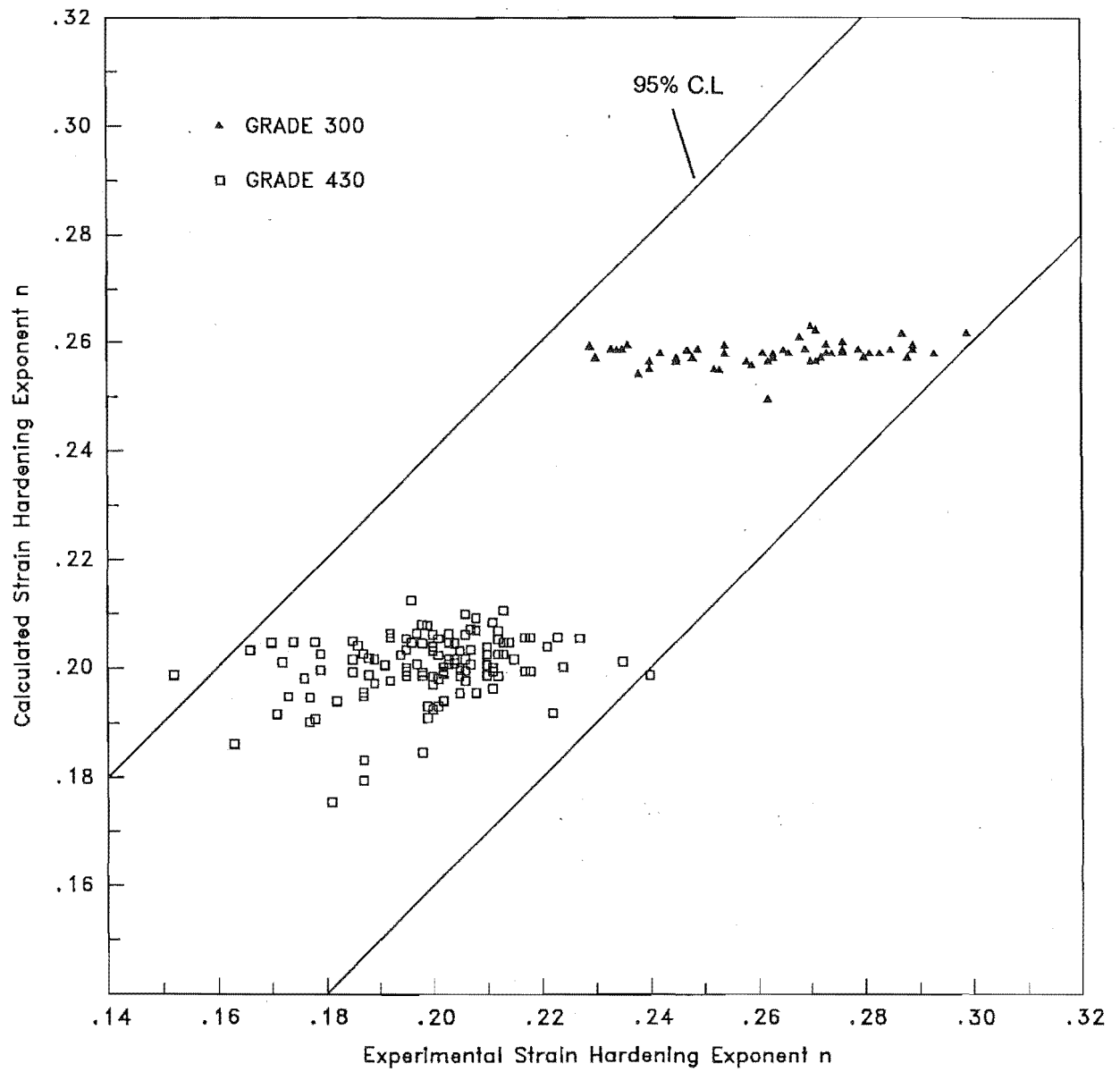


Figure 5.8: Calculated and observed strain hardening exponent n for Grade 300 and Grade 430 reinforcing steels using Equation 5.18

$$k(\text{MPa}) = 1691(\%C) + 178(\%Mn) + 533 \quad - \text{Eqn. 5.20}$$

$$(>0.00002\%) \quad (0.5\%)$$

$$k(\text{MPa}) = 1649(\%C) + 150(\%Mn) + 577 \quad - \text{Eqn. 5.21}$$

$$(>0.00002\%) \quad (>0.00002\%)$$

Figure 5.9 shows the calculated k values from Equation 5.21 plotted against the experimental values, with the lines representing the 95% confidence limits of ± 108 MPa.

Although it is generally acknowledged³⁰ that the exponent n and coefficient k are affected by changes in ferrite grain size, their exact relationship with grain size is not known. In Erasmus' work⁴³, n was found to be linearly proportional to the reciprocal of the square root of the grain size and the coefficient k was independent of grain size for a given material. It has been postulated⁴⁴ that a fine grained polycrystalline material contains a greater number of stored dislocations than the corresponding coarse grained polycrystalline material. On this basis, fine grained materials would strain harden at a higher rate than coarse grained materials. Since carbon and manganese are known⁴⁵ to reduce grain size, these elements would be expected to increase the strain hardening exponent. The effect of increasing carbon and manganese on the strain hardening exponent is further enhanced by an increase in the volume fraction of pearlite, since pearlite makes a greater contribution to work-hardening than ferrite^{35,38}. As can be seen in Equations 5.16, 5.17 and 5.18, carbon was found significant but there was no correlation with manganese. Bar diameter which has an indirect effect on the grain size was found to be only significant at a level less than 50% with a very low regression coefficient, this parameter was consequently dropped from the regression analysis.

The negative regression coefficient for vanadium is unexpected. In view of the grain size dependency, the reduction in grain size associated with vanadium should increase the strain hardening exponent. The regression coefficient for vanadium in Equation 5.17 corresponds to a reduction of 0.05(26%) in n value when adding 0.04% of vanadium to Grade 430 steel.

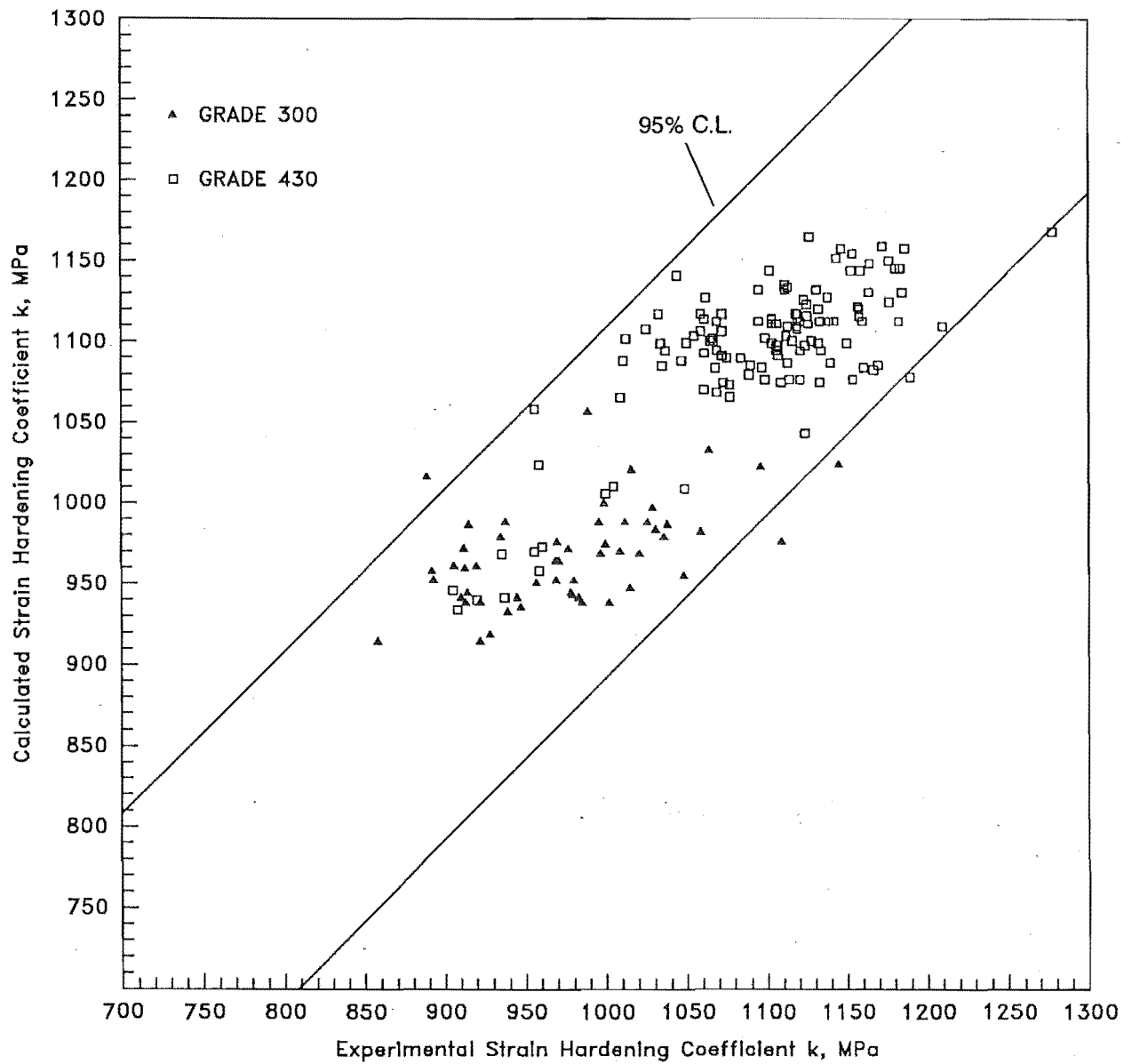


Figure 5.9: Calculated and observed strain hardening coefficient k for Grade 300 and Grade 430 reinforcing steels using Equation 5.21

From Equations 5.19, 5.20 and 5.21 the strain hardening coefficient is expected to be a function of carbon and manganese contents. The statistical work of Erasmus³⁰ on structural steel sections yielded a regression equation showing a strong dependency of k on carbon and manganese. Since increasing carbon and manganese are known to improve the strength, it follows that higher strength material would have higher k values. The difference in the mean k value between Grade 300 and Grade 430 steels is considered to be due to the difference in the manganese content. Equation 5.21 predicts an increase in k value of 103 MPa when increasing the manganese content from the mean value of 0.57% in Grade 300 to 1.25% in Grade 430.

Since it is predicted that n and k are increased by increasing carbon content and n can be reduced by adding vanadium to steels, high strength steels with lower strain hardening rates can be achieved by reducing the carbon content and adding vanadium. In this case, vanadium has dual roles; improving the strength while at the same time lowering the strain hardening exponent and consequently the strain hardening rate.

5.7 THE REGRESSION OF STRAIN AGEING PARAMETERS

Strain ageing at ambient temperature in hot-rolled reinforcing steels has been shown^{11,46} to be influenced by nitrogen. Since nitrogen content is not available for the regression analysis, vanadium content is used as a representative of the effect of nitrogen on strain ageing parameters. Although three parameters measuring the strain ageing index of Grade 300 and Grade 430 steels were determined, the yield related strain ageing parameter ΔY , (where ΔY = post strain age lower yield stress - prestrain flow stress), was mainly used in the regression as the dependent variable, because this parameter gives the most consistent indication of strain ageing. No regression was carried out on Grade 300 data because the mean vanadium content is only 0.003%.

The regression of Grade 430 data yielded Equation 5.22 which has a strong correlation with vanadium.

$$\Delta Y(\text{MPa}) = 136 - 95(\%C) - 0.66(d) - 1240(\%V) \quad - \text{Eqn. 5.22}$$

(2.5%) (0.01%) (0.005%)

Equation 5.22 has a F-value of 17.5 and is significant at a level much greater than 0.1%. A comparison between the experimental data and the calculated values of ΔY from Equation 5.22 is shown in Figure 5.10. Also shown are lines representing the 95% confidence limits of ± 23.5 MPa.

When silicon was included as a variable in the regression, Equation 5.23 was obtained.

$$\Delta Y(\text{MPa}) = 112 - 99(\%C) - 0.61(d) + 58(\%Si) - 1140(\%V) \quad - \text{Eqn. 5.23}$$

(5%) (0.05%) (10%) (0.02%)

The regression coefficients for the remaining parameters do not differ much when compared to Equation 5.22, but the corresponding significance levels were found to be lower.

The predicted effect of vanadium in reducing the strain ageing parameter, ΔY , as shown in Equations 5.22 and 5.23 is not unexpected. The addition of vanadium to low carbon steels will result in the combination of the active nitrogen with vanadium to form stable vanadium nitride precipitates and so suppress strain ageing. In order to combine sufficient of the available nitrogen as vanadium nitride to successfully render the steel non-strain ageing, vanadium contents of 0.04% to 0.06% have been shown¹⁹ to be necessary. Using Equation 5.22, the amount of vanadium required to completely eliminate strain ageing in Grade 430 reinforcing steel was found to be approximately 0.08%, which is well in excess of the stoichiometric requirement for steels which contain 0.005% - 0.006% nitrogen. Unfortunately, the nitrogen content is not available to confirm the above estimation. Pussegoda¹⁹ found that for optimum properties after strain ageing, particularly the transition temperature, the V/N ratio should be between 7 and 9.

The negative regression coefficient for bar diameter in Equations 5.22 and 5.23 predicts higher magnitude of ΔY for small diameter bars. The grain size is related

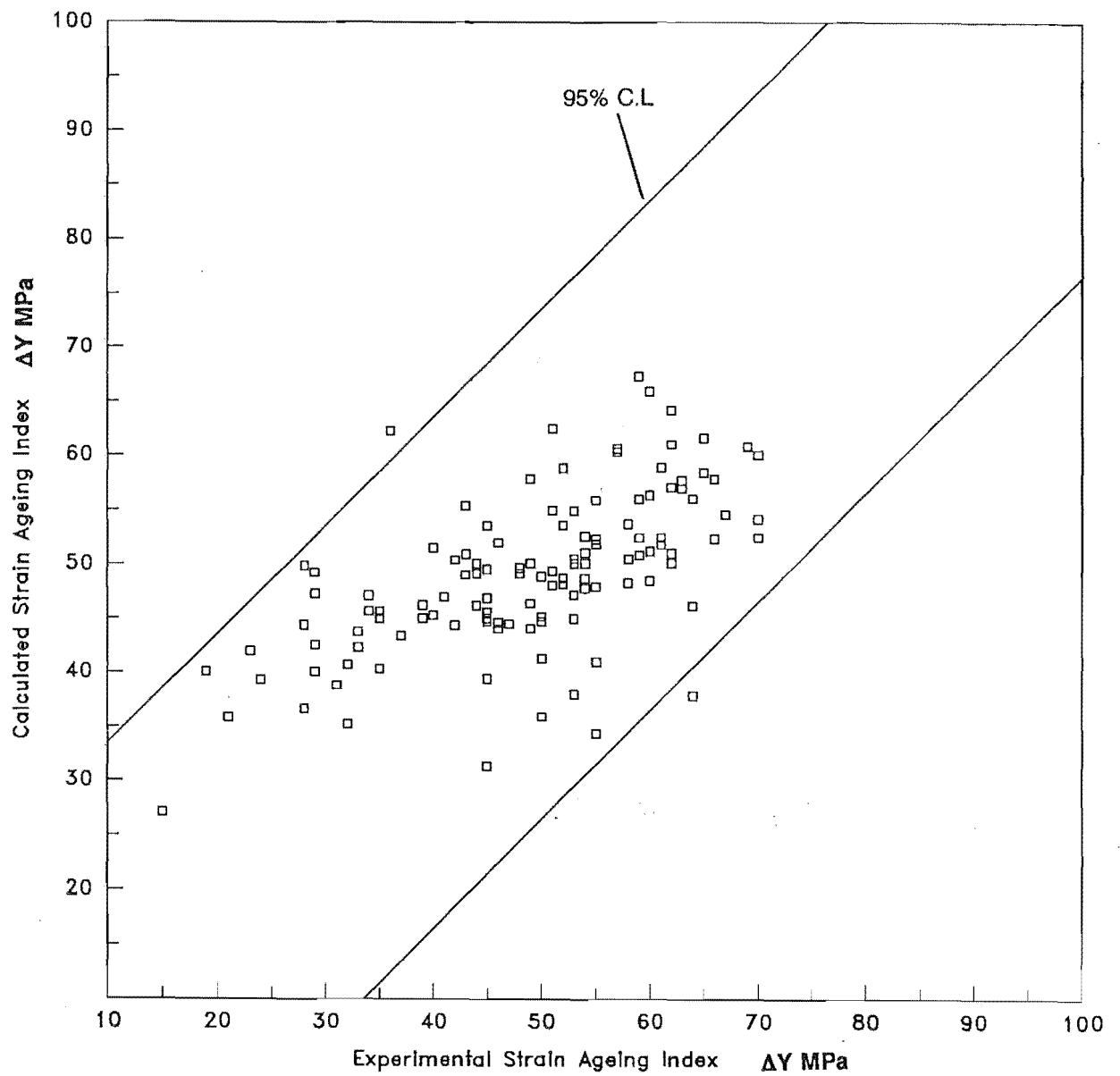


Figure 5.10: Calculated and observed strain ageing index ΔY for Grade 430 reinforcing steel using Equation 5.22

to bar diameter and smaller bar will have finer grain size, suggesting that steels of finer grain size are more susceptible to strain ageing. This phenomenon agrees with earlier research work^{47,48} where the grain size dependence of strain ageing has been established.

The effect of carbon in reducing ΔY , predicted by Equations 5.22 and 5.23, is inconsistent with the grain size dependency of strain ageing. Since increasing carbon is known to contribute to a reduction of grain size, an increase in ΔY would be expected. It is speculated that the predicted effect of carbon could be similar to manganese, in retarding strain ageing by slowing the rate at which nitrogen segregates to grain boundaries^{46,49}. In the analysis, manganese was found significant at less than the 50% level and consequently was dropped from the regression. However, the regression coefficient for manganese was found to be negative, implying that ΔY decreases with increasing manganese content.

Equation 5.23 predicts an increase in ΔY with an increase in silicon content. The prediction is inconsistent with the study of Robert et al⁵⁰ and Arrowsmith⁵¹ where an addition of 0.3% silicon has been shown to result in the precipitation of manganese-silicon nitrides which can inhibit strain ageing in low carbon steels by removing nitrogen. It may be the small range of silicon considered is responsible for the unexpected effect of silicon in Equation 5.23.

Equations 5.24 and 5.25 also reveal the significance of vanadium in reducing strain ageing.

$$\Delta U(\text{MPa}) = 46 - 627(\%V) \quad - \text{Eqn. 5.24}$$

(20%)

$$\Delta El(\%) = 1.52 - 18.8(\%V) \quad - \text{Eqn. 5.25}$$

(20%)

These equations can be used in conjunction with Equations 5.22 or 5.23 to predict the strain ageing behaviour for Grade 430 reinforcing steel.

5.5 SUMMARY

All the regression equations presented in this chapter are summarised in Table 5.5, which also shows the significance level of each coefficient and of the equation as a whole. It can be seen from the table that the significance levels of the equations (given by the F value) as well as of the coefficients were markedly improved when Grade 430 and the combined data were used in the regression analysis. This is mainly due to the larger data sets and an increase in the range of chemical composition associated with the combined data. Equations derived from the combined data generally involve the same parameters as those produced by Grade 430 data, but with alterations in the regression coefficients.

From the regression analysis, increasing bar diameter was found to have an adverse effect on the strengths as well as the ductility and Luder strain of the reinforcing steels. The predicted effect of bar diameter on lower yield strength and tensile strength is not unexpected since smaller bars will have a faster cooling rate. Consequently, a finer grain size and higher strength would be expected. However, the argument for grain size effect on ductility and Luder strain is not very convincing. It was also found that strain ageing is enhanced in smaller diameter bars. This prediction is consistent with other research work assuming that the diameter is related to the grain size. However, calculated values of lower yield strength, and tensile strength for four different bar diameters of the "low carbon trial heats" do not correspond well with the experimental data.

In general, carbon and manganese were found to increase strength but decrease ductility and Luder strain. Elements such as silicon, nickel and copper were also found to be beneficial to the strengths. The regression equation for ΔY predicts that a high carbon content reduces strain ageing, and that steels of lower vanadium content are more susceptible to strain ageing. The latter prediction is not unexpected since addition of vanadium results in the precipitation of vanadium nitrides and consequently reduces strain ageing by removing active nitrogen. Using the equation, the vanadium content required to completely eliminate strain ageing in Grade 430 reinforcing steel was estimated to be approximately 0.08%. The predicted effect of carbon on ΔY is not really understood.

From the regression analysis, vanadium was found to reduce ductility and Luder strain, but the effect was small when compared to the total elongation and Luder strain of Grade 300 and Grade 430 reinforcing steels. By contrast, the effect of vanadium on the strain hardening exponent n was to reduce it significantly. Generally, the addition of vanadium to reinforcing steels has been found to be beneficial with regard to the strength, strain hardening rate and strain ageing without significantly affecting ductility and Luder strain.

The regression equations derived from the available data are only of statistical significance for the samples that were tested. The significance of each regression coefficient and the equation as a whole is a function of the range of chemical composition considered. Nevertheless, these linear equations enable predictions of mechanical properties and strain ageing behaviour for Grade 300 and Grade 430 reinforcing bars from production variations in chemical composition.

Table 5.5: Summary of significant equations from Multiple Linear Regression analysis

Eqn. No.	Grade	Data Sets	Dependent Variable	Regression Coefficients and (Significance Levels)									Constant	Eqn. F Value	Eqn. Signif. Level
				%C	%Mn	%CEQ	d	%Si	%Ni	%Mo	%Cu	%V			
5.1	300	55	LYS(MPa)	133 (10%)			- 1.0 (1%)		319 (0.5%)				307	5.10	0.5%
5.2	430	125	LYS(MPa)	523 (>0.00002%)	105 (0.02%)		- 0.97 (0.01%)				43 (10%)	750 (20%)	203	31.58	> > 0.1%
5.3	430	125	LYS(MPa)			313 (>0.00002%)	- 1.10 (0.001%)				80 (0.05%)	1323 (0.5%)	272	34.00	> > 0.1%
5.4	Combined	180	LYS(MPa)	469 (>0.00002%)	98 (0.01%)		- 1.11 (0.00005%)				46 (1%)	1253 (0.2%)	205	481	> > 0.1%
5.5	Combined	180	LYS(MPa)			281 (>0.00002%)	- 1.26 (0.00002%)				71 (0.01%)	2226 (>0.00002%)	256	548	> > 0.1%
5.6	300	55	TS(MPa)	264 (0.2%)				103 (5%)					424	7.00	> > 0.1%
5.7	430	125	TS(MPa)	695 (>0.00002%)	141 (0.2%)		- 0.87 (2%)				66 (10%)	768 (20%)	277	23.40	> > 0.1%
5.8	Combined	180	TS(MPa)	659 (>0.00002%)	131 (0.005%)		- 0.92 (0.2%)				62 (2%)	992 (10%)	290	308.60	> > 0.1%

Table 5.5 continued ...

Eqn. No.	Grade	Data Sets	Dependent Variable	Regression Coefficients and (Significance Levels)									Constant	Eqn. F Value	Eqn. Signif. Level
				%C	%Mn	%CEQ	d	%Si	%Ni	%Mo	%Cu	%V			
5.9	300	55	Elongation (%)	- 28 (0.2%)			- 0.18 (0.005%)				- 4.8 (10%)		46	21.60	> > 0.1%
5.10	430	125	Elongation (%)	- 28 (>0.00002%)	- 4.6 (2%)		- 0.10 (0.001%)			- 96 (2%)			44.4	23.97	> > 0.1%
5.11	Combined	180	Elongation (%)	- 30 (>0.00002%)	- 3.9 (5%)		- 1.12 (>0.00002%)			- 66 (5%)		- 54 (20%)	46	131.72	> > 0.1%
5.12	300	55	LS(%)				- 0.02 (5%)						2.53	5.55	2.5%
5.13	430	125	LS(%)	- 1.8 (1%)	- 0.64 (2%)		- 0.02 (0.1%)						3.0	29.44	> > 0.1%
5.14	Combined	180	LS(%)	- 1.53 (5%)	- 0.98 (0.1%)		- 0.02 (0.02%)						3.4	153	> > 0.1%
5.15	Combined	180	LS(%)	- 1.33 (10%)	- 0.62 (5%)		- 0.02 (0.02%)					- 6.92 (50%)	3.16	116	> > 0.1%
5.16	300	55	n	0.085 (20%)			0.166 (10%)						0.216	1.16	25%

Table 5.5 Continued ...

Eqn. No.	Grade	Data Sets	Dependent Variable	Regression Coefficients and (Significance Levels)									Constant	Eqn. F Value	Eqn. Signif. Level
				%C	%Mn	%CEQ	d	%Si	%Ni	%Mo	%Cu	%V			
5.17	430	125	n	0.073 (10%)								- 1.31 (0.2%)	0.240	5.70	1%
5.18	Combined	180	n	0.070 (10%)								- 1.55 (0.01%)	0.250	158	> > 0.01%
5.19	300	55	k(MPa)	1345 (1%)									719	7.71	> > 0.1%
5.20	430	125	k(MPa)	1691 (>0.00002%)	178 (0.5%)								533	45.4	> > 0.1%
5.21	Combined	180	k(MPa)	1649 (>0.00002%)	150 (>0.00002%)								577	159	> > 0.1%
5.22	430	125	ΔY (MPa)	- 95 (2.5%)			- 0.66 (0.01%)					- 1240 (0.005%)	136	17.5	> > 0.1%
5.23	430	125	ΔY (MPa)	- 99 (5%)			- 0.61 (0.05%)	58 (10%)				- 1140 (0.02%)	112	14.33	> > 0.1%
5.24	430	125	ΔU (MPa)									- 627 (20%)	46	2.18	25%
5.25	430	125	ΔEI (%)									- 18.8 (20%)	1.52	2.10	25%

CHAPTER 6

CONCLUSIONS

Using data supplied by Pacific Steel Ltd and data generated in the Materials Laboratory of the Department, a statistical analysis of lower yield strength, tensile strength, elongation at fracture, Luder strain at the yield point, strain hardening rate, and three parameters measuring the strain ageing index has been carried out for Grade 300 and Grade 430 reinforcing steels. Distributions of these properties were produced from three different sets of data (machined specimen, lab deformed and Pacific Steel deformed). The mean lower yield strengths of machined specimen data were 339.8 MPa for Grade 300 and 466.7 MPa for Grade 430 steels. For both grades of steel, the 95% characteristic strengths of machined specimen data and Pacific Steel deformed data were found to comply with the test properties specified in NZS 3402:1989.

Variation in the distributions and mean values of lower yield strength and tensile strength determined from different sets of data were found to be mainly attributed to the different strain rates employed in the tensile tests. The type of test piece only affects the tensile strength and % elongation at fracture. However, Luder strain was found to be insensitive to strain rate and the geometry of test specimen.

Grade 430 reinforcing steel was found to have a mean % elongation at fracture of 28.7% and a mean Luder strain of 1.3% which are higher than those of the previous Grade 380 steel. In addition, Grade 430 steel has a lower strain hardening rate and is less susceptible to strain ageing. The improved properties are mainly due to the addition of 0.04% vanadium as revealed by the multiple linear regression analysis.

The multiple linear regression analysis has successfully yielded equations which provide an indication of how the mechanical properties, strain hardening characteristic and strain ageing index of Grade 300 and Grade 430 reinforcing steels are affected by the percentages of the different chemical elements. These simple

equations are particularly useful for Pacific Steel Ltd in predicting the properties from production variations in chemical composition.

From the analysis of the regression equations, bar diameter was found to have an adverse effect on strength, particularly lower yield strength. The effect of bar diameter on strength is believed to be related to the grain size. Smaller diameter bar has a higher cooling rate and so a finer grain size, consequently the strength is higher. However, tensile strength was found to be less affected by bar diameter, due to the fact that ferrite grain size has less effect on tensile strength.

Carbon and manganese were found to increase strength. This is believed to be through grain refinement and solid-solution hardening mechanisms. However, they adversely affect the ductility and Luder strain, which are probably related to the pearlite content and the strain hardening rate. The lower yield strength, tensile strength, % elongation at fracture and Luder strain of Grade 300 and Grade 430 reinforcing steel can be predicted using the following equations.

$$\text{LYS(MPa)} = 469(\%C) + 98(\%Mn) - 1.11(d) + 46(\%Cu) + 1253(\%V) + 205$$

- Eqn. 5.4

$$\text{TS(MPa)} = 659(\%C) + 131(\%Mn) - 0.92(d) + 62(\%Cu) + 992(\%V) + 290$$

- Eqn. 5.8

$$\text{Elongation at Fracture(\%)} = 46 - 30(\%C) - 3.9(\%Mn) - 0.12(d) - 66(\%Mo) - 54(\%V)$$

- Eqn. 5.11

$$\text{LS(\%)} = 3.4 - 1.53(\%C) - 0.98(\%Mn) - 0.02(d)$$

- Eqn. 5.14

Following the regression equations, it can be concluded that the addition of 0.04% vanadium to Grade 430 steel has been very beneficial. Vanadium was found to increase the strengths without significantly reducing the ductility and Luder strain. On the other hand, vanadium was found to reduce the strain hardening exponent n and strain ageing. These improved properties would enhance the use of Grade 430 steel in plastic hinge zones in reinforced concrete structures.

REFERENCES

1. Disney, L.A., "Steel Reinforcement. Cutting. Bending. Fixing", 1st Published, 1954, Concrete Publications Limited, London.
2. Park, R. and Paulay, T., "Reinforced Concrete Structures", 1975, John Wiley & Sons, New York.
3. Andriono, T., "Properties of Reinforcing Steel Used in Seismic Design", M.E. Thesis, 1986, Dept. of Civil Eng., University of Canterbury, New Zealand.
4. Smaill, J.S. et al, "Effects of Titanium Additions on Strain Ageing Characteristics and Mechanical Properties of Carbon-Manganese Reinforcing Steels", Metal Technology, 1976, vol. 3, p 194.
5. Standards Association of New Zealand, "Specification for Hot-Rolled Steel Bars for the Reinforcement of Concrete", NZS 3402:1989.
6. Hundy, B.B., "Accelerated Strain Ageing of Mild Steel", Journ. Iron & Steel Inst., 1954, vol. 178, p 34.
7. British Standards Institution, "Methods for Tensile Testing of Metals", BS18, 1987.
8. Standards Association of New Zealand, "Code of Practice for the Design of Concrete Structures", NZS 3101:Part 1, 1982.
9. Mander, J.B., "Seismic Design of Bridge Piers", Ph.D. Thesis, 1984, Dept. of Civil Eng., University of Canterbury, New Zealand.

10. Erasmus, L.A., "Nitrogen in Steel. Friend or Foe?", Proceeding Australasian Conference on Materials for Industrial Development, I.M.M.A., 1987, Christchurch.
11. Pussegoda, L.N., "Strain Age Embrittlement in Reinforcing Steels", Ph.D. Thesis, 1978, Dept. of Mechanical Eng., University of Canterbury, New Zealand.
12. Mirza, S.A. and MacGregor, J.G., "Variability of Mechanical Properties of Reinforcing Bars", Journ. of the Structural Division, ASCE, 1979, vol. 105, p 921.
13. Johnson, R.F., "The Measurement of Yield Stress", 1967, B.I.S.R.A./I.S.I. Conference on Strong Tough Structural Steels.
14. Bodner, S.R. and Symonds, P.S., "Experimental and Theoretical Investigation of the Plastic Deformation of Cantilever Beams Subjected to Impulsive Loading", Journ. of Applied Mechanics, 1962, vol. 29, p 719.
15. ACI Committee 439, "Effect of Steel Strength and Reinforcement Ratio on the Mode of Failure and Strain Energy Capacity of Reinforced Concrete Beams", Journ. ACI, 1968, vol. 66, p 165.
16. Standards Association of Australia, "Methods for Tensile Testing of Metals", AS 1391, 1974.
17. Andriono, T. and Park, R., "Seismic Design Considerations of the Properties of New Zealand Manufactured Steel Reinforcing Bars", Proceeding Pacific Conference on Earthquake Eng., N.Z. National Society for Earthquake Eng., 1987, Wairakei, New Zealand.
18. Andriono, T. and Park, R., "Stress-Strain Properties of New Zealand Manufactured Micro-Alloy Reinforcing Steel Used in Seismic Design", Internal Report, 1986, Dept. of Civil Eng., University of Canterbury, New Zealand.

19. Erasmus, L.A. and Pussegoda, L.N., "The Strain Ageing Characteristics of Reinforcing Steel with a Range of Vanadium Contents", *Metallurgical Transactions*, 1980, vol. 11A, p 231.
20. Mansoor, J., "Fracture Toughness of Micro-Alloyed Reinforcing Steel", B.E. Project Report, 1987, Dept. of Mechanical Eng., University of Canterbury, New Zealand.
21. Edwards, A.L., "An Introduction to Linear Regression and Correlation", 1st Edition, 1976, W.H. Freeman & Company, San Fransisco.
22. Volk, W., "Applied Statistics for Engineers", 2nd Edition, 1969, McGraw-Hill Inc., New York.
23. Hines, W.W. and Montgomery, D.C., "Probability and Statistics in Engineering and Management Science", 2nd Edition, 1980, John Wiley & Sons, New York.
24. Blank, L., "Statistical Procedures for Engineering, Management and Science", International Student Edition, 1982, McGraw-Hill Inc., Tokyo.
25. Fisher, R.A. and Yates, F., "Statistical Tables for Biological, Agricultural and Medical Research", 6th Edition, 1963, Oliver and Boyd Ltd, London.
26. Enrico, T.F., "Extended Tables of the Percentage Points of Student's t Distribution", *Journ. of the American Statistical Association*, 1959, p 683.
27. Gladman, T. and Pickering, F.B., "Effect of Manganese on the Precipitation of Nitrogen from Ferrite", *Journ. Iron & Steel Inst.*, 1965, vol. 203, p 1212.
28. Gouzou, J., "Analysis of the Grain Size Dependence of the Lower Yield Stress in Steel", *Acta Metallurgical*, 1964, vol. 12, p 785.
29. Sage, A.M., "Effect of Vanadium, Nitrogen and Aluminium on the Mechanical Properties of Reinforcing Bar Steels", *Metals Technology*, 1976, vol. 3, p 65.

30. Erasmus, L.A., "Statistical Analysis of Mechanical Properties Obtained on Structural Section", HERA Research Report, R4-01, 1983.
31. Gladman, T., McIvor, I.D. and Pickering, F.B., "Some Aspects of the Structure-Property Relationships in High-Carbon Ferrite-Pearlite Steels", Journ. Iron & Steel Inst., 1972, vol. 210, p 916.
32. Rollason, E.C., "Metallurgy for Engineers", 4th Edition, 1973, Edward Arnold, Norwich.
33. Honeycombe, R.W.K., "Steels, Microstructures and Property", 1981, Edward Arnold, London.
34. Pui, C.C., "The Effect of Copper and Other Residual Elements on the Properties of Pacific Steels Rod", B.E. Project Report, 1987, Dept. of Mechanical Eng., University of Canterbury, New Zealand.
35. Gladman, T., Holmes, B. and Pickering, F.B., "Work Hardening of Low Carbon Steels", Journ. Iron & Steel Inst., 1970, vol. 208, p 172.
36. Avner, S.H., "Introduction to Physical Metallurgy", 2nd Edition, 1974, McGraw-Hill, New York.
37. Anya, C.C. and Baker, T.N., "The Effect of Silicon on the Grain Size and the Tensile Properties of Low Carbon Steels", Materials Sci. & Eng., 1989, A118, p 197.
38. Anya, C.C. and Baker, T.N., "Effect of Silicon on Microstructures and Some Mechanical Properties of Low Carbon Steels", Materials Sci. & Tech., 1966, vol. 6, p 554.
39. Erasmus, L.A. et al, "Engineering Metallurgy", 2nd Edition, 1980, University of Canterbury, New Zealand.

40. Krauss, G., "Steels Heat Treatment and Processing Principles", 1st Edition, 1989, ASM International.
41. Hutchison, M.M., "Considerations Relevant to Lower Yield Stress", Metal Science Journ., 1973, vol. 7, p 26.
42. Evans, R.W., "Effect of Prior Cold Reduction on Ductility of Annealed Rimmed Steel", Journ. Iron & Steel Inst., 1967, vol. 205, p 1150.
43. Erasmus, L.A., "Factors Affecting the Tensile Flow Curve for Low Carbon Steel", 1969, The Second Australasian Conference on the Mechanics of Structures and Materials, University of Adelaide, Australia.
44. Soh, K.S., "The Effect of Grain Size on the Tensile Flow Curve of Low Carbon Steel", M.E. Thesis, 1970, Dept. of Mechanical Eng., University of Canterbury, New Zealand.
45. Rollason, E.C., "Fundamental Aspects of Molybdenum on Transformation of Steel", Dept. of Industrial Metallurgy, University of Birmingham, London.
46. Erasmus, L.A., "Strain Ageing in Carbon/Manganese Steels - the Independence of Nitrogen, Manganese and Grain Size", Proceeding of the 1987 Australasian Conference on the Mechanics of Structures and Materials, University of Canterbury, New Zealand.
47. Wilson, D.V. and Russell, B., "The Contribution of Precipitation to Strain Ageing in Low Carbon Steels", Acta Metallurgical, 1960, vol. 8, p 468.
48. Wilson, D.V., "Grain-Size Dependence of Discontinuous Yielding in Strain-Aged Steels", Acta Metallurgical, 1968, vol 16, p 743.
49. Baird, J.D., "The Effect of Strain-Ageing Due to Interstitial Solutes on the Mechanical Properties of Metals", Metals & Materials, Metallurgical Review 149, 1971, vol. 5, p 1.

50. Robert, W., Grieveson, P. and Jack, K.H., "Precipitation of Silicon Nitrides and Manganese Silicon Nitrides in Steel", Journ. Iron & Steel Inst., 1972, vol. 210, p 931.
51. Arrowsmith, J.M., "A New Silicon Nitride Phase in Commercial Silicon Killed Steels", Journ. Iron & Steel Inst., 1963, vol. 201, p 699.

CHEMICAL COMPOSITION OF REINFORCING STEEL

Table A.1: Chemical composition of Grade 300 reinforcing steel

Cast Number	Diameter (mm)	Chemical Analysis										
		C	Mn	Si	S	P	Ni	Cr	Mo	Cu	Sn	V
61414	32	0.20	0.60	0.19	0.040	0.029	0.14	0.11	0.019	0.37	0.036	0.003
61473	32	0.22	0.54	0.14	0.023	0.019	0.10	0.08	0.013	0.37	0.036	0.003
63139	32	0.19	0.56	0.17	0.038	0.042	0.09	0.11	0.015	0.52	0.043	0.003
63210	32	0.20	0.54	0.15	0.022	0.020	0.09	0.07	0.014	0.34	0.029	0.003
63228	32	0.20	0.53	0.12	0.034	0.031	0.12	0.11	0.018	0.56	0.034	0.003
63236	32	0.20	0.54	0.16	0.038	0.039	0.12	0.14	0.018	0.52	0.034	0.003
63261	32	0.19	0.61	0.14	0.042	0.026	0.10	0.09	0.016	0.46	0.038	0.003
63279	32	0.24	0.56	0.16	0.021	0.018	0.10	0.08	0.014	0.35	0.030	0.002
63287	32	0.19	0.52	0.17	0.044	0.040	0.10	0.08	0.015	0.40	0.038	0.003
58317	28	0.17	0.58	0.13	0.042	0.021	0.10	0.09	0.017	0.42	0.032	0.003
58325	28	0.20	0.53	0.13	0.030	0.015	0.10	0.07	0.015	0.37	0.037	0.003
58350	28	0.18	0.64	0.16	0.034	0.050	0.09	0.12	0.017	0.36	0.045	0.003
58368	28	0.18	0.57	0.15	0.025	0.042	0.10	0.11	0.018	0.35	0.037	0.003
58376	28	0.16	0.65	0.15	0.022	0.025	0.16	0.09	0.017	0.41	0.034	0.004
58392	28	0.21	0.62	0.14	0.033	0.028	0.11	0.10	0.016	0.40	0.038	0.003
58406	28	0.18	0.54	0.15	0.031	0.020	0.10	0.08	0.018	0.40	0.032	0.003
58465	28	0.18	0.60	0.11	0.033	0.028	0.12	0.11	0.017	0.40	0.039	0.003
58473	28	0.16	0.82	0.16	0.033	0.041	0.10	0.13	0.015	0.32	0.032	0.007
58503	28	0.19	0.57	0.14	0.038	0.022	0.10	0.09	0.017	0.36	0.039	0.002
60635	28	0.22	0.56	0.13	0.024	0.025	0.10	0.11	0.018	0.37	0.037	0.003
60741	28	0.21	0.51	0.15	0.038	0.017	0.09	0.08	0.013	0.37	0.030	0.002
60759	28	0.18	0.58	0.16	0.042	0.020	0.10	0.09	0.014	0.36	0.030	0.003
60783	28	0.20	0.51	0.15	0.028	0.017	0.09	0.08	0.013	0.24	0.030	0.001
60805	28	0.18	0.63	0.33	0.032	0.026	0.09	0.09	0.012	0.26	0.033	0.003
60813	28	0.17	0.56	0.16	0.032	0.028	0.09	0.08	0.013	0.33	0.048	0.002
61091	28	0.22	0.55	0.11	0.029	0.027	0.12	0.10	0.016	0.46	0.034	0.002
58511	24	0.19	0.57	0.17	0.031	0.020	0.09	0.10	0.017	0.34	0.033	0.002
60236	24	0.17	0.50	0.13	0.022	0.009	0.10	0.05	0.012	0.26	0.030	0.001

Table A.1 continued ...

Cast Number	Diameter (mm)	Chemical Analysis										
		C	Mn	Si	S	P	Ni	Cr	Mo	Cu	Sn	V
60317	24	0.18	0.52	0.14	0.027	0.012	0.11	0.06	0.018	0.36	0.034	0.002
60325	24	0.21	0.49	0.14	0.026	0.012	0.10	0.05	0.013	0.33	0.035	0.002
60333	24	0.16	0.49	0.11	0.023	0.020	0.11	0.08	0.015	0.40	0.035	0.003
61457	24	0.17	0.56	0.16	0.021	0.019	0.10	0.08	0.018	0.38	0.040	0.003
61503	24	0.17	0.57	0.19	0.024	0.019	0.09	0.09	0.011	0.37	0.033	0.002
63724	24	0.17	0.54	0.14	0.028	0.013	0.11	0.07	0.016	0.36	0.030	0.002
63741	24	0.17	0.58	0.19	0.040	0.026	0.12	0.13	0.023	0.44	0.037	0.003
63872	24	0.18	0.52	0.15	0.044	0.025	0.12	0.11	0.019	0.42	0.041	0.003
63902	24	0.19	0.59	0.16	0.036	0.020	0.12	0.10	0.017	0.47	0.043	0.003
63929	24	0.20	0.54	0.17	0.039	0.015	0.11	0.09	0.019	0.40	0.039	0.003
63937	24	0.18	0.58	0.17	0.037	0.012	0.09	0.06	0.015	0.38	0.035	0.002
63961	24	0.20	0.54	0.14	0.034	0.016	0.11	0.08	0.018	0.44	0.034	0.003
64066	20	0.23	0.51	0.19	0.025	0.010	0.11	0.09	0.017	0.30	0.030	0.002
64074	20	0.17	0.54	0.15	0.043	0.027	0.10	0.13	0.018	0.42	0.032	0.003
64082	20	0.15	0.63	0.19	0.042	0.028	0.12	0.15	0.020	0.41	0.035	0.003
64091	20	0.17	0.63	0.16	0.037	0.032	0.12	0.14	0.020	0.40	0.033	0.004
64112	20	0.18	0.56	0.13	0.022	0.028	0.09	0.06	0.013	0.27	0.020	0.002
64121	20	0.18	0.60	0.17	0.042	0.019	0.10	0.11	0.019	0.42	0.039	0.003
64104	20	0.15	0.60	0.12	0.043	0.019	0.12	0.10	0.021	0.49	0.042	0.003
64147	20	0.17	0.56	0.13	0.024	0.016	0.10	0.11	0.019	0.36	0.035	0.003
64155	20	0.19	0.59	0.16	0.032	0.022	0.10	0.11	0.017	0.38	0.034	0.003
64171	20	0.17	0.60	0.14	0.019	0.021	0.09	0.08	0.014	0.34	0.032	0.003
64228	20	0.17	0.52	0.18	0.042	0.014	0.11	0.08	0.020	0.42	0.040	0.002
64201	20	0.19	0.54	0.16	0.038	0.024	0.11	0.11	0.019	0.37	0.056	0.003
64236	20	0.17	0.54	0.21	0.038	0.018	0.11	0.11	0.019	0.42	0.039	0.002
64244	20	0.19	0.54	0.17	0.038	0.014	0.11	0.07	0.020	0.43	0.039	0.002
64210	20	0.18	0.51	0.17	0.038	0.016	0.10	0.07	0.016	0.34	0.040	0.002

Table A.2: Chemical composition of Grade 430 reinforcing steel

Cast Number	Diameter (mm)	Chemical Analysis										
		C	Mn	Si	S	P	Ni	Cr	Mo	Cu	Sn	V
63171	32	0.23	1.14	0.26	0.028	0.018	0.09	0.09	0.013	0.38	0.034	0.036
63198	32	0.21	1.29	0.24	0.020	0.020	0.09	0.07	0.013	0.35	0.032	0.044
63341	32	0.20	1.21	0.33	0.039	0.018	0.13	0.10	0.027	0.54	0.041	0.041
63376	32	0.21	1.20	0.36	0.026	0.017	0.12	0.10	0.021	0.48	0.040	0.040
63384	32	0.24	1.28	0.32	0.033	0.026	0.10	0.10	0.018	0.41	0.037	0.038
63392	32	0.23	1.14	0.31	0.042	0.021	0.10	0.09	0.016	0.43	0.033	0.039
63414	32	0.22	1.15	0.38	0.037	0.020	0.10	0.07	0.017	0.37	0.034	0.040
63422	32	0.21	1.29	0.29	0.042	0.017	0.10	0.07	0.017	0.43	0.036	0.037
63431	32	0.21	1.25	0.30	0.031	0.014	0.12	0.06	0.019	0.45	0.037	0.040
63449	32	0.20	1.29	0.32	0.041	0.015	0.11	0.08	0.019	0.44	0.036	0.041
63457	32	0.19	1.46	0.23	0.037	0.020	0.12	0.08	0.020	0.47	0.038	0.056
63465	32	0.19	1.36	0.27	0.038	0.024	0.12	0.13	0.023	0.50	0.036	0.046
63473	32	0.21	1.26	0.32	0.034	0.023	0.12	0.11	0.021	0.45	0.035	0.040
63481	32	0.21	1.28	0.30	0.036	0.014	0.16	0.11	0.026	0.54	0.040	0.045
63490	32	0.22	1.28	0.33	0.032	0.033	0.09	0.11	0.015	0.39	0.037	0.040
63503	32	0.20	1.27	0.32	0.029	0.026	0.10	0.11	0.016	0.42	0.034	0.039
63511	32	0.19	1.33	0.28	0.016	0.046	0.10	0.14	0.015	0.41	0.044	0.044
63520	32	0.19	1.36	0.26	0.025	0.036	0.11	0.12	0.018	0.38	0.036	0.041
63538	32	0.22	1.36	0.30	0.031	0.026	0.12	0.11	0.020	0.39	0.030	0.043
63562	32	0.23	1.25	0.32	0.036	0.018	0.12	0.09	0.022	0.46	0.032	0.038
63571	32	0.21	1.39	0.37	0.034	0.023	0.11	0.11	0.019	0.43	0.035	0.051
63589	32	0.19	1.31	0.33	0.036	0.019	0.10	0.08	0.018	0.41	0.036	0.039
63597	32	0.20	1.37	0.32	0.030	0.027	0.12	0.09	0.019	0.47	0.039	0.044
63546	32	0.19	1.31	0.30	0.029	0.033	0.12	0.13	0.017	0.38	0.031	0.041
63601	32	0.22	1.30	0.28	0.043	0.022	0.12	0.09	0.020	0.42	0.036	0.045
63619	32	0.21	1.24	0.26	0.037	0.024	0.13	0.12	0.024	0.44	0.033	0.043
63635	32	0.22	1.27	0.24	0.022	0.023	0.13	0.12	0.027	0.48	0.032	0.046

Table A.2 continued ...

Cast Number	Diameter (mm)	Chemical Analysis										
		C	Mn	Si	S	P	Ni	Cr	Mo	Cu	Sn	V
63651	32	0.21	1.25	0.32	0.036	0.035	0.11	0.15	0.020	0.41	0.036	0.041
63660	32	0.19	1.23	0.29	0.034	0.033	0.12	0.15	0.019	0.41	0.030	0.045
63694	32	0.21	1.24	0.36	0.037	0.015	0.13	0.09	0.020	0.48	0.042	0.040
63759	32	0.25	1.12	0.33	0.041	0.030	0.14	0.14	0.023	0.46	0.036	0.036
63767	32	0.20	1.25	0.32	0.039	0.022	0.10	0.09	0.020	0.37	0.031	0.037
63783	32	0.23	1.12	0.33	0.034	0.015	0.12	0.09	0.021	0.31	0.029	0.039
63775	32	0.21	1.23	0.37	0.035	0.022	0.12	0.11	0.018	0.37	0.034	0.044
63805	32	0.21	1.18	0.38	0.041	0.030	0.12	0.10	0.019	0.40	0.036	0.039
63813	32	0.24	1.15	0.35	0.044	0.029	0.11	0.12	0.023	0.37	0.033	0.039
63830	32	0.21	1.19	0.35	0.046	0.024	0.12	0.12	0.019	0.33	0.034	0.037
63406	32	0.19	1.36	0.27	0.033	0.022	0.10	0.09	0.017	0.44	0.034	0.038
57961	28	0.18	1.50	0.40	0.030	0.045	0.09	0.12	0.016	0.31	0.037	0.053
58015	28	0.19	1.48	0.27	0.019	0.030	0.09	0.09	0.014	0.39	0.042	0.051
58023	28	0.18	1.35	0.31	0.025	0.018	0.09	0.08	0.013	0.35	0.039	0.041
58040	28	0.21	1.26	0.30	0.030	0.021	0.10	0.10	0.019	0.31	0.029	0.042
58058	28	0.22	1.34	0.35	0.035	0.022	0.10	0.11	0.020	0.37	0.029	0.047
58066	28	0.21	1.29	0.33	0.028	0.023	0.11	0.12	0.022	0.39	0.029	0.041
58074	28	0.21	1.22	0.29	0.033	0.023	0.09	0.10	0.017	0.35	0.031	0.038
58104	28	0.23	1.30	0.34	0.035	0.031	0.11	0.12	0.021	0.43	0.037	0.041
58163	28	0.20	1.22	0.30	0.029	0.021	0.08	0.08	0.012	0.29	0.034	0.038
58171	28	0.21	1.32	0.44	0.032	0.028	0.09	0.10	0.013	0.33	0.037	0.033
58180	28	0.21	1.22	0.30	0.033	0.039	0.09	0.10	0.013	0.40	0.039	0.050
58198	28	0.20	1.28	0.38	0.037	0.037	0.09	0.10	0.016	0.75	0.038	0.037
58201	28	0.23	1.34	0.37	0.032	0.030	0.09	0.09	0.015	0.46	0.029	0.048
58210	28	0.20	1.13	0.29	0.011	0.038	0.12	0.14	0.016	0.38	0.034	0.039
58228	28	0.24	1.30	0.36	0.029	0.027	0.11	0.11	0.016	0.35	0.031	0.038
60872	28	0.21	1.19	0.32	0.031	0.036	0.08	0.08	0.011	0.33	0.031	0.038

Table A.2 continued ...

Cast Number	Diameter (mm)	Chemical Analysis										
		C	Mn	Si	S	P	Ni	Cr	Mo	Cu	Sn	V
60881	28	0.24	1.18	0.33	0.028	0.028	0.08	0.08	0.012	0.32	0.034	0.037
60899	28	0.22	1.20	0.34	0.029	0.031	0.09	0.12	0.014	0.32	0.032	0.039
60902	28	0.24	1.21	0.36	0.040	0.036	0.10	0.10	0.015	0.37	0.039	0.042
60911	28	0.22	1.18	0.30	0.035	0.049	0.10	0.11	0.015	0.34	0.038	0.038
60937	28	0.21	1.14	0.30	0.037	0.041	0.12	0.13	0.016	0.44	0.037	0.036
60953	28	0.20	1.28	0.33	0.032	0.030	0.10	0.09	0.013	0.35	0.040	0.036
62911	28	0.21	1.29	0.36	0.047	0.033	0.11	0.07	0.017	0.38	0.027	0.038
62937	28	0.22	1.27	0.33	0.034	0.016	0.09	0.06	0.016	0.34	0.031	0.046
62945	28	0.19	1.29	0.33	0.037	0.022	0.09	0.07	0.018	0.34	0.035	0.041
62953	28	0.21	1.27	0.34	0.034	0.019	0.09	0.09	0.019	0.34	0.040	0.038
62961	28	0.19	1.26	0.34	0.029	0.031	0.09	0.10	0.017	0.36	0.040	0.038
62970	28	0.19	1.38	0.38	0.037	0.018	0.09	0.09	0.016	0.39	0.046	0.040
62996	28	0.18	1.35	0.28	0.030	0.020	0.09	0.07	0.016	0.34	0.035	0.040
63007	28	0.21	1.35	0.36	0.033	0.020	0.08	0.08	0.014	0.39	0.033	0.039
63015	28	0.21	1.27	0.33	0.030	0.027	0.09	0.09	0.015	0.36	0.035	0.038
63066	28	0.22	1.29	0.33	0.032	0.039	0.10	0.13	0.014	0.38	0.038	0.038
63082	28	0.22	1.15	0.34	0.033	0.021	0.10	0.11	0.020	0.42	0.035	0.037
63091	28	0.23	1.25	0.33	0.041	0.020	0.10	0.08	0.016	0.48	0.037	0.039
54465	24	0.23	1.26	0.32	0.028	0.014	0.08	0.07	0.013	0.32	0.031	0.038
54457	24	0.21	1.28	0.31	0.031	0.024	0.08	0.10	0.012	0.31	0.037	0.042
58082	24	0.19	1.24	0.31	0.037	0.022	0.10	0.10	0.020	0.38	0.035	0.036
58155	24	0.18	1.31	0.28	0.034	0.029	0.09	0.08	0.016	0.48	0.047	0.041
58252	24	0.19	1.19	0.33	0.035	0.022	0.09	0.10	0.020	0.42	0.040	0.037
60121	24	0.20	1.31	0.36	0.037	0.014	0.09	0.06	0.015	0.50	0.049	0.040
60139	24	0.20	1.36	0.27	0.031	0.029	0.09	0.10	0.014	0.36	0.036	0.047
60155	24	0.21	1.33	0.37	0.037	0.021	0.09	0.07	0.014	0.37	0.037	0.044

Table A.2 continued ...

Cast Number	Diameter (mm)	Chemical Analysis										
		C	Mn	Si	S	P	Ni	Cr	Mo	Cu	Sn	V
60431	24	0.20	1.30	0.32	0.016	0.037	0.09	0.11	0.014	0.41	0.030	0.044
60520	24	0.22	1.20	0.35	0.036	0.030	0.08	0.10	0.014	0.49	0.035	0.039
60538	24	0.21	1.26	0.37	0.042	0.039	0.09	0.11	0.017	0.40	0.039	0.041
60554	24	0.23	1.35	0.37	0.032	0.034	0.09	0.11	0.014	0.36	0.031	0.041
60597	24	0.24	1.17	0.33	0.032	0.020	0.09	0.07	0.013	0.34	0.033	0.036
60601	24	0.22	1.15	0.33	0.036	0.027	0.09	0.09	0.019	0.34	0.035	0.038
60619	24	0.20	1.19	0.36	0.040	0.035	0.13	0.13	0.024	0.40	0.044	0.039
60627	24	0.20	1.17	0.35	0.030	0.035	0.13	0.14	0.025	0.50	0.042	0.037
63201	24	0.19	1.22	0.37	0.017	0.022	0.12	0.09	0.017	0.43	0.034	0.041
63295	24	0.20	1.21	0.33	0.043	0.027	0.12	0.09	0.016	0.48	0.039	0.038
63309	24	0.21	1.23	0.33	0.036	0.036	0.11	0.11	0.018	0.54	0.036	0.039
63368	24	0.20	1.18	0.33	0.033	0.015	0.11	0.07	0.018	0.44	0.035	0.037
63627	24	0.20	1.23	0.27	0.040	0.025	0.12	0.10	0.022	0.44	0.034	0.039
63708	24	0.18	1.36	0.38	0.038	0.022	0.10	0.11	0.024	0.46	0.029	0.045
64317	24	0.20	1.24	0.32	0.030	0.011	0.10	0.05	0.017	0.34	0.035	0.039
57899	20	0.19	1.30	0.29	0.034	0.028	0.09	0.10	0.017	0.37	0.033	0.041
60147	12	0.20	1.27	0.33	0.041	0.033	0.09	0.10	0.014	0.37	0.036	0.041
60163	12	0.19	1.29	0.39	0.033	0.022	0.09	0.09	0.014	0.39	0.035	0.040
60198	12	0.20	1.19	0.29	0.035	0.040	0.12	0.11	0.023	0.31	0.030	0.039
60210	12	0.22	1.15	0.34	0.039	0.034	0.10	0.11	0.018	0.34	0.030	0.039
60244	12	0.19	1.23	0.32	0.029	0.023	0.10	0.10	0.015	0.38	0.031	0.041
60295	12	0.21	1.18	0.34	0.032	0.017	0.10	0.09	0.013	0.36	0.035	0.038
60368	12	0.18	1.13	0.36	0.032	0.038	0.11	0.11	0.016	0.50	0.046	0.039
60384	12	0.19	1.12	0.36	0.040	0.026	0.12	0.10	0.015	0.39	0.033	0.038
60392	12	0.20	1.29	0.37	0.036	0.026	0.11	0.09	0.017	0.33	0.032	0.041
60414	12	0.20	1.28	0.28	0.028	0.019	0.09	0.06	0.014	0.35	0.031	0.043
60422	12	0.20	1.28	0.30	0.027	0.020	0.09	0.08	0.013	0.32	0.031	0.041

Table A.2 continued ...

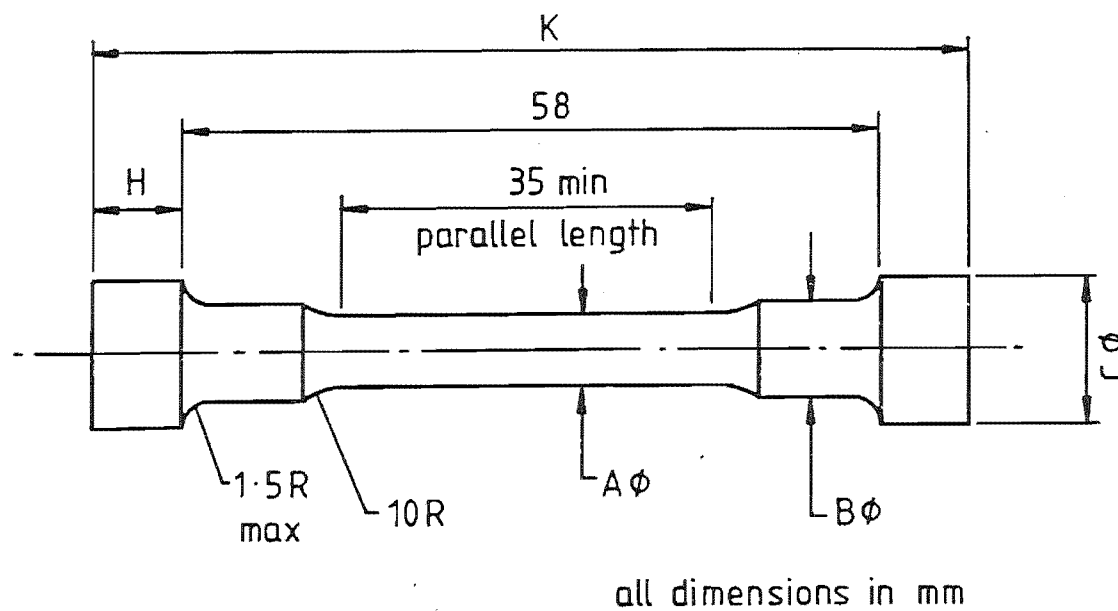
Cast Number	Diameter (mm)	Chemical Analysis										
		C	Mn	Si	S	P	Ni	Cr	Mo	Cu	Sn	V
55911	10	0.19	1.34	0.34	0.035	0.034	0.12	0.12	0.024	0.45	0.032	0.042
55929	10	0.22	1.28	0.32	0.035	0.022	0.10	0.10	0.019	0.52	0.041	0.042
55937	10	0.24	1.17	0.37	0.021	0.030	0.10	0.12	0.019	0.36	0.030	0.042
55961	10	0.18	1.28	0.35	0.027	0.025	0.08	0.09	0.013	0.37	0.027	0.040
58121	10	0.19	1.23	0.32	0.033	0.026	0.10	0.11	0.015	0.34	0.036	0.036
58147	10	0.19	1.17	0.29	0.032	0.027	0.09	0.09	0.015	0.32	0.032	0.035

Table A.3: Chemical composition of "low carbon trial heats"

Cast Number	Diameter (mm)	Chemical Analysis										
		C	Mn	Si	S	P	Ni	Cr	Mo	Cu	Sn	V
12439	32	0.11	1.25	0.34	0.025	0.024	0.12	0.10	0.014	0.29	0.029	0.038
	28	0.11	1.21	0.32	0.024	0.024	0.12	0.10	0.014	0.27	0.029	0.037
	24	0.11	1.17	0.31	0.022	0.023	0.12	0.09	0.014	0.27	0.029	0.035
	20	0.11	1.22	0.33	0.021	0.023	0.12	0.10	0.014	0.27	0.030	0.036
12447	32	0.12	1.22	0.34	0.026	0.016	0.11	0.09	0.014	0.25	0.027	0.038
	28	0.13	1.21	0.34	0.026	0.016	0.11	0.09	0.014	0.25	0.026	0.038
	24	0.13	1.18	0.32	0.024	0.017	0.11	0.09	0.015	0.25	0.028	0.037
	20	0.13	1.19	0.32	0.023	0.018	0.11	0.10	0.014	0.25	0.028	0.037
12455	32	0.16	1.22	0.36	0.028	0.016	0.10	0.09	0.015	0.24	0.030	0.039
	28	0.15	1.23	0.35	0.030	0.016	0.10	0.09	0.014	0.24	0.029	0.039
	24	0.15	1.24	0.35	0.024	0.015	0.10	0.09	0.015	0.24	0.030	0.038
	20	0.15	1.21	0.34	0.023	0.015	0.10	0.09	0.015	0.24	0.030	0.038

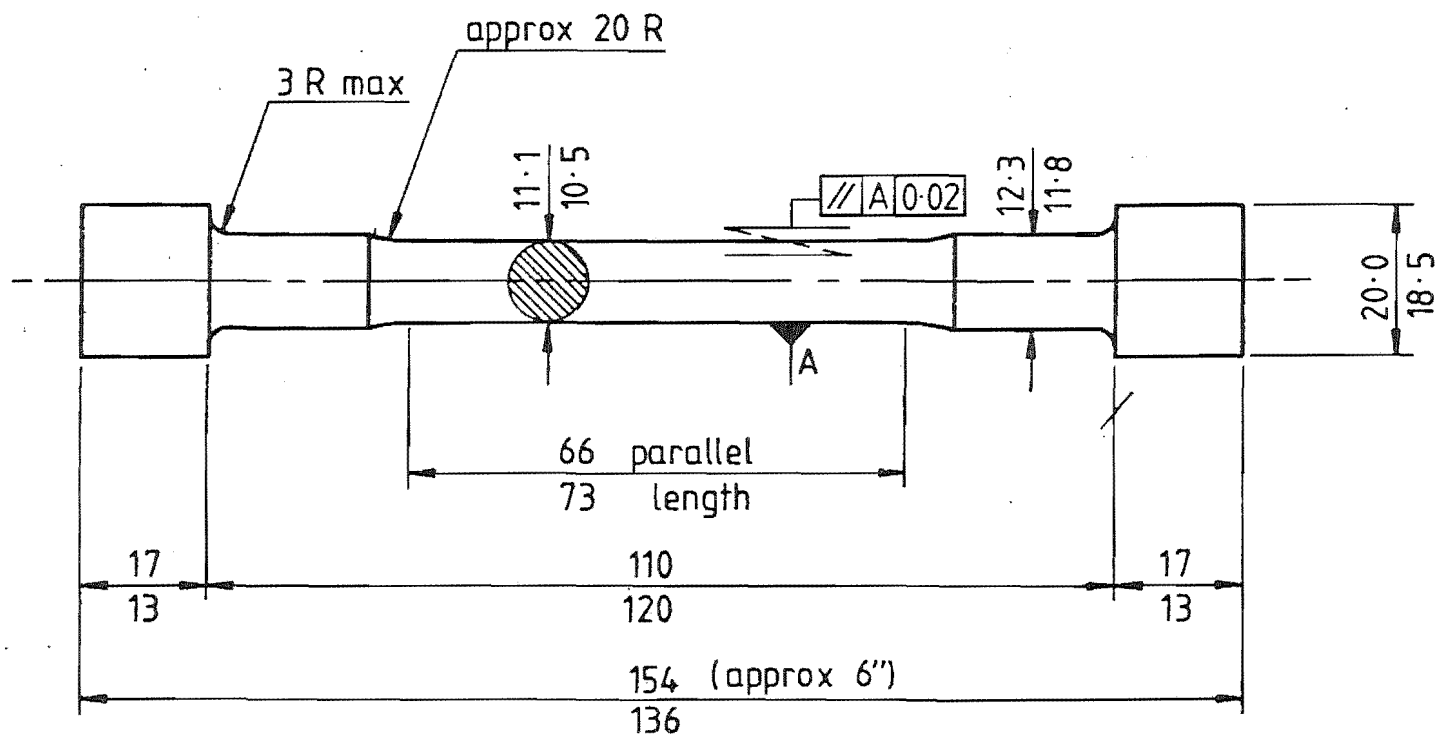
APPENDIX B

DETAILED DIMENSION OF THE MACHINED SPECIMEN



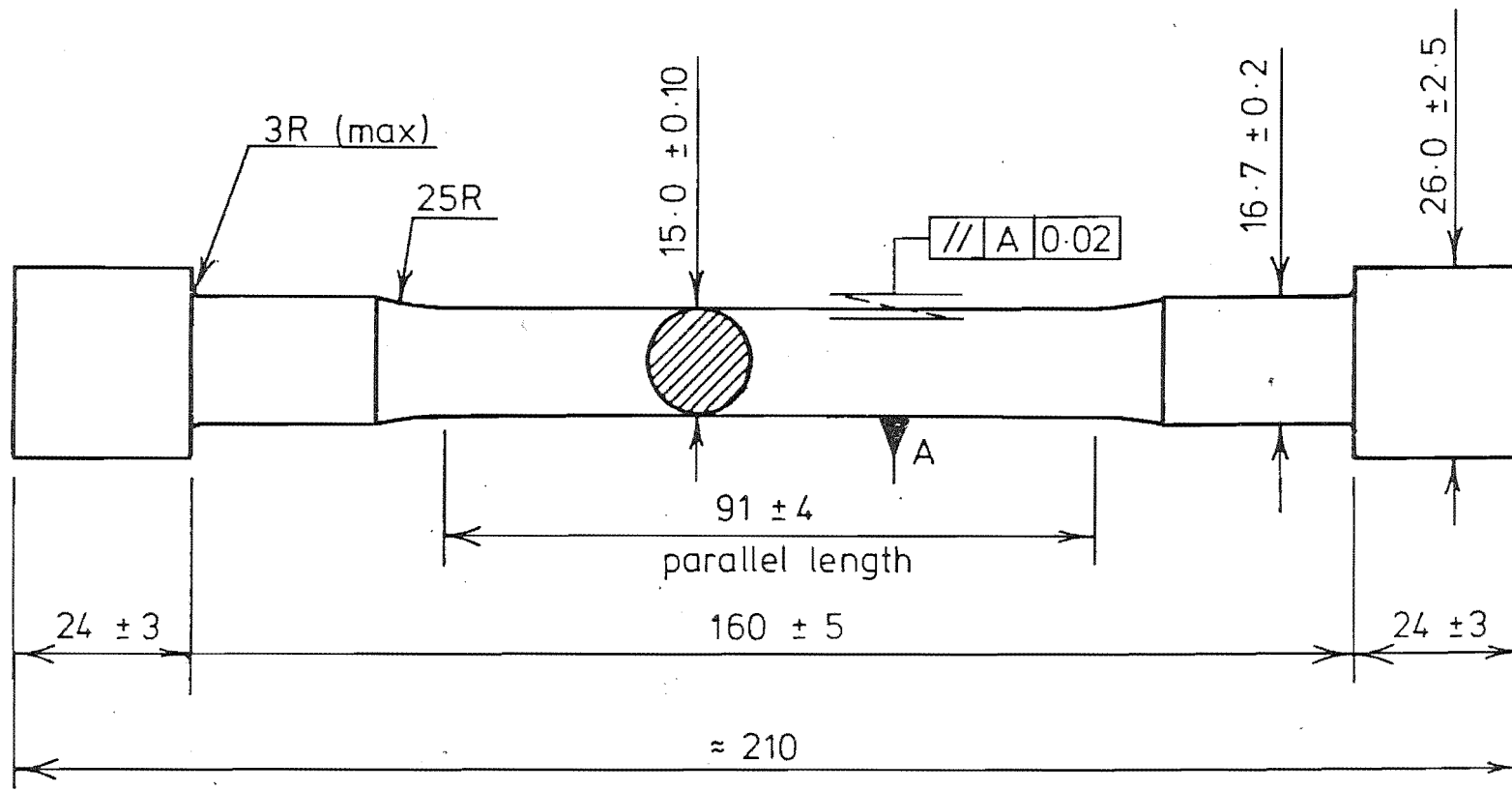
Diameters - (mm)			Lengths (mm)	
A	B	C	H	K
5.06 5.04	7.15 6.80	11.3 10.1	8	74

Figure B.1: Details of the tensile specimen machined from 10 mm/12 mm deformed bar



NOTE: All dimensions in mm

Figure B.2: Details of the tensile specimen machined from 20 mm deformed bar



NOTE: All dimensions in mm

Figure B.3: Details of the tensile specimen machined from 24 mm/28 mm/32 mm deformed bar.

APPENDIX C

TENSILE RESULTS OF REINFORCING STEEL

Table C.1: Tensile results of Grade 300 reinforcing steel

CAST NO.	Bar Diameter mm	Machined Specimen									Lab Deformed			P.S. Deformed		
		LYS MPa	TS MPa	EI %	LS %	n	k MPa	ΔY MPa	ΔU MPa	ΔEI %	LYS MPa	TS MPa	LS %	LYS MPa	TS MPa	EI %
61414	32	344	490	32	2.3	0.289	1029	70	53	4	302	460	2.0	319	462	33
61473	32	336	492	32	2.2	0.276	1016	64	44	3	297	450	2.2	320	466	34
63139	32	317	478	30	1.5	0.283	1000	68	81	4	312	475	1.5	325	461	31
63210	32	324	493	33	1.7	0.279	1012	56	47	4	290	451	1.7	338	488	34
63228	32	342	498	32	1.9	0.285	1038	67	45	4	305	460	2.0	316	452	31
63236	32	354	513	30	1.9	0.265	1026	75	52	1	307	473	1.8	326	470	30
63261	32	323	488	34	2.2	0.293	1059	70	51	5	305	454	2.2	320	456	29
63279	32	329	492	33	2.0	0.270	989	69	51	4	294	458	2.0	321	468	27
63287	32	333	484	33	2.0	0.281	997	62	66	7	312	466	2.1	325	462	29
58317	28	334	482	33	1.7	0.240	914	68	45	6	312	420	1.8	306	451	31
58325	28	340	474	35	1.9	0.234	915	62	50	6	311	429	1.9	321	457	26
58350	28	328	499	33	2.1	0.272	1009	58	43	5	318	429	2.3	353	484	24
58368	28	341	484	35	2.0	0.245	913	67	49	6	304	417	2.2	324	451	29
58376	28	343	493	35	1.8	0.238	913	68	53	6	318	430	2.0	348	474	29
58392	28	349	489	33	2.0	0.229	889	68	48	5	312	422	1.9	357	504	31
58406	28	327	495	33	2.0	0.288	1048	71	48	3	311	426	1.7	317	444	27
58465	28	354	501	33	1.9	0.248	971	69	43	5	322	430	2.0	344	465	29
58473	28	342	493	35	2.2	0.262	969	68	40	5	314	426	2.0	332	469	29
58503	28	342	502	33	1.9	0.254	970	69	47	6	315	421	1.9	341	480	33
60635	28	332	479	33	2.1	0.206	1145	65	47	4	304	455	2.1	308	441	33

Table C.1 continued ...

CAST NO.	Bar Diameter mm	Machined Specimen									Lab Deformed			P.S. Deformed		
		LYS MPa	TS MPa	EI %	LS %	<i>n</i>	<i>k</i> MPa	ΔY MPa	ΔU MPa	ΔEI %	LYS MPa	TS MPa	LS %	LYS MPa	TS MPa	EI %
60741	28	337	498	32	2.0	0.268	999	72	42	4	314	433	1.9	326	475	30
60759	28	314	470	35	1.9	0.263	920	73	49	7	298	398	1.9	300	445	34
60783	28	317	477	33	1.9	0.299	1031	60	49	6	303	443	1.9	318	464	33
60805	28	327	496	35	2.1	0.280	1021	63	43	6	305	463	2.0	332	474	32
60813	28	373	482	33	1.9	0.273	983	68	85	6	322	484	1.7	326	456	31
61091	28	342	512	33	1.9	0.287	1096	61	43	6	315	476	1.9	339	486	29
58511	24	343	510	33	2.1	0.289	1109	76	39	5	306	407	2.0	343	479	32
60236	24	321	468	35	2.6	0.273	939	75	43	4	288	365	1.8	372	503	34
60317	24	339	481	35	2.3	0.269	980	72	46	6	297	409	1.8	319	457	38
60325	24	349	484	35	1.7	0.151	748	79	48	6	340	385	1.8	325	469	31
60333	24	338	469	36	2.1	0.259	922	71	39	7	277	378	1.8	318	437	32
61457	24	340	488	35	2.3	0.258	945	71	42	6	312	396	1.8	321	457	32
61503	24	339	495	35	2.1	0.266	979	76	44	7	304	389	1.8	323	458	35
63724	24	346	487	35	1.6	0.242	922	72	40	7	319	396	1.7	325	453	36
63741	24	349	499	33	2.1	0.262	978	74	40	5	319	402	1.9	333	461	34
63872	24	340	485	35	1.2	0.230	893	71	49	7	310	391	1.2	332	461	34
63902	24	352	510	33	2.0	0.274	1036	76	47	6	304	416	1.9	345	477	30
63929	24	340	488	33	2.1	0.276	996	76	47	4	304	389	2.0	319	460	32
63937	24	342	490	33	1.6	0.233	906	75	46	4	306	382	1.7	320	464	32
63961	24	367	487	35	1.9	0.247	938	86	120	6	299	391	1.6	326	458	31
64066	20	364	529	33	2.5	0.271	1064	73	44	4	332	491	2.1	348	468	36
64074	20	341	490	33	2.4	0.270	985	66	40	2	326	455	1.9	332	451	36
64082	20	351	484	37	1.8	0.252	928	40	58	4	321	451	1.5	337	472	35
64091	20	352	504	35	1.8	0.253	969	70	34	5	326	465	1.5	343	485	34
64112	20	336	483	35	2.2	0.235	892	71	42	4	307	441	2.3	332	469	34
64121	20	326	463	36	2.7	0.181	755	65	38	4	311	426	2.7	320	464	35
64104	20	331	460	37	2.3	0.240	858	68	46	5	302	421	2.0	315	424	37
64147	20	333	479	37	1.9	0.245	910	69	42	7	303	372	2.6	332	455	36

Table C.1 continued ...

CAST NO.	Bar Diameter mm	Machined Specimen									Lab Deformed			P.S. Deformed		
		LYS MPa	TS MPa	EI %	LS %	<i>n</i>	<i>k</i> MPa	ΔY MPa	ΔU MPa	ΔEI %	LYS MPa	TS MPa	LS %	LYS MPa	TS MPa	EI %
64155	20	348	489	36	2.2	0.254	935	74	44	5	315	444	2.4	338	468	35
64171	20	338	478	36	2.5	0.271	1015	60	60	5	328	465	2.6	327	455	35
64228	20	335	485	36	2.3	0.261	947	72	50	7	323	450	2.3	319	444	34
64201	20	348	500	35	2.2	0.263	977	65	41	6	323	455	2.6	341	479	35
64236	20	347	491	34	2.1	0.276	1002	68	55	3	323	460	1.7	335	459	35
64244	20	337	495	35	1.9	0.236	912	63	42	6	313	452	1.5	325	468	35
64210	20	352	497	34	2.1	0.249	957	75	53	6	313	451	1.7	329	467	35

Table C.2: Tensile results of Grade 430 reinforcing steel

CAST NO.	Bar Diameter mm	Machined Specimen									Lab Deformed			P.S. Deformed		
		LYS MPa	TS MPa	EI %	LS %	n	k MPa	ΔY MPa	ΔU MPa	ΔEI %	LYS MPa	TS MPa	LS %	LYS MPa	TS MPa	EI %
63171	32	457	631	27	1.3	0.208	1138	51	28	3	393	566	1.3	451	602	19
63198	32	434	595	29	1.3	0.208	1072	29	15	2	395	550	1.4	445	573	23
63341	32	424	586	29	1.3	0.211	1047	50	19	2	402	535	1.3	451	583	24
63376	32	465	623	27	1.3	0.203	1112	39	16	1	424	572	1.3	448	583	22
63384	32	455	622	28	1.3	0.212	1127	46	18	4	410	596	1.3	458	614	22
63392	32	455	638	28	1.0	0.170	1062	28	4	0	440	560	1.0	450	600	18
63414	32	440	607	28	1.3	0.201	1069	49	16	2	410	563	1.4	446	583	18
63422	32	435	585	34	1.5	0.290	1033	52	50	7	405	560	1.4	443	579	24
63431	32	461	630	28	1.3	0.206	1126	53	22	2	422	579	1.2	447	590	22
63449	32	463	634	28	1.1	0.202	1128	45	22	3	429	587	1.1	448	584	20
63457	32	506	713	25	1.0	0.181	1210	15	20	3	490	654	1.0	533	691	21
63465	32	445	592	30	1.5	0.199	1037	45	15	2	402	546	1.5	454	587	19
63473	32	459	621	25	1.1	0.204	1095	45	24	1	424	514	1.1	457	592	22
63481	32	474	654	27	1.1	0.182	1125	31	11	1	458	578	1.1	498	646	19
63490	32	458	617	29	1.2	0.201	1095	46	35	2	427	581	1.2	502	650	24
63503	32	453	611	28	1.3	0.212	1107	53	23	3	407	563	1.4	454	597	25
63511	32	444	612	29	1.1	0.202	1084	23	15	1	405	560	1.1	450	577	25
63520	32	435	609	29	1.0	0.198	1069	35	19	2	407	547	1.2	451	585	25
63538	32	447	615	26	1.2	0.206	1102	35	16	1	414	566	1.2	479	619	22
63562	32	469	643	25	1.2	0.206	1153	45	22	0	424	584	1.0	458	603	22
63571	32	478	645	27	1.2	0.198	1131	45	9	1	446	591	1.2	473	598	19
63589	32	499	662	26	1.0	0.188	1140	52	39	0	473	624	1.0	505	641	19
63597	32	502	665	27	1.2	0.187	1133	55	30	1	478	618	1.5	500	631	21
63546	32	458	647	27	1.0	0.188	1113	34	6	2	424	576	1.0	461	598	20
63601	32	493	662	28	1.0	0.177	1111	64	51	7	468	627	1.1	505	643	20
63619	32	474	630	26	1.1	0.200	1113	50	29	2	449	603	1.1	472	614	28
63635	32	483	665	26	1.0	0.201	1185	28	16	1	458	617	1.2	503	624	26

Table C.2 continued ...

CAST NO.	Bar Diameter mm	Machined Specimen									Lab Deformed			P.S. Deformed		
		LYS MPa	TS MPa	EI %	LS %	n	k MPa	ΔY MPa	ΔU MPa	ΔEI %	LYS MPa	TS MPa	LS %	LYS MPa	TS MPa	EI %
63651	32	453	619	27	1.2	0.205	1106	33	15	4	410	560	1.2	443	578	24
63660	32	460	618	30	1.2	0.200	1109	32	9	2	432	547	1.4	439	586	19
63694	32	446	612	27	1.2	0.215	1119	35	24	1	410	563	1.2	461	600	21
63759	32	483	652	25	1.2	0.213	1187	64	35	0	439	603	1.4	451	580	21
63767	32	458	609	29	1.4	0.223	1134	48	27	1	412	560	1.4	444	577	26
63783	32	462	655	28	1.1	0.204	1177	42	19	2	432	598	1.2	451	584	21
63775	32	454	625	27	1.1	0.205	1119	19	19	1	417	578	1.2	463	598	26
63805	32	450	615	29	1.0	0.205	1116	44	16	1	414	569	1.1	440	583	22
63813	32	470	648	25	1.3	0.212	1181	37	13	0	422	583	1.2	464	613	23
63830	32	439	601	28	1.3	0.203	1066	54	28	1	405	548	1.5	444	574	26
63406	32	462	631	29	1.2	0.195	1106	51	9	4	440	570	1.2	458	596	29
57961	28	501	665	27	1.3	0.187	1150	55	23	3	487	601	1.3	493	622	25
58015	28	480	669	27	1.1	0.187	1142	50	8	4	478	596	1.0	458	597	31
58023	28	486	669	27	1.0	0.176	1121	29	20	2	478	594	1.0	517	648	27
58040	28	463	630	29	1.4	0.205	1119	50	7	4	430	549	1.3	452	593	28
58058	28	459	633	29	1.1	0.171	1044	53	19	5	430	555	1.0	476	617	24
58066	28	481	643	28	1.3	0.195	1119	49	14	2	441	552	1.1	469	612	24
58074	28	481	645	28	1.3	0.174	1072	44	13	2	455	577	1.2	473	636	28
58104	28	499	671	27	1.4	0.185	1144	47	10	3	473	592	1.5	488	635	21
58163	28	456	612	29	1.6	0.200	1075	54	24	2	427	542	1.3	458	590	27
58171	28	473	661	28	1.0	0.196	1157	60	19	2	454	578	1.1	471	624	24
58180	28	486	652	27	1.2	0.163	1059	32	6	0	473	593	1.3	496	636	21
58198	28	486	659	27	1.2	0.192	1132	55	26	4	468	586	1.1	480	626	23
58201	28	517	685	33	1.4	0.178	1147	21	7	6	489	612	1.3	502	651	22
58210	28	463	633	29	1.2	0.187	1154	28	7	2	440	561	1.1	466	609	24
58228	28	505	707	26	1.1	0.208	1278	29	9	1	477	625	1.1	504	667	19
60872	28	455	605	29	1.2	0.214	1099	62	27	3	408	565	1.3	443	573	25

Table C.2 continued ...

CAST NO.	Bar Diameter mm	Machined Specimen									Lab Deformed			P.S. Deformed		
		LYS MPa	TS MPa	EI %	LS %	<i>n</i>	<i>k</i> MPa	ΔY MPa	ΔU MPa	ΔEI %	LYS MPa	TS MPa	LS %	LYS MPa	TS MPa	EI %
60881	28	470	645	28	1.3	0.211	1177	60	24	2	439	599	1.4	475	616	27
60899	28	470	628	28	1.4	0.210	1132	55	25	1	433	586	1.3	468	601	22
60902	28	481	643	27	1.4	0.207	1154	33	22	1	446	606	1.3	468	611	25
60911	28	463	631	28	1.3	0.201	1118	44	20	1	430	583	1.3	457	597	22
60937	28	461	635	29	1.0	0.199	1121	54	26	4	427	585	1.0	449	590	25
60953	28	452	617	29	1.2	0.207	1103	52	18	4	414	565	1.2	443	586	23
62911	28	466	629	29	1.0	0.178	1059	49	20	2	433	601	1.0	471	610	22
62937	28	475	660	27	1.0	0.199	1164	24	14	1	447	614	1.0	485	630	21
62945	28	430	595	29	1.2	0.210	1068	58	27	3	401	562	1.2	447	588	25
62953	28	443	596	28	1.1	0.203	1061	53	44	4	414	572	1.1	439	586	26
62961	28	448	610	29	1.3	0.207	1089	46	23	1	414	568	1.0	447	576	26
62970	28	457	621	29	1.2	0.202	1106	45	18	1	422	577	1.0	469	598	29
62996	28	456	616	27	1.3	0.206	1099	58	29	3	420	577	1.3	467	606	23
63007	28	457	635	29	1.1	0.200	1123	50	14	2	427	568	1.2	455	597	22
63015	28	456	633	28	1.1	0.196	1103	54	16	3	427	588	1.2	457	600	22
63066	28	465	636	28	1.2	0.195	1113	48	24	3	438	588	1.1	493	642	24
63082	28	468	644	29	1.1	0.208	1160	42	21	2	438	604	1.1	466	607	26
63091	28	466	658	27	1.0	0.198	1159	41	8	2	438	611	1.0	462	607	26
54465	24	493	658	27	1.3	0.200	1184	59	14	4	360	658	1.2	462	603	20
54457	24	485	640	27	1.3	0.212	1158	54	13	1	442	539	1.2	468	609	23
58082	24	484	634	29	1.2	0.197	1114	62	110	3	429	531	1.1	462	597	28
58155	24	447	602	28	1.1	0.201	1061	55	81	3	410	522	1.1	457	583	28
58252	24	469	629	28	1.0	0.185	1069	55	12	4	427	522	1.1	455	584	23
60121	24	470	637	29	1.1	0.172	1055	60	15	3	433	515	1.0	466	620	23
60139	24	486	654	30	1.1	0.177	1103	29	9	4	446	535	1.0	487	621	25
60155	24	478	650	28	1.1	0.187	1125	40	13	2	433	526	1.0	466	603	24
60431	24	463	615	29	1.3	0.173	1013	39	6	0	342	550	1.2	478	617	24

Table C.2 continued ...

CAST NO.	Bar Diameter mm	Machined Specimen									Lab Deformed			P.S. Deformed		
		LYS MPa	TS MPa	EI %	LS %	n	k MPa	ΔY MPa	ΔU MPa	ΔEI %	LYS MPa	TS MPa	LS %	LYS MPa	TS MPa	EI %
60520	24	463	627	29	1.6	0.221	1158	53	10	0	420	526	1.5	458	602	30
60538	24	477	634	29	1.7	0.211	1139	43	6	2	438	531	1.2	463	612	24
60554	24	481	647	29	1.4	0.189	1173	34	32	3	444	528	1.2	485	633	22
60597	24	469	647	28	1.2	0.206	1165	66	21	2	427	526	1.1	456	607	23
60601	24	463	631	28	1.4	0.227	1183	61	16	1	429	508	1.0	463	608	21
60619	24	475	641	29	1.4	0.213	1170	59	15	2	429	506	1.2	457	597	28
60627	24	451	629	29	1.0	0.217	1167	51	7	1	412	506	1.0	447	598	15
63201	24	509	679	28	1.2	0.152	1077	43	9	3	472	535	1.2	479	604	21
63295	24	445	600	31	1.1	0.186	1011	58	11	3	394	495	1.1	457	581	26
63309	24	471	630	29	1.1	0.166	1025	40	8	2	455	517	1.1	462	590	26
63368	24	462	618	29	1.4	0.218	1161	53	15	1	416	519	1.3	448	577	23
63627	24	440	599	28	1.6	0.210	1072	70	25	2	399	493	1.7	453	581	28
63708	24	469	632	28	1.1	0.222	1190	45	5	0	310	546	1.2	481	617	23
64317	24	478	635	29	1.1	0.179	1061	61	13	2	433	528	1.2	463	596	23
57899	20	456	601	30	1.4	0.195	1035	45	31	0	434	566	1.5	487	633	22
60147	12	470	630	28	1.7	0.218	1124	66	29	4	487	625	2.0	480	629	24
60163	12	474	637	30	1.7	0.224	1097	70	6	1	467	609	1.8	474	612	23
60198	12	439	647	27	1.2	0.213	1090	57	3	5	446	611	1.3	449	587	25
60210	12	445	636	29	1.6	0.200	1121	97	41	3	502	648	1.7	475	621	23
60244	12	473	610	33	2.1	0.240	1133	52	4	1	472	600	2.2	475	622	25
60295	12	468	617	32	2.0	0.213	1067	57	21	4	465	602	2.1	467	598	29
60368	12	461	627	32	2.1	0.235	1124	92	5	0	469	605	2.2	454	577	28
60384	12	433	634	30	1.8	0.195	956	51	1	1	434	566	1.8	463	579	33
60392	12	494	656	32	1.7	0.195	1065	92	7	2	487	625	1.7	487	602	28
60414	12	480	623	32	2.0	0.211	1034	43	5	8	460	587	2.0	475	603	21
60422	12	481	624	30	1.8	0.217	1050	49	25	2	458	613	2.2	494	609	32
55911	10	485	720	28	1.4	0.189	1107	61	2	4	485	641	1.5	475	635	26

Table C.2 continued ...

CAST NO.	Bar Diameter mm	Machined Specimen									Lab Deformed			P.S. Deformed		
		LYS MPa	TS MPa	EI %	LS %	<i>n</i>	<i>k</i> MPa	ΔY MPa	ΔU MPa	ΔEI %	LYS MPa	TS MPa	LS %	LYS MPa	TS MPa	EI %
55929	10	470	661	30	1.2	0.185	1111	64	22	2	461	650	1.0	493	662	25
55937	10	435	496	35	1.8	0.261	922	70	143	4	346	461	1.9	505	649	25
55961	10	489	658	28	1.3	0.179	1009	36	10	3	461	607	1.3	492	633	30
58121	10	491	652	29	2.0	0.192	1073	36	5	1	494	629	2.1	483	625	28
58147	10	483	638	33	1.7	0.198	1077	30	7	2	469	612	1.9	457	617	25

Table C.3: Tensile results of "low carbon trial heats"

CAST NO.	Bar Diameter mm	Machined Specimen									Lab Deformed			P.S. Deformed		
		LYS MPa	TS MPa	EI %	LS %	<i>n</i>	<i>k</i> MPa	ΔY MPa	ΔU MPa	ΔEI %	LYS MPa	TS MPa	LS %	LYS MPa	TS MPa	EI %
12439	32	400	535	31	1.6	0.192	905	63	26	2	371	463	1.4	398	512	26
	28	406	538	32	1.9	0.198	920	69	32	2	382	452	1.9	399	515	30
	24	409	541	32	2.1	0.194	908	60	22	2	377	460	1.7	388	504	29
	20	396	534	34	1.3	0.204	937	59	34	4	381	472	1.4	393	524	30
12447	32	395	556	30	1.2	0.200	959	59	21	4	381	476	1.0	394	507	27
	28	403	552	30	1.5	0.202	961	63	19	0	385	487	1.5	405	521	31
	24	403	545	32	1.5	0.197	936	65	24	3	377	460	1.6	392	512	28
	20	406	549	33	1.4	0.203	956	62	32	3	400	452	1.4	393	531	31
12455	32	397	551	32	1.4	0.205	959	62	22	6	378	478	1.5	414	537	27
	28	426	599	29	1.1	0.202	1049	67	19	1	422	526	1.3	425	554	28
	24	428	588	30	1.3	0.191	1005	65	23	1	412	502	1.4	422	554	24
	20	407	565	33	1.3	0.210	1000	62	32	4	405	472	1.3	420	564	31